Impacts of non- and whole-fat milk supplementation on metabolic dysfunction-associated steatotic liver disease (MASLD) in C57BL/6 mice

by

Emily Berg

A thesis submitted in partial fulfillment of the requirements for the degree of

Master of Science

Department of Physiology

University of Alberta

Abstract

The pathophysiology behind metabolic dysfunction-associated steatotic liver disease (MASLD) and mechanisms underlying the progression of the disease are highly complex, complicating treatment options, leaving diet and weight loss as the standard of care. Functional foods can mitigate MASLD progression by improving glucose and lipid homeostasis with many studies focusing on the role of dairy products; however, the mechanism of action has not been elucidated.

This study aims to compare MASLD-related outcomes after feeding non- (NFM) versus whole-fat milk (WFM) in a high-fat diet (HFD)-induced obese mouse model. I hypothesize that (1) both WFM and NFM will significantly reduce diet-induced hepatic lipid accumulation and prevent the progression of early-stage MASLD in obese, male C57BL/6 mice but via different mechanisms and that (2) increased capacity for substrate uptake and metabolism in skeletal muscle may act as a mediator of reduced hepatic steatosis.

After 8 weeks of providing 0.425 mL for 5 days per week of either NFM or WFM milk to mice, mice were euthanized, and tissues collected in a fasted state. NFM significantly reduced body weight (BW) gain and fat mass, hepatic triglyceride (TG), lipid droplet (LD) number, and total area covered by LD compared to HFD ($p < 0.05$). This was accompanied by an increase in hepatic mitochondrial complex abundance ($p < 0.05$) and a trend towards enhanced microsomal triglyceride transfer protein (MTP) abundance ($p = 0.076$). WFM trended towards a reduction in total area covered by LD ($p = 0.051$) compared to HFD but had significantly higher TG compared to NFM ($p < 0.05$). Enzymes involved in *de novo* lipogenesis were increased in WFM, including fatty acid binding protein 4 (FABP4) ($p = 0.059$), fatty acid synthase (FAS) ($p < 0.05$), and the proportion of phosphorylated acetyl-CoA carboxylase (p-ACC / ACC) ($p < 0.05$)

compared to NFM. There was also an increase in carnitine palmitoyl transferase 1α (CPT1α) protein abundance ($p < 0.05$) in WFM compared to HFD and *Opa1* expression ($p < 0.05$) in WFM compared to NFM.

In skeletal muscle, no significant differences were seen in protein kinase B (Akt), or adenosine-monophosphate (AMP) activated kinase (AMPK), which are enzymes involved in glucose metabolism. Within lipid metabolism pathways, CD36 abundance was downregulated in both WFM and NFM compared to HFD ($p < 0.05$), and Sirtuin-1 (SIRT1) abundance was enhanced in WFM compared to NFM ($p < 0.05$). No differences were seen in CPT1α and peroxisome proliferator-activated receptor-gamma coactivator 1α (PGC1α).

Overall, NFM displayed greater beneficial effects than WFM in mitigating MASLD progression by increasing the capacity for hepatic oxidative phosphorylation and fatty acid (FA) export, which were associated with reduced hepatic fat accumulation. Skeletal muscle metabolism did not display an enhanced capacity for substrate uptake, and only WFM demonstrated an enhanced abundance of SIRT1 with no further alterations downstream.

In conclusion, this thesis provides evidence that NFM is may be superior to WFM in promoting beneficial effects in an HFD-induced obese mouse model through reduced hepatic lipid accumulation and improved utilization of FA. These results may outline a potential tool for early intervention to prevent and attenuate the progression of MASLD.

Key words: Dairy, metabolic dysfunction-associated steatotic liver disease, mitochondria, lipid metabolism, hepatic steatosis.

Dedication

I dedicate this thesis to my parents, whose unwavering resilience has continuously inspired me to persevere and rise stronger with each challenge.

"What you do makes a difference, and you have to decide what kind of difference you want to make." – Jane Goodall

Acknowledgements

Conducting this thesis would not have been possible without the support, encouragement, and patience from so many people. I would like to first thank my soon to be husband, John Holowaychuk, for listening to me every time I came home talking about western blots and nodding along even though you had no idea what I was talking about. You have pushed me to pursue my dreams and without you, I wouldn't have made it this far. Thank you to my parents, Dr. Todd and Michelle Berg, for telling that little girl to use her powers for good so that she could do anything she put her mind to. This year has been a test to us all, but through everything, you have shown immense strength and endless love. Thank you to my brother and all my friends and loved ones who were always there to pick me up and celebrate my wins, you know how special you are to me. I love you.

I want to deeply thank my supervisor, Dr. Catherine Chan, for believing in me and giving me a chance to achieve what seemed impossible at times. You have allowed me to flourish as a junior scientist, always leading me back to the path when I went a little crazy with my ideas. You have taught me to appreciate science even when it doesn't make sense and allowed me the space to reach for my dreams. Thank you for pushing me out of my comfort zone and supporting me through every step of this process.

Thank you to my committee members and examiners, Dr. Robin Clugston, Dr. Spencer Proctor, and Dr. Jessica Yue. Your expertise, suggestions, and kindness have shaped who I am as a researcher and played a large role in my professional trajectory.

To my lab mates, there is so much to say. Thank you, Dr. Stepheny Zani, for taking me under your wing and showing me almost everything I know today. I owe so much of my graduate experience to you, and I will be forever grateful for your support, coffee dates, and endless

laughs. Emad Yuzbashian, thank you for always lending me a helpful hand or eye when I just couldn't understand what my computer was spitting out at me, and for being a constant reminder of how much we love western blots. Thank you to my undergraduate honours' student, JJ Diaz, for reminding me that science can be fun, but it's better when done together. You were my first student to supervise, and I will always hold you near my heart. Thank you for your work on my project, and for helping me become a better teacher. To all the undergraduates that I have been able to work with and mentor over my two years, Aaron Getachew, Dineli Fernando, Linden Stuart, and Maria Janisz, thank you. You have been a source of laughter and joy in my daily lab life, and you can count on me for anything you need in the future.

Finally, thank you to everyone I have met along the way. All my PGSA crew, ADI TWG execs, and fellow grad students. Grad school was everything and nothing of what I expected, and each person I met and formed a bond with I am so grateful for. A special mention to Dr. Shereen Hamza for pointing me in this direction and being a consistent mentor and support during this journey. Thank you to Dr. Saswati Das for your friendship and kindness over the past few years, I sincerely appreciate being able to call my favourite professors my colleagues.

Table of Contents

List of Tables

List of Figures

Chapter 1: Introduction & Literature Review

1.1 Introduction and purpose

The global prevalence of chronic metabolic disorders has grown exponentially over the last few decades. Overweight and obesity affects more than 2.5 billion adults, type 1 diabetes (T1D) and type 2 diabetes (T2D) affect over 545 million individuals, metabolic syndrome (MetS) prevalence estimates range between 20-45% of the global population, and 2.31 billion individuals are diagnosed with metabolic dysfunction-associated steatotic liver disease (MASLD) [1], [2], [3], [4], [5]. An individual can be diagnosed with more than one metabolic disorder, thereby increasing morbidity, mortality, and drastically reducing quality of life [6]. These disorders progress over time, and their preclinical signs often go undetected, resulting in irreversible pathologic progression. Thus, almost half of the world's population is at risk of developing a chronic metabolic condition that results in trillions of dollars spent on health care and loss of economic productivity [7]. Individuals require lifelong monitoring and, in the case of diabetes, administration of exogenous insulin or another pharmacotherapy. This can cause an extreme burden, not only financially, but mentally and physically with almost 64% of adults displaying severe distress with concerns over complications and disease management [8]. Polypharmacy is another clinical concern and has been associated with decreased therapeutic benefit among patients with MetS [9]. Pharmacotherapy is provided once clinical thresholds are met, reducing its efficacy and applicability for the prevention of disease progression [10].

Early intervention after identification of preclinical markers or risk factors could prevent progression to clinical disease, preventing comorbidities and overall mortality. Lifestyle interventions are integral to prevent and treat chronic disorders such as obesity, diabetes, MASLD, and hypertension [6]. Adopting long-term lifestyle modifications such as consistent

physical activity, limiting alcohol intake, and refraining from smoking significantly reduces mortality, hepatic steatosis, and hyperglycemia [11], [12], [13]. Low-energy diets, omega-3 fatty acid-rich diets, and the Mediterranean diet effectively reduce visceral adiposity, dyslipidemia, blood pressure, hepatic fat accumulation, and improve glycemic control [14], [15]. Multiple lifestyle intervention studies combining diet and physical activity programs significantly improve weight, glycemic control, and dyslipidemia over 2-4 years [16], [17]. Overall, diet and physical activity are recommended before pharmacotherapy for early intervention and mitigation of chronic disease progression [6].

In our research, we examine how whole foods contribute to health, disease prevention, and treatment. We seek to identify foods, that if consumed in greater quantity, could alleviate the burden of chronic disease. Our past preclinical research on dairy products suggests benefits on BW gain, diabetes-related outcomes, and hepatic steatosis, but there is controversy in the literature about the wisdom of consuming of dairy because some dairy products are high in saturated fat [18]. However, in our preliminary research studying the effects of dairy milk on these outcomes, we saw indications that both non-fat (NFM) and whole-fat milk (WFM) had benefits [19]. In this thesis, I will extend these preliminary studies to characterize and compare the effects of dairy milk on body weight (BW) gain, diabetes-related outcomes, and hepatic steatosis in a mouse model of obesity, preclinical diabetes, and hepatic steatosis. My overall aim is to assess dairy milk efficacy as an early intervention tool to mitigate the initiation of metabolic dysfunction.

1.2. Metabolic syndrome: a global clinical problem

1.2.1 Global epidemic: metabolic dysfunction

MetS is a complex condition characterized by concurrent comorbidities resulting in an enhanced risk for cardiovascular disease (CVD) and mortality [20]. Some comorbidities include T2D, hypertension, MASLD, dyslipidemia, and obesity.

The prevalence of MetS varies due to differing diagnostic criteria globally, however, estimates range between 20-45% of the global population, a number expected to increase to 53% by 2035 [4]. To be diagnosed with MetS in Canada, three or more of the following criteria must be met: elevated waist circumference, elevated triglycerides (TG), reduced high-density lipoprotein cholesterol (HDL-C), elevated blood pressure (BP), and elevated fasting blood glucose (FBG) [21]. In Canada, approximately one in five adults are diagnosed with metabolic syndrome, with over 44% on the cusp of diagnoses with two risk factors [22]. The diagnostic thresholds used can be seen in Figure 1.1.

The pathophysiology and etiology of MetS is complex as they involve multiple physiological systems and environmental risk factors. Some risk factors for the disorder include family history, increased age, obesity, low socioeconomic status, and western dietary patterns [23]. Insulin resistance (IR) in combination with enhanced FA flux is thought to be the primary driver of MetS, resulting in lipid accumulation in multiple tissues such as the liver, adipose tissue, and skeletal muscle. This can then lead to a proinflammatory state as the expansion of adipose tissue causes immune cell infiltration, reactive oxygen species production, and cytokine mediator release. Chronic inflammation alongside IR can result in tissue fibrosis, atherogenesis and consequently CVD [24].

MetS diagnostic criteria encompasses multiple concurrent disorders, with this thesis focusing on two disorders: T2D and MASLD. T2D is denoted by dysfunctional insulin secretion and production by pancreatic β-cells and/or the inability of tissues to respond appropriately to insulin signalling, resulting in hyperglycemia [25]. T2D represents 90% of all diabetes diagnoses, with approximately 537 million prevalent cases in 2021 [3]. This number is expected to increase to 1.31 billion by 2050 with no countries expected to reduce their prevalence rates. Individuals who have T2D present with elevated blood glucose, visceral adiposity, sedentary lifestyle, and poor nutrition [26]. T2D is a multi-organ disorder affecting the pancreas, liver, adipose tissue, brain, skeletal muscle, and small intestine [27].

Diagnostic criteria for both T1D and T2D in Canada include either an 8-hour fasting blood glucose (FBG) ≥ 7.0 mmol/L, a glycated hemoglobin A1C (A1C) ≥ 6.5 % in adults, 2-hour plasma glucose (PG) in a 75g oral glucose tolerance test (OGTT) ≥ 11.1 mmol/L, or a random PG ≥ 11.1 mmol/L [21]. Individuals with T1D are generally under the age of 25, thin, and have absent insulin production whereas T2D patients are generally overweight (>90%), have a frequent familial history of T2D, and have insulin production.

MASLD is a disease comprised of metabolic dysfunction-associated steatotic liver (MASL) and metabolic dysfunction-associated steatohepatitis (MASH) and is described as the hepatic manifestation of MetS [28]. Without proper management, MASLD can progress to cirrhosis and hepatocellular carcinoma, which are leading causes of liver transplantation globally [29]. A summary of the progression of MASLD can be seen in Figure 1.2. In 2019, the global prevalence of MASLD was 29.8%, with North America having the highest prevalence of 35.7% [5]. MASLD is a risk factor for several global epidemics such as obesity and T2D, with almost 56% of T2D patients and 70% of obese patients also diagnosed with MASLD [30], [31].

To diagnose MASLD, a liver biopsy is the gold standard to distinguish between MASL and MASH histologically [32]. However, conducting a liver biopsy is invasive, expensive, and creates a risk for further complications [33]. Thus, non-invasive techniques such as magnetic resonance imaging-derived proton density fat fraction, transient elastography, and biomarkers such as plasma cytokeratin, aspartate transaminase (AST), alanine aminotransferase (ALT), and microbiome metabolites are all being investigated to provide earlier diagnosis and prognosis.

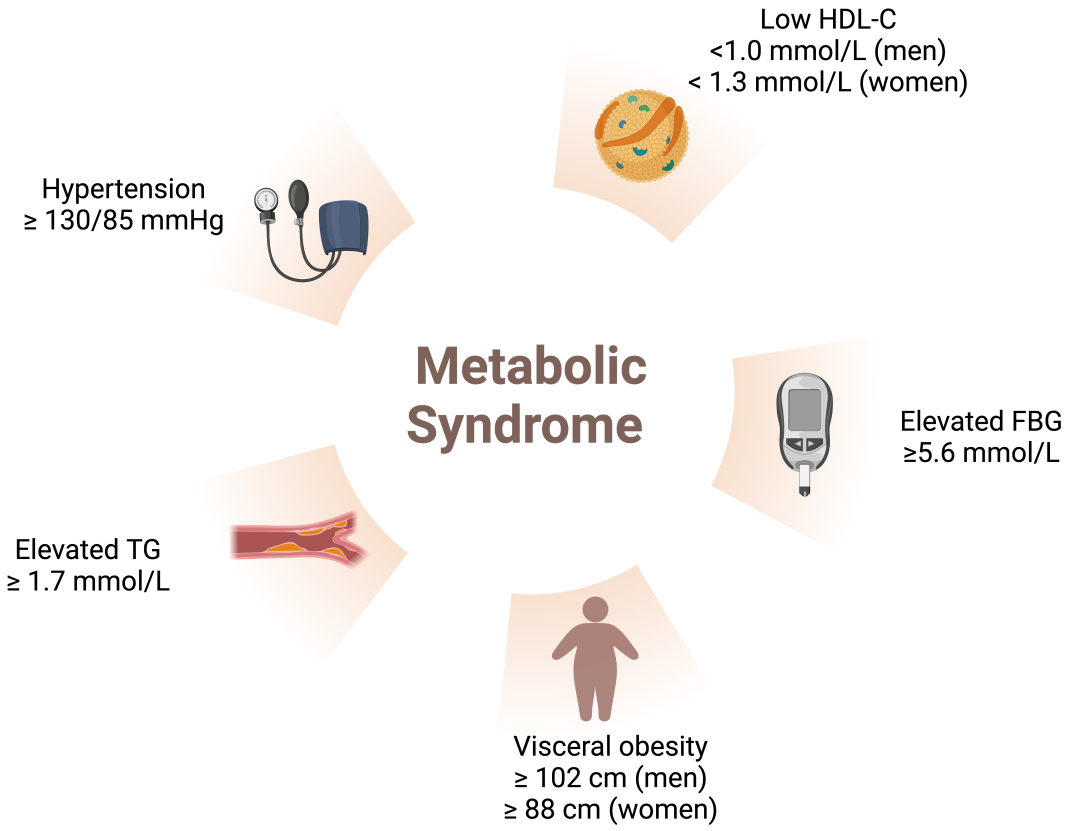

Figure 1.1. Diagnostic thresholds for MetS diagnosis according to Diabetes Canada [21]. TG, triglycerides; HDL-C, high-density lipoprotein cholesterol; BP, blood pressure; FBG, fasting blood glucose. Created by EB with Biorender.com.

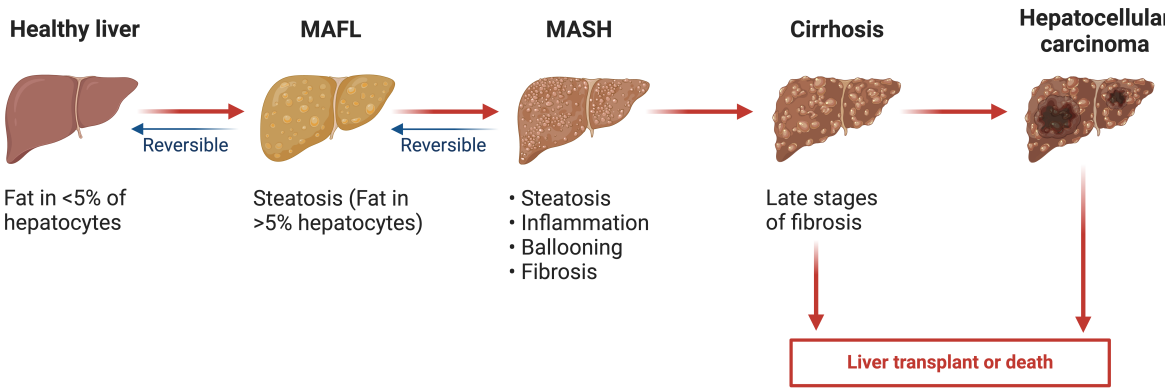

Figure 1.2. Summary figure of MASLD progression and morphological changes. MAFL, metabolic dysfunction-associated fatty liver; MASH, metabolic dysfunction-associated steatohepatitis. Created by EB with Biorender.com.

1.2.2 Preclinical MetS-related conditions: interconnected pathophysiology

Prior to reaching clinical status, metabolic diseases such as T2D and MASLD have preclinical windows of intervention. Prediabetes is characterized by elevated FBG between 6.1-6.9 mmol/L, 2hPG in a 75g OGTT between 7.8-11 mmol/L, or an A1C between 6-6.4%, putting people at an enhanced risk of developing diabetes within their lifetime [21]. The global prevalence of prediabetes in 2021 was around 762 million individuals, a number expected to increase to over 1 billion by 2045 [34]. Although MASLD does not have a defined preclinical stage like prediabetes, it does have preclinical windows of intervention before reaching later stages of MAFL and MASH. Both MASLD and T2D are 'silent' as they progress, with many patients presenting with mild hyperglycemia, dyslipidemia, or being asymptomatic until advanced stages are reached [35]. However, they share similar alterations to normal physiology that may allow for earlier diagnosis and concurrent management of the disorders prior to meeting

clinical thresholds. A brief overview of these connections will be described in this section, with a deeper understanding of normal versus pathological physiology explored in the next section.

Enhanced adipose tissue expansion resulting in visceral obesity is one of the starting points for the pathologic progression of prediabetes and MASLD [36]. Excessive consumption of a westernized diet resulting in hyperglycemia and hyperlipidemia causes an increase in insulin production and secretion by pancreatic β-cells. However, these compensatory mechanisms cannot be sustained long-term, resulting in reductions in glucose sensitivity leading to IR of key regulator tissues such as the liver, adipose tissue, and muscle. Adipose tissue expansion also leads to an enhanced production of proinflammatory mediators, which can dysregulate β-cell function through various pathways, ultimately resulting in the progression of IR and prediabetes into a diabetic state. IR within the liver enhances gluconeogenesis, exacerbating hyperglycemia and pushing the progression of both T2D and MASLD. To mitigate hyperglycemia and hyperlipidemia, hepatic *de novo* lipogenesis is upregulated, increasing hepatic TG content, and progressing MASLD status [37]. A summary of the events that occur during T2D progression is outlined in Figure 1.3. T2D and MASLD are intrinsically linked through their pathophysiology and preceding risk factors, with almost 56% of patients with T2D concurrently diagnosed with MASLD [38]. Thus, if clinical intervention can occur at a preclinical window to mitigate obesity, proinflammatory states, and IR, we not only would mitigate T2D progression but also MASLD and other concurrent metabolic disorders that affect over half of the global population. Further discussion on solutions is covered in Section 1.4.

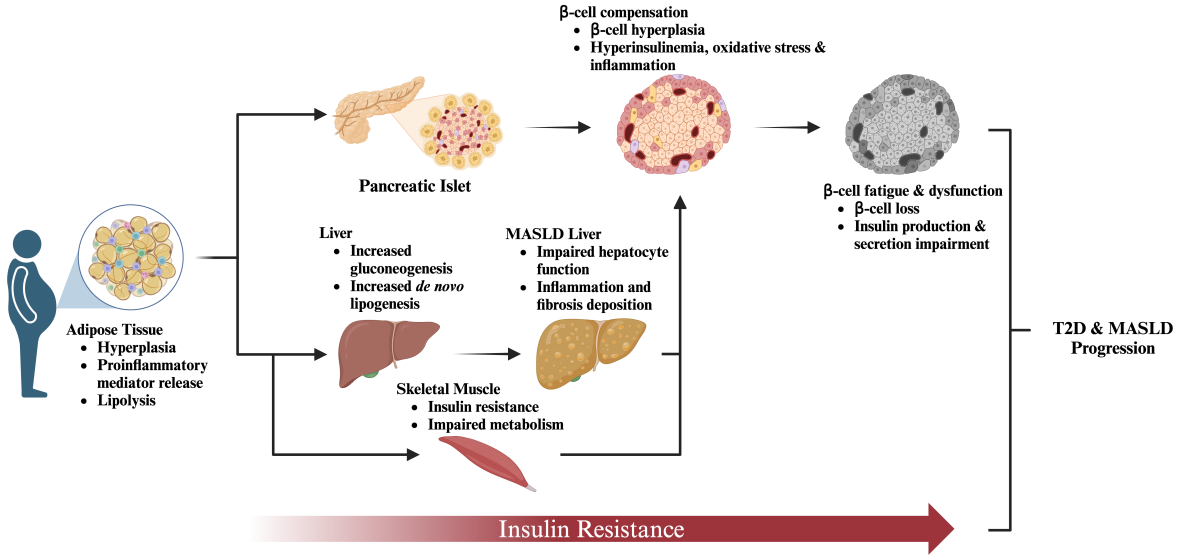

Figure 1.3. Overview of pathologic progression of IR from obesity resulting in T2D and MASLD. MASLD, metabolic dysfunction-associated steatotic liver disease; T2D, type 2 diabetes. Created by EB with Biorender.com and adapted from Dludla et al. [36].

1.3 Allowing chronic disease to progress: pathophysiology of chronic metabolic conditions

1.3.1 Glucose homeostasis & pathophysiology

Ensuring stable blood glucose necessitates intricate coordination among various physiological processes, demanding a continual balance between glucose storage, synthesis, and utilization. Insulin and glucagon, hormones secreted by the pancreas with opposing functions, collectively regulate blood glucose [39]. After consuming a meal, glucose is absorbed in the small intestine through sodium-dependent glucose cotransporter 1 (SGLT1) and into the systemic circulation through a facilitated-diffusion glucose transporter (GLUT2) [40]. GLUT2 transporters are also present on pancreatic β-cells, and sense the elevation in blood glucose,

resulting in the release of insulin into the circulation [39]. This results in a cascade of events in insulin-sensitive tissues, culminating in glucose uptake and storage for later use.

When blood glucose drops during fasting, pancreatic α-cells secrete glucagon, which acts in the liver to inhibit glycogenesis and promote gluconeogenesis and glycogenolysis to elevate blood glucose for metabolism. Both insulin and glucagon can be regulated by the central nervous system (CNS) and other circulating hormones; however, the focus of this thesis will be on insulin and glucagon actions in the liver and skeletal muscle to regulate glucose metabolism and homeostasis.

1.3.2 Hepatic glucose metabolism: gluconeogenesis, glycogenesis, de novo lipogenesis

The liver is a vital organ in glucose homeostasis as it is the primary tissue producing glucose in a fasted state to support maintenance of FBG [41]. GLUT2 transporters are responsible for insulin-independent glucose uptake into hepatocytes as well as glucose release into the circulation. Once taken up, glucose can be utilized through glycolysis, generating glucose-6-phosphate (G6P) which is a precursor for glycogenesis [42]. G6P can also be metabolized into pyruvate and shuttled to the mitochondria for oxidative phosphorylation or used to synthesize FA through *de novo* lipogenesis (DNL) [42].

In a fasted state, glucagon acts to promote glycogenolysis and gluconeogenesis to elevate circulating blood glucose [39]. During short-term fasting, glycogenolysis is the main source of circulating glucose; however, chronic fasting results in a depletion of hepatic glycogen stores, requiring *de novo* production of glucose through gluconeogenesis [42]. Gluconeogenesis produces glucose from non-carbohydrate precursors such as lactate from glycolysis, glycerol from lipolysis and amino acids through the citric acid cycle [43]. Glucagon activates signalling

cascades that result in an increased concentration of cyclic adenosine monophosphate (cAMP) which phosphorylates pyruvate kinase, enhancing phosphoenolpyruvate carboxykinase (PEPCK) expression [42]. PEPCK catalyzes the formation of phosphoenolpyruvate from oxaloacetate and is one of the rate-limiting steps of gluconeogenesis alongside pyruvate carboxylase, fructose 1,6-biphosphatase, and glucose-6-phosphatase (G6Pase) [41]. Further biochemical reactions result in the production of G6P, which is converted to glucose by G6Pase, and glucose is then released into the circulation. Increases in the abundance of gluconeogenic enzymes can increase the capacity for gluconeogenesis in IR, and this capacity can be measured using a pyruvate tolerance test (as described in Chapter 3).

Insulin impacts hepatic glucose metabolism by stimulating glycolysis through enhanced expression of hepatic glucokinase, promoting the conversion of glucose to G6P [39]. Glycogenesis is also upregulated through activating glycogen synthase kinase, resulting in glycogen synthase activation. Insulin also suppresses PEPCK and G6Pase expression, resulting in enhanced storage of glucose in the liver and inhibition of gluconeogenesis. Glucose can also be stored in the form of TG through DNL (see section 1.3.5). Once glycolysis occurs, pyruvate is shuttled to the mitochondria and is metabolized into acetyl-CoA [39]. In the cytoplasm, acetyl-CoA is carboxylated by ACC to form malonyl-CoA, which fatty acid synthase (FAS) uses to synthesize FA. Insulin stimulates DNL postprandially through the activation of mammalian target of rapamycin complex 1 (mTORC1) and Akt. Overall, the liver is a critical organ in maintaining blood glucose concentrations, operating a tight balance between glycogenesis, DNL, glycogenolysis, and gluconeogenesis.

1.3.3 Skeletal muscle glucose metabolism: glycolysis and glycogenesis

The skeletal muscle accounts for approximately 85% of systemic glucose uptake and therefore plays a large role in maintaining glucose homeostasis [44]. Postprandially, insulin-dependent glucose uptake is the most important. Insulin secreted in response to glucose and other meal-associated secretagogues binds to its receptor, which initiates a cascade of reactions including autophosphorylation of the tyrosine kinase subunit of the receptor, followed by phosphorylation of insulin receptor substrate proteins (IRS). This promotes recruitment of phosphatidylinositol-3-which leads to phosphorylation of Akt, which is frequently measured as an index of activation of insulin-dependent glucose uptake. Akt phosphorylates Akt substrate 160 (AS160), stimulating GLUT4 translocation from the cytosol to the plasma membrane. Glucose then enters myocytes via facilitated transport to be phosphorylated by hexokinase into G6P, which serves as the initial substrate of further glucose utilization or storage [45]. During fasting or active muscle contraction (i.e. exercise), insulin-independent uptake is facilitated by basal GLUT1 or GLUT4 respectively [46]. Exercise effects are dependent on AMP-activated protein kinase (AMPK), which is highly sensitive to changes in cellular energy. Like Akt, AMPK also increases GLUT4 insertion into the plasma membrane via phosphorylation of AS160. The calcium influx associated with muscle contraction potentiates GLUT4 translocation through calmodulin-dependent kinase (CAMK) [47]. Glucose has four fates within the skeletal muscle; however, this thesis will focus on two, glycolysis and glycogenesis.

Glycolysis is a ten-step process that results in the conversion of glucose into pyruvate [48]. Split into two stages, key enzymes of the first stage include hexokinase, which catalyzes the first conversion of glucose to G6P, and phosphofructokinase-1, which catalyzes the conversion of fructose-6-phosphate (F6P) to fructose 1,6-biphosphate (F1,6BP). One more conversion by

aldolase converts F1,6BP into glyceraldehyde 3-phosphate. The first stage requires two molecules of adenosine triphosphate (ATP) and is known as the investment stage. The key enzyme of the second stage is pyruvate kinase, which catalyzes the final step of glycolysis, converting phosphoenol pyruvate (PEP) to pyruvate. The second stage produces four molecules of ATP and is known as the payoff stage. Pyruvate has two main fates. In the presence of oxygen, it is converted to acetyl-CoA and enter the citric acid cycle to produce ATP, or in the absence of oxygen, it is converted to lactate [49].

Glycogenesis is the conversion of glucose into glycogen and is the main source of energy for skeletal muscle [50]. As hexokinase converts glucose into G6P, further reactions occur until insulin-dependent glycogen synthase converts uridine diphosphate glucose (UDPG) into glycogen [50]. Gluconeogenesis occurs in skeletal muscle, but glucose is not released to the circulation due to the absence of G6Pase, the enzyme required for the conversion of G6P to glucose; therefore, it can be catalyzed by muscle or used to rebuild glycogen stores [51].

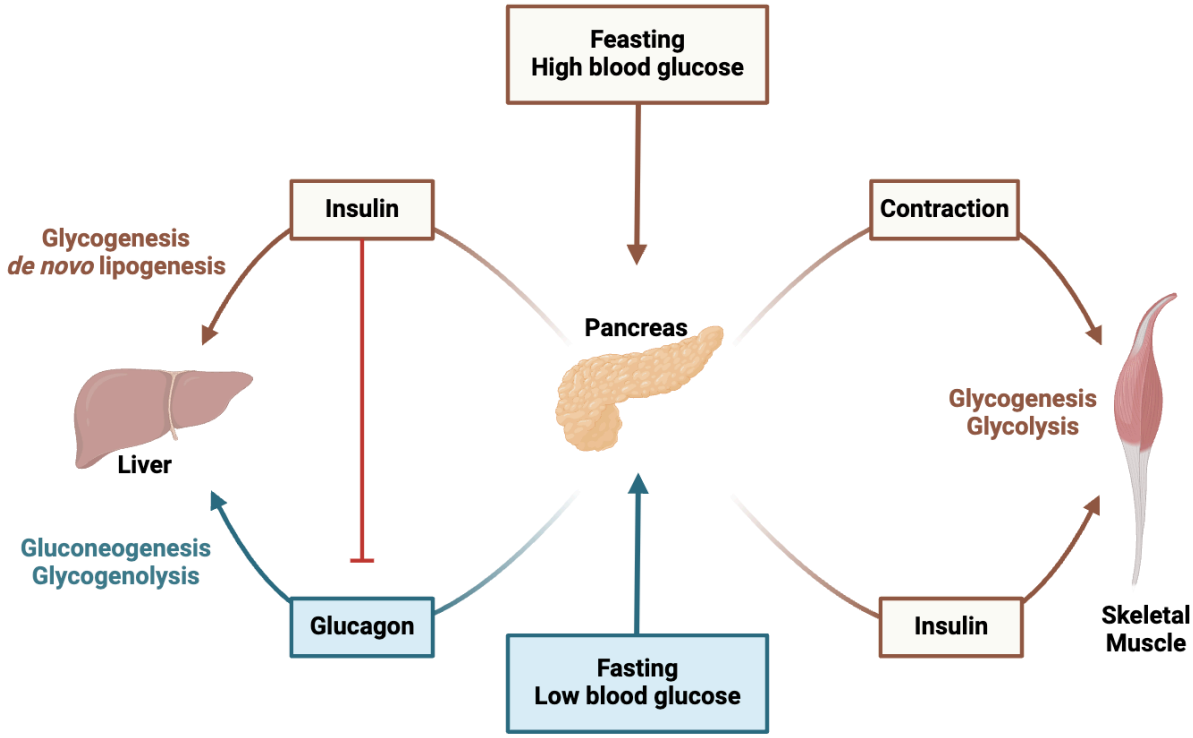

Figure 1.4. Summary figure of glucose homeostasis and metabolism in the liver and skeletal muscle. Created by EB with Biorender.com.

1.3.4 Pathophysiology of glucose metabolism in T2D & MASLD

In T2D and MASLD, glucose metabolism is dysregulated in both the liver and skeletal muscle. As briefly mentioned in the previous section, nutritional excess resulting in adipose tissue expansion, hyperglycemia, and hyperlipidemia can initiate the transition between healthy physiology and pathophysiology [37]. Reduced insulin sensitivity triggers β-cell hypersecretion of insulin to maintain normoglycemia through hyperinsulinemia [35]. However, chronic hyperfunction of pancreatic β-cells causes fatigue and dysfunction, leading to insulin deficiency and hyperglycemia. IR and β-cell dysfunction pose a conflicting argument within the literature in terms of what arises first. One perspective is that IR is primary resulting in hyperinsulinemia due

to diet-induced disruption of integral peripheral tissues such as the liver and skeletal muscle [52]. The opposing viewpoint is that hyperinsulinemia is primary resulting in the downregulation of insulin pathways in peripheral tissues, resulting in IR [52]. However, physiological changes do not occur in isolation, suggesting that both perspectives may be valid and occurring simultaneously, resulting in the overall presentation of hyperglycemia, dyslipidemia, and IR.

Hepatic IR results in impaired inhibition of gluconeogenesis, either indirectly or directly. Indirectly, IR promotes lipolysis in white adipose tissue (WAT), and increased NEFA and glycerol content in the circulation, which are taken up by the liver to act as substrates for lipogenesis and gluconeogenesis [53]. Peripheral IR in the skeletal muscle impairs glucose uptake resulting in enhanced hepatic glucose uptake and DNL. Directly, IR impairs the inhibition of gluconeogenesis, exacerbating the production of glucose and hyperglycemia. Insulin inhibits hepatic gluconeogenesis by binding to its receptor, subsequently phosphorylating Akt, which inhibits forkhead box O1 (FOXO1) from entering the nucleus, reducing transcription and activation of PEPCK and G6Pase [53].

In T2D and MASLD, the IRS/PI3K/Akt/AS160 insulin-dependent pathway (described in section 1.3.4) is disrupted due to IR, attenuating the translocation of GLUT4 to the plasma membrane and glucose influx into the myocytes [45]. Hepatic steatosis has been significantly linked with reduced Matsuda index 72 of 72 Japanese patients diagnosed with MASLD, suggesting a central role of peripheral resistance and skeletal muscle IR [54]. In diabetic rats, expression of *Irs-1, Akt,* and *Glut4* are significantly reduced [55], and decreasing human myotubular IRS-1 or Akt2 using gene silencing impairs insulin-stimulated glucose uptake [56]. A vicious cycle ensues, in which IR exacerbates hyperglycemia, leading to hyperinsulinemia, worsened IR, and progression of T2D and MASLD.

IR is associated with a whole host of complications. One main consequence of hyperglycemia is the production of reactive oxygen species (ROS) resulting in impaired cellular function, damage, and death [57]. Microvascular complications associated with IR include diabetic retinopathy, neuropathy, nephropathy, and amputation [58]. Macrovascular complications include cardiovascular disease, cerebrovascular disease, and peripheral artery disease. Intervention at a preclinical window prior to loss of control over glycemic parameters is imperative to prevent complications, reduced quality of life, and overall mortality.

1.3.5 Lipid homeostasis and pathophysiology

Approximately 35% of our daily average caloric intake comes from dietary fats, of which TG is the predominant form [59]. Dietary TG is first broken down by pancreatic lipases and absorbed through intestinal enterocytes before being re-esterified into TG. Uptake of dietary fats occurs either through transport proteins or through passive diffusion through the apical membrane [60]. Once inside, dietary TG and other fats can be packaged into chylomicrons or stored as cytosolic LD for fatty acid oxidation. TG are packaged into chylomicrons by microsomal triglyceride transport protein (MTP) and apolipoprotein B (apoB). Chylomicrons are TG-rich lipoproteins that have a phospholipid monolayer surface and a lipid-rich core [61]. The chylomicrons exit the enterocyte into the lymphatic system in a controlled manner to prevent excess secretion and enter the systemic circulation through the thoracic duct. Lipoprotein lipases (LPL) catalyze the hydrolysis of TG within chylomicrons, liberating FFA that are taken up by tissues for various metabolic and cellular pathways [59]. Lipids are also stored, produced, and released into the circulation by the liver through DNL and lipolysis. They can also be stored and released by adipose tissue; however, this thesis will not focus on the adipose tissue role. Lipid

homeostasis is a tight balance between absorption, production, utilization, and storage, of which the liver and skeletal muscle play integral roles.

1.3.6 Hepatic lipid metabolism: lipid uptake, DNL, oxidation, and lipolysis

There are four arms of liver lipid metabolism: FA uptake and DNL, which increase TG content of the liver, and FA oxidation and export, which decrease TG content in the liver and potentially enhance serum TG levels. These arms require tight regulation to maintain lipid homeostasis and when these arms become dysregulated, pathophysiology such as MASLD can occur.

FA uptake in the liver occurs when TG is hydrolyzed by LPL, producing glycerol and FA [62]. Non-esterified FA (NEFA) are taken up by the liver in three ways, either through FA transport proteins (FATP), CD36, or through simple diffusion. Once across the plasma membrane, NEFA is bound to FA binding proteins (FABP) or acyl-CoA synthetase (ACS) and activated to channel towards either storage or FA oxidation. TG synthesis occurs to store FA as TG and primarily uses the glycerol-3-phosphate (G3P) pathway [63]. First, FA is esterified to G3P by G3P acyltransferases (GPAT), then G3P undergoes multiple reactions to become phosphatidic acid (PA) by acylglycerol-3-phosphate acyltransferases (AGPAT). PA is converted to diacylglycerol (DAG) by lipin enzymes. DAG is then converted to TG by diacylglycerol acyltransferases (DGAT) then packaged into lipid droplets (LD) or very-low-density lipoproteins (VLDL) to be secreted into the circulation.

Via DNL, the liver has the capacity to generate FA from non-lipid substrates, notably carbohydrates [64]. As mentioned above (section 1.4.2), glucose can be converted to citrate through glycolysis and the citric acid cycle, acting as a substrate for ATP-citrate lyase to produce acetyl-CoA. ACC and FAS then catalyze the conversion of acetyl-CoA to palmitate. Insulin and

high-carbohydrate diets can regulate DNL, enhancing the expression of genes within the DNL pathway [65]. Excess TG produced enters the same fate as dietary TG, i.e., either stored as LD or packaged into VLDL molecules to be secreted into circulation.

VLDL molecules are assembled by the ER, requiring MTP and apoB proteins [63]. MTP is responsible for incorporating TG to apoB proteins in the ER lumen and packaging additional TG in the golgi apparatus. VLDL molecules are then secreted into the circulation. LD are also formed in the ER but are not dependent on MTP and apoB. The outer layer of LD is comprised of multiple proteins such as perilipins, Cidea, and microsomal fat-inducing transmembrane protein, and a phosphatidylcholine surfactant monolayer with a TG-rich core.

Lipolysis is the breakdown of TG into FA and is dependent on adipose triglyceride lipase (ATGL) [63]. TG is hydrolyzed by ATGL into DAG, which is hydrolyzed by hormone-sensitive lipase (HSL) into monoacylglycerol (MAG). Finally, monoacylglycerol lipase hydrolyzes MAG into FA and glycerol. FA can be converted to acyl-CoA by ACS and shuttled to undergo FA oxidation or esterified back into TG. β-oxidation of FA primarily occurs in the mitochondria but can also occur in peroxisomes. Carnitine palmitoyltransferase-1 (CPT-1) is the rate-limiting step of β-oxidation and is responsible for shuttling FA into the mitochondria [62]. Through β-oxidation, electrons are transferred to flavin-adenine dinucleotide (FAD) and nicotinamide-adenine dinucleotide (NAD^+), which then donate electrons to the electron transport chain (ETC) to produce ATP. Overall, the liver is a principal organ involved in lipid homeostasis, regulating lipid uptake, storage, oxidation, and export.

1.3.7 Skeletal muscle lipid metabolism: lipid uptake, storage, lipolysis, and oxidation

Skeletal muscle not only utilizes glucose as a fuel source but also uses FA and amino acids to sustain metabolic requirements. As in the liver, circulating FA enter myocytes via FATP and CD36, then are bound to FABP and FA transport proteins (FATP) [66]. Although muscle can readily utilize FA for energy, depending on the overall energy balance, substrate availability and energy requirements of the muscle, lipid storage in droplets may occur and this is called intermuscular adipose tissue or intramyocellular lipids (IMCL). TG synthesis is catalyzed by MAG acyltransferases (MGAT) and DAG acyltransferases (DGAT) [67]. In normal physiological conditions, IMCL is utilized for fuel during acute and chronic physical activity when circulating glucose is limited or glycogen is depleted.

Lipolysis in the skeletal muscle follows a similar pathway as in the liver with ATGL and HSL acting as the major enzymes responsible for TG hydrolysis [68], with the resulting FA available for oxidation. During prolonged exercise, and depending on the muscle type (i.e., slow-twitch vs fast-twitch), skeletal muscle relies more on FA oxidation [69]. However, in insulin-resistant states, IMCL may become elevated and contribute to worsening IR, with its attendant complications, as explained in earlier sections [70].

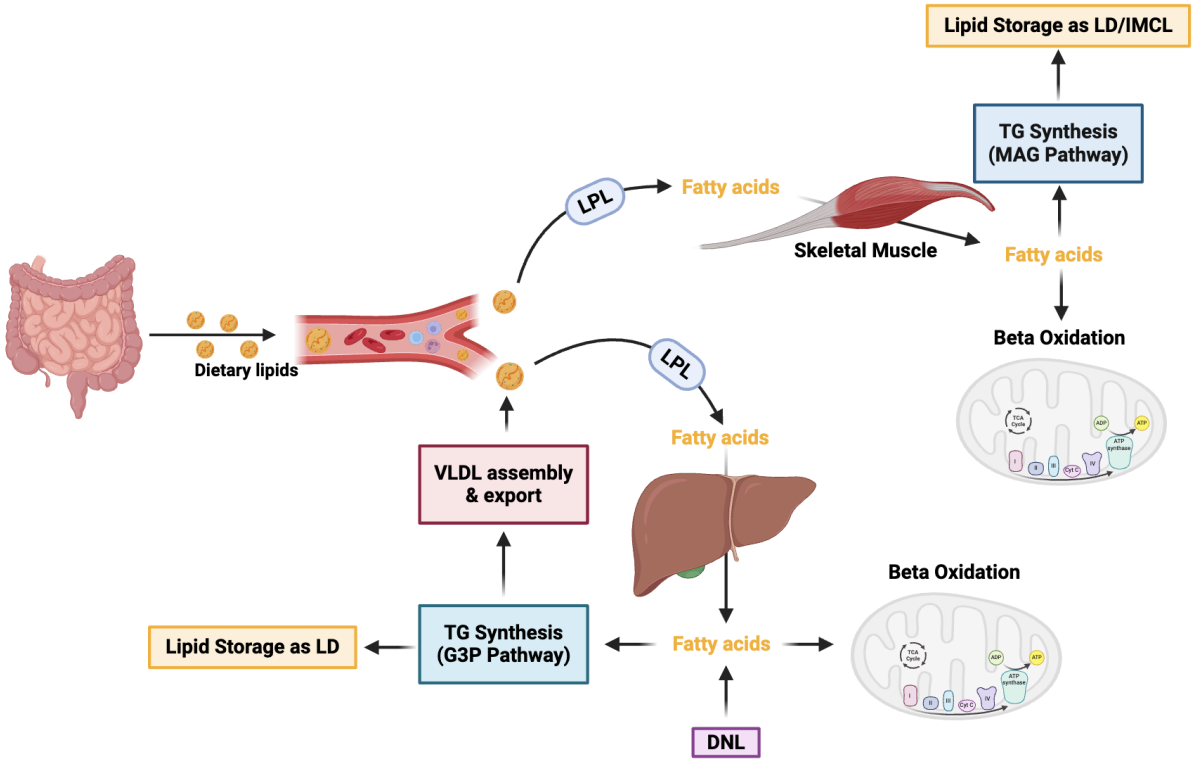

Figure 1.5. Summary of lipid homeostasis and metabolism in the liver and skeletal muscle. LPL, lipoprotein lipase; DNL, de novo lipogenesis; TG, triglyceride; G3P, glycerol-3-phosphate; LD, lipid droplets; VLDL, very low density lipoprotein; MAG, monoacylglycerol; IMCL, intramyocellular lipids. Created by EB with Biorender.com.

1.3.8 Pathophysiology of lipid metabolism in T2D & MASLD

Systemic lipid homeostasis is tightly regulated; however, in pathologic states like T2D and MASLD, this tight regulation is lost, resulting in dyslipidemia and lipotoxicity. MASLD results from the inability of the liver to utilize or export FA imported or produced by DNL. The pathophysiology of MASLD is complex, with the multi-hit hypothesis accounting for various components resulting in the initiation and progression of the disease.

The multi-hit hypothesis proposes that nutrition, genetics, organ cross talk, and inflammatory pathways all play a role in MASLD progression. Initially, excessive consumption of a westernized diet and genetic factors leads to the expansion of WAT past its capacity, resulting in WAT inflammation, IR, and enhanced lipolysis [71]. Resultant hyperlipidemia causes the liver to take up FA to normalize lipid concentrations. IR due to hyperglycemia and hyperlipidemia intensifies DNL, resulting in an increased load on the liver to utilize and handle. The microbiome also plays a role in worsening MASLD progression, with multiple microbial metabolites associated with MASLD progression and severity [72].

Enhanced DNL in IR in T2D and MASLD is contradictory to what is seen in knockout-induced hepatic IR [73]. In insulin receptor KO mice, hepatic gluconeogenesis is increased with a decrease in DNL as expected through normal physiological pathway inhibition [74]. However, the opposite is seen in T2D and MASLD models, suggesting induction of selective IR in the liver [55]. This may be caused by either enhanced substrate availability due to impaired lipolysis in WAT or altered brain-liver interactions where insulin signalling counteracts hyperglycemic signals in the brain, resulting in lipid production and accumulation [75].

Regardless, increased FA uptake and DNL results in hepatic TG accumulation, and the formation of toxic lipid species, increased mitochondrial biogenesis, and oxidative DNA damage [76]. There is also a reduction in FA export, denoted by a reduction in apoB and MTP abundance in individuals with MASLD [77]. Key genes have been associated with hepatic fibrosis, steatosis, and enhanced hepatic FA flux, playing an additive role, and promoting MASLD progression. Overall, there is a net accumulation of FA within the liver, exacerbating MASLD and metabolic dysfunction. Due to the complex nature of both MASLD and T2D, mitigation of

disease progression and early intervention are imperative to reducing disease burden and mortality.

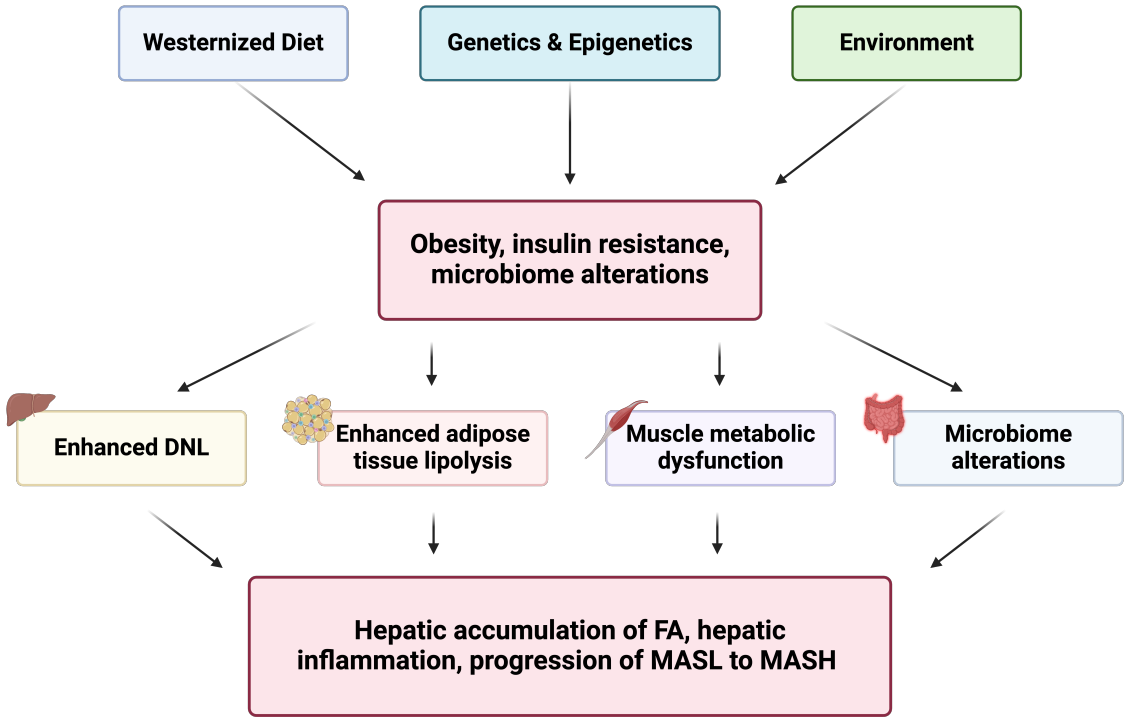

Figure 1.6. Overview of the multiple hit hypothesis for the progression of MASLD. DNL, de novo lipogenesis; FA, FA; MASL, metabolic dysfunction associated steatotic liver; MASH, metabolic dysfunction-associated steatohepatitis. Created by EB with Biorender.com.

1.4 Current modes of treatment

1.4.1 Pharmaceutical interventions

Pharmacological interventions for T2D can complement lifestyle interventions if A1C remains > 1.5% above the clinical target at the 3-month mark or can be administered at the time of diagnosis if individuals display symptoms of hyperglycemia or metabolic dysfunction [10]. Metformin is the first line of pharmacological treatment; however other drug categories

have shown efficacy in reaching clinical goals such as insulin, glucagon-like peptide-1 (GLP-1) receptor agonists, sodium-glucose co-transporter (SGLT2) inhibitors, dipeptidyl peptidase 4 (DPP-4) inhibitors, insulin secretagogues, or thiazolidinediones. The mechanism of action of these drugs varies; however, all are used to reach the clinical end goal of improved glycemic control. The out-of-pocket costs of pharmaceuticals in addition to the side-effect burden result in low adherence of patients to treatment protocols, compromising disease management [78], [79].

MASLD pharmacotherapies are currently underdeveloped with only one recently FDA-approved medication targeted to directly improve MASH and liver fibrosis [80]. However multiple drug types such as *de novo* lipogenesis inhibitors, GLP-1 agonists, SGLT-2 inhibitors, and PPAR agonists target the associated comorbidities, such as glycemic control and obesity, to improve clinical markers of MASLD [81]. Although, it is important to highlight that to treat with pharmaceuticals, patients must have reached clinical thresholds and diagnosis status, missing a critical intervention window to prevent disease initiation. For this reason, lifestyle interventions remain as the first line of treatment and management for early-stage T2D and MASLD.

1.4.2 Lifestyle interventions as a public health approach

Lifestyle interventions are the first line of treatment for MASLD and T2D with a goal of clinically relevant weight loss to improve hepatic steatosis and fibrosis [82]. Diet interventions such as the Mediterranean diet reduce visceral adipose tissue, hepatic fat content, and serum TG in an adult population [15]. Exercise interventions also demonstrate a reduction in liver steatosis and stiffness [13]. Adopting long-term lifestyle modifications such as consistent physical activity, limiting alcohol intake, and refraining from smoking reduces mortality and incident T2D risk [11]. An optimal activity dose of approximately 183 to 367 minutes per week of moderate-

intensity activity was calculated to reduce AIC levels [83]. Both high-intensity and low-intensity functional training are effective at reducing FBG, insulin, A1C, blood pressure and homeostatic model assessment for IR (HOMA-IR) in elderly T2D patients [12]. Low-energy diets alone have demonstrated efficacy in treating T2D, with reversal of the disease back to a healthy status within 12 months seen in 50% of patients in multiple studies [84], [85].

Multiple lifestyle intervention studies combining diet control and physical activity programs have significantly improved weight, glycemic control, and dyslipidemia over 2-4 years [16], [17]. The Look AHEAD (Action for Health in Diabetes) trial also assessed medication usage with fewer participants in the lifestyle intervention group requiring blood glucose or blood pressure medications after the trial [16]. These studies provide support for lifestyle interventions to manage metabolic disorders such as T2D and MASLD, however, they require life-long compliance and adherence, which can be challenging [86]. Thus, finding aspects of daily living that are easily accessible and adhered to, such as consuming well-liked foods as part of a usual diet, is critical to achieving lifelong management and prevention of metabolic disorders.

1.4.3 Dairy's role in metabolic health

Dairy as a functional food is globally consumed with over 94 national dietary guidelines recommending adequate consumption to reduce the global burden of metabolic disorders [87]. Previous research by our group sought to determine whether different types of dairy, such as cheese, yogurt, and milk, would affect glycemic control among other aspects of metabolic health. Supplementing HFD-induced obese C57BL/6 mice with a low dose (less than one serving equivalent) of WFM, yogurt or cheese demonstrated significant reductions in serum TG and

hepatic steatosis, specifically within the milk group [19]. This suggests that dairy milk may confer protective effects to hepatic lipid metabolism under the strain of HFD.

1.4.4 Dairy milk impacts from human and animal models

Dairy milk consumption and its impacts on metabolic health have been explored in animal and human studies, demonstrating an overall beneficial effect and mitigation of cardiometabolic disease risk. In a recent meta-analysis of observational studies, milk consumption was inversely related to MASLD occurrence, with a greater overall consumption reducing risk by 10% [88]. Total dairy consumption and low-fat milk consumption were associated with 15% and 41% lower risk of T2D respectively in adult participants [89]. Milk consumption has also been noted to reduce the overall risk of MetS, with 200 g/day (< 1 serving) associated with a 15% reduction in the incidence of MetS [90]. In adult participants enrolled in a randomized control trial (RCT), 6 weeks of low-fat dairy supplementation significantly reduced ALT, AST, hepatic steatosis index scores, and inflammatory cytokine expression [91]. Similar effects were seen in adolescents as dairy fat intake, marked by plasma C15:0 and C17:0 FA, was inversely related to hepatic steatosis [92]. In a multinational cohort study, increased consumption of whole-fat dairy was associated with a lower incidence of diabetes and hypertension and a lower prevalence of MetS [93]. However, in a RCT of 111 patients with T2D, increasing consumption of low- and whole-fat dairy did not affect HbA1c, BW, BP, or lipid profile [94]. This was suggested to be due to the advanced disease status of these patients while previous studies were looking into a prediabetes window of intervention, highlighting the importance of lifestyle interventions prior to disease progression.

Animal models demonstrate similar effects of dairy intake on metabolic parameters. C57BL/6 mice supplemented with phospholipid-rich dairy milk had reduced liver weight, TG, cholesterol, and serum lipids compared to controls [95]. Supplementation with calcium-fortified dairy milk in aP2-agouti transgenic mice reduced weight gain and increased expression of uncoupling protein (UCP) 3 and peroxisome proliferator-activated receptor-α (PPARα) in skeletal muscle [96]. In C57BL/6 male mice, 17-week supplementation with WFM (3%) or low-fat (1%, LFM) milk resulted in opposing effects [97]. WFM had greater BW gain, higher serum cholesterol, TG, and glucagon, and reduced abundance of Akt, p-Akt, and AMPK in the liver and WAT compared to chow-fed animals. Whereas LFM had unchanged lipid profiles, stable BW, and higher abundance of Akt, p-AKT, and p-AMPK than the HFD group. This may suggest that different nutritional components of milk have distinct effects on metabolism, as dairy milk contains multiple bioactive components that have different effects documented in the literature.

1.4.5 Dairy milk matrix, bioactive components, and metabolic health

Foods consist of multiple nutrients that are bound together in a complex structure called the food matrix, which determines the nutrients' digestion and absorption thereby controlling the overall metabolic effect [98]. Thus, food matrices may confer altered effects when compared to supplementation of their isolated nutrients. The dairy milk matrix is composed of macronutrients such as fat, protein and carbohydrates, and micronutrients such as vitamins, minerals and other bioactive molecules that may all exert effects on metabolism, growth, inflammation, and disease states [99]. Isolated and purified macro- and micronutrients range from triple to quadruple the cost of simple milk products, with similar to lesser effects [100]. This section will describe

various bioactive components of milk with a central focus on the additive effect of molecules within the dairy matrix rather than the effect of these components in isolation.

Whey and casein are the two major proteins in dairy products and have demonstrated efficacy in mitigating hepatic steatosis, obesity, and atherosclerosis in Sprague-Dawley rats and LDLr-/- Leiden mice [101], [102]. In apoE$^{-/-}$ mice, whey protein hydrolysate reduced serum and liver lipids, and alleviated hepatic steatosis, inflammation, and oxidative stress compared to controls [103]. Casein supplementation in C57BL/6 mice reduced BW gain, FBG, liver weight, and hepatic lipid accumulation [104].

Dairy milk lipids can play a role in regulating inflammation, lipid metabolism, and gastrointestinal (GI) integrity [105]. Supplementation with dairy milk gangliosides and phospholipids reduced liver mass, mesenteric adipose tissue, and hepatic lipid accumulation in C57BL/6 *ob/ob* mice. Milk fat globule membrane (MFGM) is comprised of phospholipids, polar lipids, and proteins that have bioactive properties. Supplementation of MFGM for 8 weeks in HFD and streptozotocin-induced T2D C57BL/6 mice reduced FBG, serum lipids, hepatic steatosis, and enhanced insulin sensitivity as evidenced by improved ITT and OGTT, and higher abundance of p-Akt and p-PI3K in both the liver and skeletal muscle [106]. Similar results were seen in a human RCT where 8 weeks of MFGM supplementation reduced total cholesterol, LDL cholesterol, apoB, and non-HDL cholesterol compared to diets without MFGM [107]. Individual FA such as pentadecanoic acid (C15:0), heptadecanoic acid (C17:0), and *trans*-11 vaccenic acid (VA, 18:1, n-7) also display efficacy in reducing metabolic dysfunction. In T2D male Sprague Dawley rats, VA supplementation in a diet containing butter oil as the dairy background improved insulin secretion denoted by a higher glucose infusion rate in a hyperglycemic clamp [108]. In C2C12 myotubes, *in vitro* application of pentadecanoic acid promoted GLUT4

translocation, glucose uptake, and increased phosphorylation of AS160 and AMPK, enhancing insulin sensitivity [109].

Micronutrients in milk such as choline, calcium and vitamin A also mitigate hepatic steatosis and metabolic dysfunction. Choline, which is vital for the synthesis of cell membranes and neurotransmission, is associated with MASLD, with higher intake associated with lower incidence risk [110], [111]. Choline may prevent hepatic lipid accumulation, because choline-deficient bovine hepatic cells display significantly larger LD, hepatocyte TG content, and FAS [112]. Other studies demonstrate normalization of HFD-induced weight gain in a mouse model and enhanced FA oxidation with choline supplementation *in vitro* [113], [114]. Calcium is another potential nutrient that is rich in milk and is involved in endoplasmic reticulum (ER) stress, and mitochondrial dysfunction in cells [115]. Calcium enhances the activity of Complex I and IV *in vitro* to facilitate oxidative phosphorylation [116]. Vitamin A, or the active form retinoic acid (RA), is integral in hepatic lipid metabolism with strong associations with MASLD progression [117]. Retinoic acid receptor agonist administration to HFD-induced T2D, *ob/ob*, and *db/db* mice reduced hyperglycemia, BW, hepatic steatosis, and expression of lipogenesis genes [118]. Human hepatoma HepG2 cells administered all-*trans* RA upregulated carnitine palmitoyl transferase-1 (CPT-1), enhancing cellular oxidation and FA catabolism [119].

Although the above studies remarked on the beneficial effects of these molecules in isolation, other studies were unable to replicate the same benefits or instead found opposing effects with an increase in hepatotoxicity and inflammatory biomarkers seen in male Wistar rats with long-term whey supplementation, and complete dairy supplementation improving BW and HOMA-IR in Sprague-Dawley rats compared to whey and casein supplementation alone [100], [120]. The additive effects of each bioactive molecule and nutrient within the dairy matrix may

potentiate the overall metabolic benefits conferred by dairy consumption. Currently, no study exists that compares the effects of NFM and WFM supplementation in a preclinical window to mitigate the initiation of metabolic dysfunction. The mechanism of action is also unknown, highlighting the gap this project aims to fill.

Chapter 2: Hypothesis and objectives

2.1 Hypothesis

Based on data from the above literature review in combination with previous research completed in our lab, I hypothesize that (1) both NFM and WFM will significantly reduce diet-induced hepatic lipid accumulation and prevent the initiation of early-stage MASLD in obese, male C57BL/6 mice but via different mechanisms and that (2) increased capacity for substrate uptake and metabolism in skeletal muscle may act as a mediator of reduced hepatic steatosis.

2.2 Overall aims

The overall aims of this thesis are to compare the effects of a daily dose of NFM and WFM provided to male mice fed a HFD on:

1) the metabolic phenotype including body composition, blood glucose and hepatic lipid profiles;

2) liver lipid accumulation and its regulation by lipid metabolism pathways and

3) insulin-dependent and -independent pathways regulating skeletal muscle glucose uptake and metabolism.

2.3 Specific objectives

The specific objectives of this thesis include:

1. To characterize the model of metabolic dysfunction used in this thesis

a) To characterize the metabolic phenotype of LFD versus HFD fed mice

b) To quantify the effects of LFD versus HFD on hepatic morphology and lipid accumulation

c) To identify changes in serum and hepatic lipid profiles of LFD versus HFD

d) To compare key proteins involved in lipid metabolism between LFD versus HFD

To complete objective one, an *in vivo* study was conducted using C57BL/6 mice as outlined in Figure 2.1. Outcomes examined in objective 1a included BW changes, lean to fat mass ratios, insulin sensitivity, and pyruvate tolerance. For objective 1b, histological analysis of liver tissue was completed with the key outcomes of LD number, hepatic fat accumulation, and LD size. For 1c, measurement of serum non-esterified FA, liver TG, and cholesterol were completed in addition to gas chromatography of extracted liver tissue to further characterize the hepatic lipid profile. For 1d, expression of genes involved in hepatic lipid metabolism and mitochondrial function were identified via qPCR. Protein abundance was then assessed by western blotting for the key proteins within FA uptake, *de novo* lipogenesis, FA oxidation, and FA export. Chapter 4 outlines the results of objective one.

2. To compare the effects of a low dose (less than one serving equivalent/day) of NFM and WFM on hepatosteatosis caused by HFD

a) To compare the metabolic phenotype of NFM versus WFM-supplemented mice

b) To quantify the effects of NFM versus WFM on hepatic morphology and lipid accumulation

c) To identify changes in serum and hepatic lipid profiles of supplemented mice

Similar methods were used to complete objective two as were used in objective one. An *in vivo* study was conducted using C57BL/6 mice as outlined in Figure 2.1. Outcomes examined

in objective 2a included BW changes, lean to fat mass ratios, insulin sensitivity, and pyruvate tolerance. For objective 2b, histological analysis of liver tissue was completed with the key outcomes of LD number, hepatic fat accumulation, and LD size. For 2c, measurement of serum non-esterified FA, liver TG, and cholesterol were completed in addition to gas chromatography of extracted liver tissue to further characterize the hepatic lipid profile. Chapter 5 outlines the results of objective two.

3. To identify and compare regulation of hepatic lipid metabolic pathway(s) by NFM and WFM

To complete objective 3, the expression of genes involved in hepatic lipid metabolism and mitochondrial function were identified via qPCR. Protein abundance was then assessed by western blotting for the key proteins within FA uptake, *de novo* lipogenesis, FA oxidation, and FA export. Chapter 6 outlines the results of objective three.

4. To measure abundance and activation of key enzymes regulating insulin-dependent and -independent uptake of substrates in skeletal muscle.

To complete objective four, protein abundance was assessed by western blotting for the key proteins, including Akt, AMPKα, CPT1α, PGC1α, CD36, and SIRT1. Chapter 7 outlines the results of objective three.

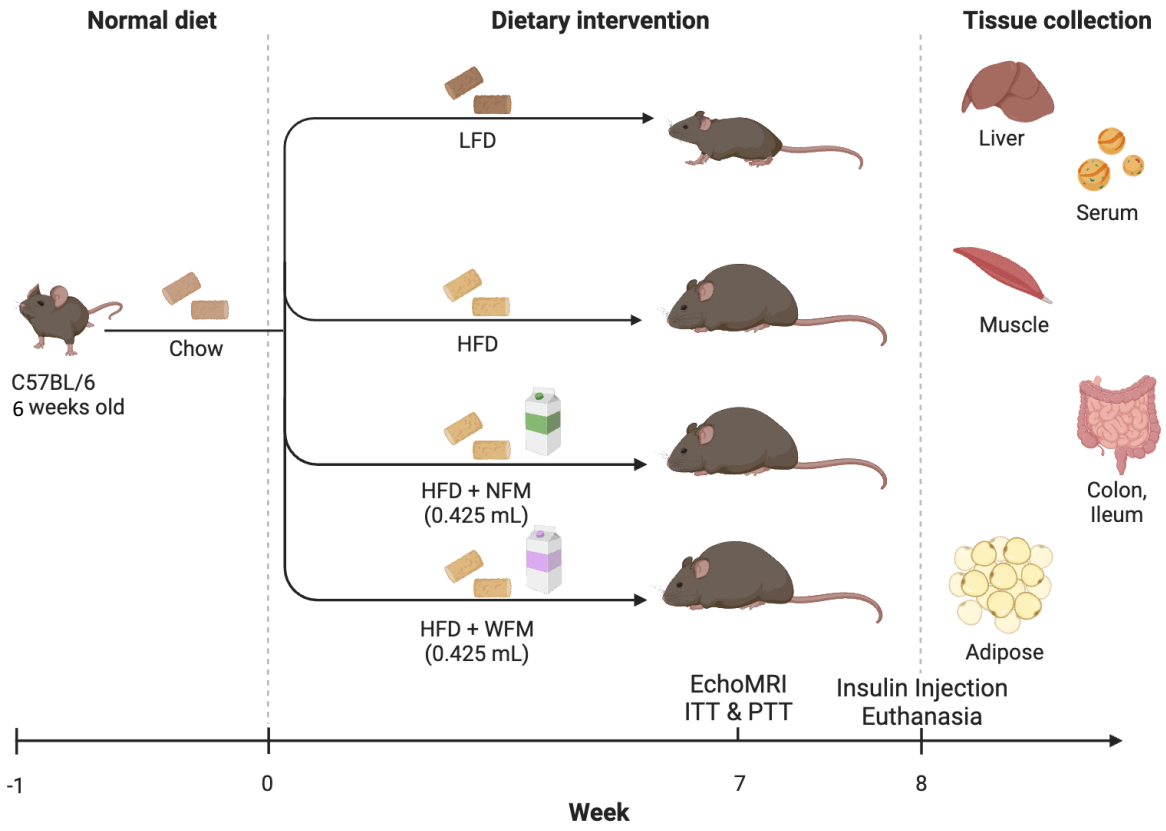

Figure 2.1. Summary of animal and diet protocol. Abbreviations: LFD, low-fat diet; HFD, high-fat diet; NFM, non-fat milk; WFM, whole-fat milk; ITT, insulin tolerance test; PTT, pyruvate tolerance test. Created by EB with biorender.com.

Chapter 3: Methods

3.1 Animal Protocol

This protocol and some results were previously published by our group [19] and approved by the Health Sciences Animal Care and Use Committee at the University of Alberta. Briefly, two cohorts of 6-week-old C57BL/6 male mice were acclimatized for 1-week post-arrival and were housed in a room with a reverse light cycle for the duration of the trial to facilitate milk feeding. Cohort one was designated for NFM (n = 24) and cohort two for WFM (n = 36). Following the acclimatization, a third of cohort one (n = 8) and cohort two (n = 12) consumed LFD ad libitum and two-thirds (n = 16; n = 24) consumed a HFD ad libitum for 1 week. The HFD mice in cohorts one and two (n = 16; n = 24) were then randomized to consume either NFM (n = 8) or WFM (n = 12) or remain on HFD (n = 20). A summary of the diet assignments is provided in Figure 3.1. At week 7, the mice were randomized (within their diet groups) to undergo either an insulin tolerance test (ITT) or a pyruvate tolerance test (PTT). At week 8, the mice underwent an overnight fast and ten minutes prior to euthanasia, half were injected intraperitoneally with 0.37 IU/kg BW of insulin in saline (n = 30). Only male mice were used in this study, but it is important to state that a group of female mice were included in cohort two (WFM). These female mice (n = 40) displayed no signs of IR or metabolic dysfunction providing the reasoning for utilizing only male mice in this study [19]. A summary of the animal and diet protocol is provided in Figure 2.1.

3.2 Diet

The mice were randomly distributed into four diet groups as follows:

1. HFD control with 45 kcal% fat
2. LFD control with 10 kcal% fat
3. HFD + Whole-fat Milk (3.25 g% fat)
4. HFD + Non-fat Milk (0 g% fat)

The HFD and LFD control groups were provided with half of a plain Cheerio daily to control for handling stress, which affects blood glucose. Diet composition was published by our group previously [19] and is summarized in Table 3.1. WFM and NFM were administered at 0.425 mL on five out of seven days in a separate dish from the pelleted diet. Food was removed for two hours at the end of the light cycle and all animals were placed in clean cages, separated into four individual compartments, and provided either half a Cheerio in the LFD and HFD groups or the supplemented milk in the WFM and NFM groups. The individual compartments ensured that each mouse received the appropriate dosage, and the restriction of food for two hours enhanced the likelihood that novel foods would be ingested. Animals in the WFM and NFM groups were trained to drink milk from a small bowl and given two hours to consume their milk prior to returning to their home cage, which was replenished with the appropriate diet. The dairy dosage used in this study was to determine whether a minimal amount of dairy added to the diet is enough to cause significant alterations to overall metabolic health as a part of total calorie intake. The dosage of milk in this study equated to 2% of the total calorie intake by our mice. The nutritional characteristics of WFM and NFM are reported in Table 3.2 and 3.3. Food intake was measured weekly for cohort 1 and for cohort 2 was measured over 24 hours three times during week 7 of the study.

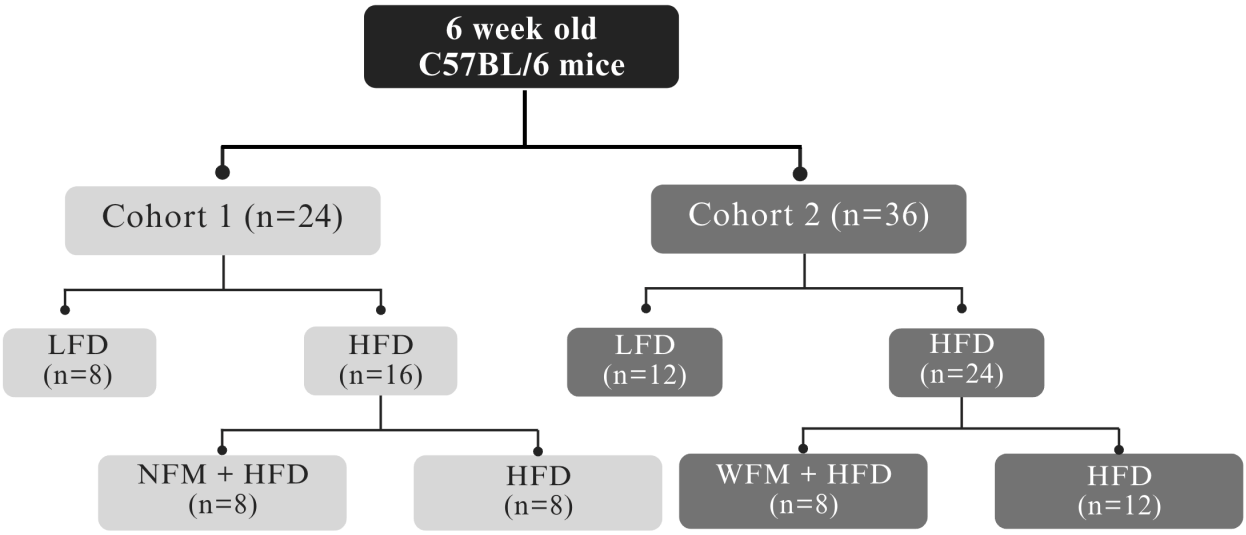

Figure 3.1. Summary of diet assignments. Abbreviations: LFD, low-fat diet; HFD, high-fat diet; NFM, non-fat milk; WFM, whole-fat milk.

Table 3.1. Nutritional composition of control diets

	HFD (D12451)	**LFD (D12450B)**
Macronutrients	Kcal (%)	Kcal (%)
Protein	20	20
Carbohydrate	35	70
Fat	45	10
Total Kcal/g	**4.73**	**3.85**
Ingredients		
Casein (g)	200	200
L-Cystine (g)	3	3
Corn Starch (g)	72.8	452.2
Maltodextrin 10 (g)	100	75
Sucrose (g)	172.8	172.8
Cellulose, BW200 (g)	50	50
Soybean Oil (g)	25	25
Lard (g)	177.5	20
Mineral Mix S10026 (g)	10	10
Dicalcium Phosphate (g)	13	13
Calcium Carbonate (g)	5.5	5.5
Potassium Citrate, 1 H2O (g)	16.5	16.5
Vitamin Mix V10001 (g)	10	10
Choline Bitartrate (g)	2	2
FD&C Red Dye #40 (g)	0.05	0.01
FD&C Yellow Dye #40 (g)	0	0.04
Total (g)	**858.15**	**1055.05**

Diet composition adapted and taken from Research Diets Inc., 2006.

Table 3.2. Nutritional composition of milk servings.

	WFM	SERVING GIVEN TO MICE	NFM	SERVING GIVEN TO MICE
MEASURE (ML)	250	**0.425**	250	**0.425**
WEIGHT (G)	249	**0.42**	246	**0.42**
ENERGY (KCAL)	152	**0.26**	83.6	**0.14**
PROTEIN (MG)	8140	**13.8**	8440	**14.4**
CARBOHYDRATE (MG)	11500	**19.6**	12100	**20.6**
TOTAL SUGAR (MG)	12000	**20.4**	12400	**21.1**
TOTAL FAT (MG)	7970	**13.6**	197	**0.33**
SATURATED FAT (MG)	4808	**7.87**	121	**0.21**
CALCIUM (MG)	306	**0.52**	325	**0.55**
AVERAGE CHOLINE (MG)	36.9	**0.06**	44.8	**0.08**
IRON (MG)	0.08	**0.00**	0.00	**0.00**
POTASSIUM (MG)	374	**0.64**	411	**0.70**
MAGNESIUM (MG)	29.6	**0.05**	30.8	**0.05**
PHOSPHOROUS (MG)	251	**0.43**	263	**0.45**
VITAMIN A (RAE)	79.7	**0.14**	157	**0.27**
VITAMIN D (MCG)	2.39	**0.00**	2.71	**0.00**
FOLATE (DFE)	0.00	**0.00**	4.92	**0.01**
VITAMIN B12 (MCG)	1.34	**0.00**	1.43	**0.00**
RIBOFLAVIN (MG)	0.34	**0.00**	0.32	**0.00**

Abbreviations: mg, milligram; mcg, microgram; RAE, rational activity equivalent; DFE, dietary folate equivalent. Nutrient composition is taken from the USDA FoodData Central, 2019; WFM (FDC ID 746782), NFM (FDC ID 746776).

Table 3.3. Energy contributed by macronutrients in each diet group.

	LFD (D12450B)	**HFD (D12451)**	**HFD + WFM (3.25%)**	**HFD + NFM (0%)**
Macronutrients	Kcal (%)	Kcal (%)	Kcal (%)	Kcal (%)
Protein	20	20	20.01	20.02
Carbohydrate	70	35	34.07	34.08
Fat	10	45	44.93	44.92
Total Kcal / day	**11.55**	**14.19**	**14.45**	**14.33**

Abbreviations: LFD, low-fat diet; HFD, high-fat diet; WFM, whole-fat milk (3.25%); NFM, non-fat milk (0%). Calculated assuming an average of 3g of chow per day for each diet group.

3.3 Insulin tolerance test (ITT), pyruvate tolerance test (PTT), and fasting glucose

At week 7, ITT and PTT were performed [121] after a four-hour fast and overnight fast respectively. Blood glucose was measured from a tail vein sample using a glucometer (Contour Next, Bayer, Leverkusen, Germany) at time zero for both tests. For ITT, human insulin (Sigma Aldrich, St. Louis, MO, United States) was first diluted with saline, then a dose of 0.75 IU/kg BW was intraperitoneally injected. For PTT, 2 g/kg of sodium pyruvate was injected intraperitoneally. Blood glucose was measured at 15, 30, 60, 90 and 120 minutes for both tests. Fasting glucose and ITT were used to interpret IR in the mice whereas PTT was used to measure hepatic gluconeogenesis [122].

3.4 BW, body composition, and tissue collection

Mice were weighed weekly with body composition measured at week 7 in fasted animals using ECHO magnetic resonance imaging (ECHO MRI) as per the standard manufacturer's protocol. Adipose tissue, lean tissue, free water, and total water were measured. At the end of week 8, all animals were fasted overnight, and half were injected with saline-diluted insulin (0.37 IU/kg BW) ten minutes prior to euthanasia. Animals were euthanized using CO_2 and 500-1000 mL blood was collected using cardiac puncture, then centrifuged for ten minutes at 4000 RPM to separate the serum. Liver, skeletal muscle, epididymal adipose, brown adipose tissue, ileum, and colon were collected. Samples of liver, epididymal adipose, and colon were prepared for histological analysis and fixed in phosphate-buffered formalin. The remaining tissues were snap-frozen in liquid nitrogen and stored at -80 °C until further analysis.

3.5 Histological analysis

Paraffin blocks of the liver were cut into 5 mm sections and fixed to glass slides. Slides were stained using the hematoxylin and eosin (H&E) protocol previously published by our group [123]. Four random photomicroscopic images of each slide (one slide per animal) were captured using a Zeiss AxioCam HR microscope 20x objective lens connected to a Canon Power Shot camera. Per group, six animals were used, with 96 images analyzed. Each image was quartered, and the top left quadrant was analyzed. ImageJ software, specifically the "freehand selections" tool, was used to quantify LD area and the total number of LDs.

3.6 Liver TG, cholesterol, and serum NEFA assays

Liver lipids were extracted using an adapted Folch extraction protocol using approximately 100 mg of tissue [124]. Tissue was homogenized in 1 mL of 1M NaCl solution and 1 mm glass beads. A total of 500 mL of the extract was mixed with 2 mL of Folch solution (2:1 chloroform: methanol), centrifuged at 3500 rpm for ten minutes and the lower phases collected into another 1.5 mL glass tube. While the lower phase was dried under nitrogen, 1 mL of Folch solution was added to the upper phase, vortexed, and spun at 3000 rpm for ten minutes. The lower phase was added to the lower phase tube, dried, resuspended with 1 mL of 2% Triton X-100 solution in chloroform, and dried again. The dried sample was then resuspended in ddH_2O and kept at -40 °C until assays were completed. TG and cholesterol content were measured using commercial kits (Infinity™, Thermo Scientific, Waltham, MA, USA). NEFA content was measured within the serum using a commercial kit (Wako Pure Chemical Industries LTD., Chuo-ku, Osaka, Japan), following the manufacturer's protocol.

3.8 Gas chromatography (GC) of liver extracts

Liver lipids were extracted using an adapted Folch protocol using approximately 100 mg of liver tissue [125], [126]. Tissue was homogenized in 1 mL KCl using 1mm glass beads in a tissue homogenizer, after which 950 mL of the extract was transferred to a glass tube, 1 mL of KCl and 8 mL of 2:1 chloroform:methanol was added, and tubes were vortexed and left to stand at 4 °C overnight. The following day, tubes were centrifuged at 1500 rpm for five minutes and the lower phase was transferred to a new tube and dried under nitrogen gas in a warming plate at 55 °C. The dried sample was resuspended in hexane and aliquoted for isolation on thin-layer chromatography on G plates. Silica plates were baked at 55 °C for an hour prior to scoring and spotting. Previously prepared aliquots were spotted on plates (eight samples per plate) and developed for 30 minutes. Plates were removed when the developing solution was one inch from the top of the plate and dried before being sprayed with ANSA spray. UV light was used to visualize triglycerides and phospholipid bands, scored around, and removed into 8 mL tubes. The tubes were then methylated by adding 1.5 mL BF_3 and 1.5 mL Hexane to the tubes and boiled at 110 °C for one hour. Tubes were cooled for five minutes, 1 mL of dd H_2O added, and put in the cold room at 4 °C overnight. The following morning, tubes were spun at 1500 rpm for five minutes and the upper phase was removed and dried under nitrogen, then resuspended in 300 mL hexane. FA were separated using automated GC and quantified as relative percent of total lipid and total phospholipid FA content.

3.9 Protein extraction and western blot

Total protein from liver and skeletal muscle was extracted using a lysis buffer (50 mM Tris HCL pH:8.0, 150 mM NaCl, 0.1% Triton X-100, 0.5% sodium deoxycholate, 0.1% SDS)

supplemented with protease and phosphatase inhibitors (2 mg/mL aprotinin (Calbiochem), 5 mM sodium fluoride, 5 mM sodium orthovanadate, and protease inhibitor cocktail (FastPrep® - 24, MP Biomedicals). Total protein content was measured using the modified Lowry protein assay protocol. Bovine serum albumin was used as a protein standard with 200 mL of Lowry reagent (Sigma, St. Louis, MO, United States) added, incubated for ten minutes, followed by 20 mL Folin & Ciocalteu Phenol Reagent 2.0 N (Thermo Scientific, Waltham, MA, United States) diluted with ddH_2O, and incubated for 30 minutes. Absorbance of 750 nm was measured using a spectrophotometer and concentrations was interpolated in GraphPad Prism 7.0 (GraphPad Software Inc., CA, United States). For immunoblotting, protein samples were diluted into a final concentration of 2 mg/mL with a lysis buffer and SDS loading buffer, boiled depending on protein sensitivity at 100 °C for five minutes. Samples were stored at -80 °C. Thawed samples were loaded and separated using an SDS-PAGE 8, 10, or 12% polyacrylamide gel, transferred to nitrocellulose membranes, and incubated overnight at 4 °C. Membranes were either incubated with fluorescent (Li-cor Biosciences) or peroxidase-coupled secondary antibodies for one hour at room temperature and then imaged using Li-cor scanners or placed in SuperSignal™ chemiluminescent substrate (Thermo Fisher Scientific) and imaged with a Bio-Rad ChemiDoc MP imaging system respectively. Images were analyzed using ImageJ software [127]. Total proteins were normalized to β-actin and phosphorylated proteins were normalized to their respective total protein and then expressed as a fold change (FC) of HFD. A summary of antibodies used can be found in Table 3.4.

Table 3.4. Antibody summary table.

ANTIBODY	COMPANY & CATALOGUE NUMBER	DILUTION
ACETYL-CoA CARBOXYLASE (ACC)	Cell Signalling - CS3676	1:1000
PHOSPHORYLATED ACC (P-ACC) (SER79)	Cell Signalling - CS11818	1:1000
AMP-ACTIVATED PROTEIN KINASE α (AMPKα)	Cell Signalling - CS2603s	1:1000
PHOSPHORYLATED AMPKα (P-AMPKα) (THR172)	Cell Signalling - CS2531s	1:1000
AMPKβ	Cell Signalling - CS12063	1:1000
p-AMPKβ (SER108)	Cell Signalling - CS23021	1:1000
ATP-CITRATE LYASE (ACL)	Cell Signalling - CS4332	1:1000
PHOSPHORYLATED ACL (P-ACL) (SER455)	Cell Signalling - CS4331	1:1000
ACYL COA SYNTHASE (ACS)	Cell Signalling - CS9189	1:1000
AKT	Cell Signalling - CS48272s	1:1000
P-AKT (SER473)	Cell Signalling - CS4060s	1:1000
ADIPOSE TRIGLYCERIDE LIPASE (ATGL)	Cell Signalling - CS2439	1:1000
CARNITINE PALMITOYL TRANSFERASE 1α (CPT1α)	Cell Signalling - CS97361	1:1000
FATTY ACID BINDING PROTEIN 4 (FABP4)	Cell Signalling - CS2120	1:1000
FATTY ACID SYNTHASE (FAS)	Cell Signalling - CS3180	1:1000
HORMONE SENSITIVE LIPASE (HSL)	Cell Signalling - CS4107s	1:1000
PHOSPHORYLATED HSL (P-HSL) (SER660)	Cell Signalling - CS4126	1:1000
MICROSOMAL TRIGLYCERIDE TRANSFER PROTEIN (MTP)	Santa Cruz - SC515742	1:500
CD36	Santa Cruz - SC7309	1:500
OXIDATIVE PHOSPHORYLATION COMPLEXES I-V (OXPHOS)	Abcam - Ab110413	1:1000
PROLIFERATOR-ACTIVATED RECEPTORS α (PPARα)	Santa Cruz - SC398394	1:500
PPARγ	Cell Signalling - CS2435	1:1000

PEROXISOME PROLIFERATOR ACTIVATED RECEPTOR-GAMMA COACTIVATOR (PGC1α)	Santa Cruz - SC518025	1:500
SIRTUIN 1 (SIRT1)	Cell Signaling – CS2310	1:1000
ANTI-MOUSE IGG	Sigma Aldrich - A9169	1:4000
ANTI-RABBIT IGG	Sigma Aldrich - A9169	1:4000
BETA-ACTIN (β-ACTIN)	Sigma Aldrich - A5441	1:2000

3.10 Liver RNA extraction and quantitative PCR (qPCR)

RNA extraction was performed using the QIAGEN RNeasy mini plus kit following the manufacturer's instructions with the following modifications. Approximately 100 mg of liver tissue was homogenized with 1 mL of TRIzol, rested for five minutes at room temperature, then added 0.2 mL of chloroform per mL of TRIzol. Samples were incubated at room temperature for three minutes, centrifuged at 12000x g for ten minutes at 4 °C, supernatant collected, and the manufacturer's instructions followed for the remaining procedure [128]. RNA concentration was measured using a Nanodrop (ThermoFisher, Waltham, MA, USA) and cDNA synthesis was conducted using the high-capacity cDNA RT kit (Applied Biosystems, Waltham, MA, USA) using 2 mg RNA per reaction. qPCR was performed using PerfeCYa SYBR Green SuperMix ROX (Quantabio, Beverly, MA, USA) in a QuantStudio3 machine (Applied Biosystems, Waltham, MA, USA). Cyclophilin A was used as the reference gene and the primer sequences for all genes are provided in Table 3.5.

Table 3.5. Primer sequences

Primer		Primer Sequence
Acaca	F 5' – 3'	CCTGAAGACCTTAAAGCCAATGC
	R 5' – 3'	CCAGCCCACACTGCTTGTA
ApoB	F 5' – 3'	ACTGTGACTTCAATGTGGAG
	R 5' – 3'	CTGAGGCAGACAGACTTGTC
Cidea	F 5' – 3'	GCCGTGTTAAGGAATCTGCTG
	R 5' – 3'	TGCTCTTCTGTATCGCCCAGT
Cd36	F 5' – 3'	TGGCTAAATGAGACTGGGACC
	R 5' – 3'	ACATCACCACTCCAATCCCAAGTAAGG
Cpt1a	F 5' – 3'	CCTACCATGGCTGGATGTTTGCAG
	R 5' – 3'	GTATCTTTGACAGCTGGGACAGGCA
Dgat1	F 5' – 3'	GAGTCTATCACTCCAGTGGG
	R 5' – 3'	GGCGGCACCACAGGTTGACA
Dgat2	F 5' – 3'	CTGGCAAGAACGCAGTCA
	R 5' – 3'	TTCTTCTGGACCCATCGG
Fasn	F 5' – 3'	CTTCCGTCACTTCCAGTTAGAGCAG
	R 5' – 3'	AGTTCAGTGAGGCGTAGTAGACAGTG
Mttp	F 5' – 3'	AGAGGACAGCTTTGTCACCG
	R 5' – 3'	TCTTCAGCTCCAATTTCTGCTTCG
Opa1	F 5' – 3'	TCTCAGCCTTGCTGTGTCAGAC
	R 5' – 3'	TTCCGTCTCTAGGTTAAAGCGCG
Ppia	F 5' – 3'	TGGCTATAAGGGTTCCTCCTTTCACAG
	R 5' – 3'	GCCAGGACCTGTATGCTTTAGGATG
Srebp1c	F 5' – 3'	GGAGCCATGGATTGCACATTTGAAGACAT
	R 5' – 3'	TTCCAGAGAGGAGGCCAGAGA

Abbreviations: *Gene symbol* is followed by its name and the encoded protein of interest: *Acaca* (acetyl-coA carboxylase alpha) encodes ACC1; *ApoB* (apolipoprotein B) encodes APOB*; Cidea* (cell-death inducing DNA fragmentation factor-like effector A) encodes CIDEA; *Cd36* encodes fatty acid translocase CD36; *Cpt1α* (carnitine palmitoyl transferase 1α) encodes CPT1α*; Dgat1* (diacylglycerol O-acyltransferase) encodes DGAT1; *Dgat2* (diacylglycerol O-acyltransferase 2) encodes DGAT2; *Fasn* (fatty acid synthase) encodes FAS; *Mttp* (microsomal triglyceride transfer protein) encodes MTP; *Opa1* (optic atrophy 1) encodes OPA1; *Ppia* (peptidylprolyl isomerase A)

encodes cyclophilin A; *Srebp1c* (sterol regulatory element binding transcription factor 1C) encodes SREBP-1c.

3.11 Statistical analysis

Statistical analysis was conducted using GraphPad Prism software 7.0 (GraphPad Software Inc., San Diego, CA, USA). Data are presented as means ± SEM with the corresponding sample size described in each figure caption. For western blot, data sets were combined with both insulin-stimulated and basal animals included for pathways independent of direct insulin action (n = 8 / group). For those with direct insulin action, data sets were separated into basal (n = 4 / group) and insulin-stimulated (n = 4 / group). LFD was compared to HFD groups using two-tailed t-tests to identify diet-related differences in Chapter 4. HFD, HFD+WFM and HFD+NFM groups were compared using one-way ANOVA or two-way ANOVA followed by Tukey's post-hoc test to study treatment effects in Chapters 5, 6 and 7. Data were checked for normal distribution using the Shapiro-Wilk test and any identified outliers (q = 0.5%) were removed. Data that did not follow a normal distribution were log-transformed prior to the statistical analysis. Statistically significant was considered if the p-value < 0.05 and a p-value of < 0.1 was considered a trend.

Chapter 4: Creating a model of metabolic dysfunction with a HFD

4.1 Results

4.1.1 Food intake, body composition, and tissue weight

Food intake was similar between the LFD and HFD groups (Figure 4.1). After 8 weeks of diet intervention, the HFD group had significantly higher BW increases than the LFD group ($p < 0.0002$) even when corrected to baseline BW (Table 4.1). Four-hour fasting blood glucose (FBG) was lower in LFD animals compared to HFD animals ($p < 0.05$), however, overnight FBG was unchanged between the LFD and HFD groups (Table 4.1). Body composition analysis showed that LFD mice had a lower fat mass % ($p < 0.0001$) when compared to the HFD animals (Table 4.1). The liver weight was unchanged between LFD and HFD, whereas the epididymal white adipose tissue (WAT) was significantly less in the LFD than the HFD group (Table 4.1).

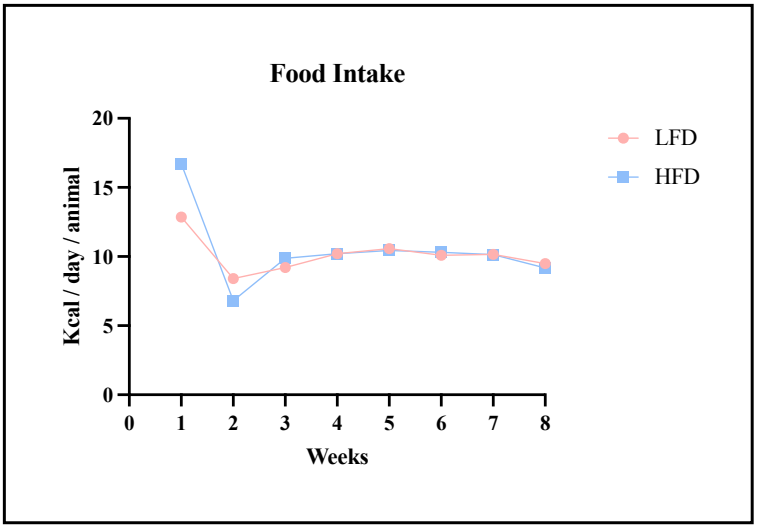

Figure 4.1. Food intake measured as Kcal per day per animal during 8 weeks of diet supplementation. Data expressed as an average per cage with n = 8 mice and analyzed by two-way ANOVA followed by Tukey's post-hoc. LFD, low-fat diet; HFD, high-fat diet.

Table 4.1. Body composition and metabolic profile of LFD and HFD mice.

	LFD	**HFD**
Body composition		
BW initial (g)	22 ± 0.28	22 ± 0.28
BW final (g)	31 ± 0.7***	36 ± 1.0
BW change (% of Baseline)	38 ± 4.0***	61 ± 3.5
Final fat mass (% BW)	23 ± 1.2****	34 ± 1.1
Final lean mass (% BW)	68 ± 0.9****	58 ± 1.0
Tissue Weight		
Liver (% BW)	3.3 ± 0.22	3.0 ± 0.16
eWAT (% BW)	3.7 ± 0.37**	5.6 ± 0.38
Plasma (fasting)		
4-hour fasted glucose (mmol/L)	9.3 ± 0.37*	11 ± 0.49
Overnight fasted glucose (mmol/L)	6.2 ± 0.34	5.9 ± 0.53
NEFA (mEq/L)	0.51 ± 0.06	0.49 ± 0.04
Liver Content (mg/g tissue)		
TG (mg/g)	39.3 ± 5.0*	71.7 ± 14.4
Cholesterol (mg/g)	1.35 ± 0.29	1.40 ± 0.23

Abbreviations: BW, body weight; eWAT, epididymal white adipose tissue; NEFA, non-esterified FA; TG, triglycerides. Data expressed as mean ± SEM of n = 8 mice / group. Analysis by two-tailed t-test. * Indicates $p < 0.05$, ** $p < 0.01$, *** $p < 0.001$, **** $p < 0.0001$.

4.1.2 ITT, PTT, and FBG

LFD animals had a significantly lower blood glucose concentration after a four-hour fast compared to the HFD group ($p < 0.05$) (Table 4.1). These values were time = 0 (baseline) in the ITT. There was no statistical difference seen between LFD and HFD after an overnight fast (Table 4.1). These values were time = 0 in the PTT.

Two-way ANOVA analysis displayed a significant time x diet interaction ($p < 0.05$), and effect of the diet ($p < 0.05$). Blood glucose during the ITT was significantly lower in LFD at the 0-minute ($p < 0.05$) and 15-minute time mark ($p < 0.01$) compared to HFD (Figure 4.2A). Once corrected to baseline, the significant differences between time x diet and diet effects were lost. Blood glucose after correction was reduced to a trend ($p = 0.09$) at the 15-minute mark and was not significantly different at any other time point (Figure 4.2B). ITT AUC values were not different both prior and after correcting for baseline FBG suggesting that marked IR may not have been established (Figure 4.2C/D). PTT was not significantly different between LFD and HFD (Figure 4.3). However, two-way ANOVA analysis displayed a significant effect of time ($p < 0.01$).

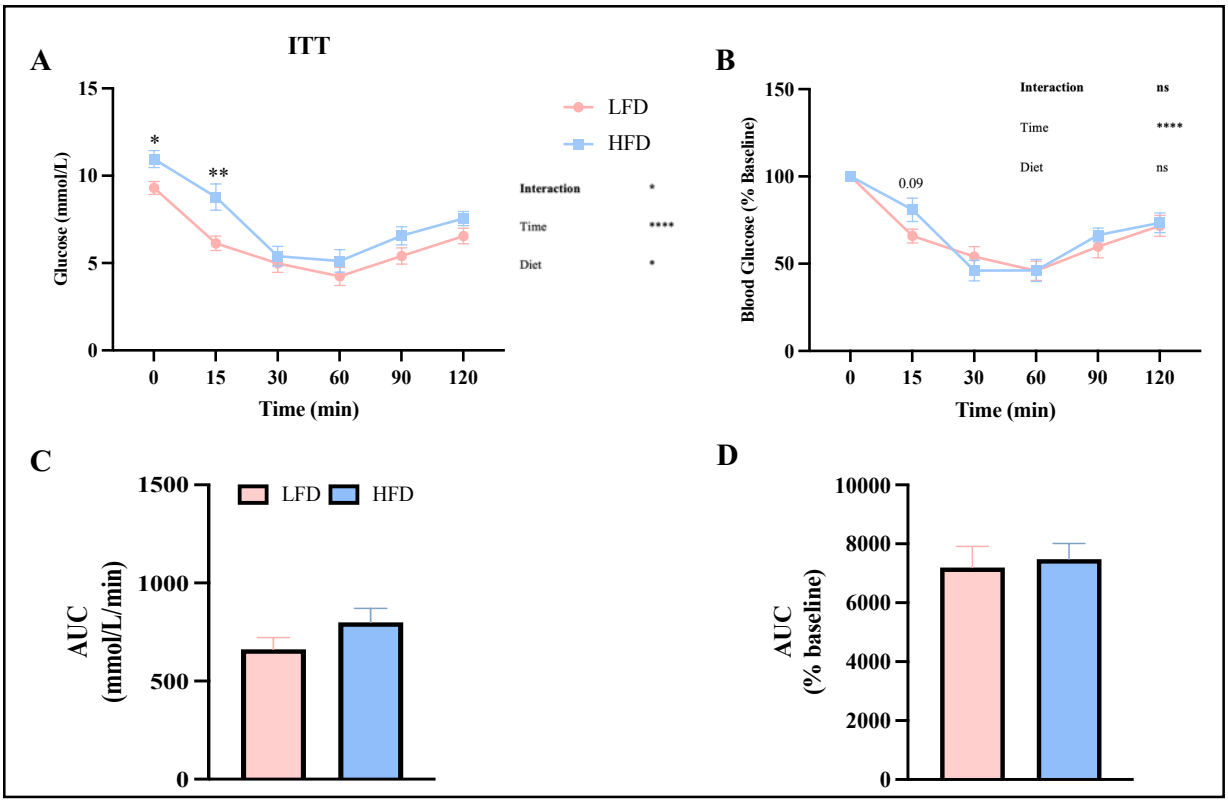

Figure 4.2. Insulin tolerance test (ITT) in 4-h fasted LFD and HFD mice. (A) ITT LFD vs HFD (n = 10 / group); (B) ITT as % of baseline fasting blood glucose concentration for LFD vs HFD; (C) ITT area under the curve (AUC) and (D) ITT AUC of baseline corrected curves. Data expressed as mean ± SEM and analyzed by two-way ANOVA followed by Tukey's post-hoc for ITT for the effect of diet (A, B) and two-tailed t-test for AUC. * Indicates $p < 0.05$, ** indicates $p < 0.01$.

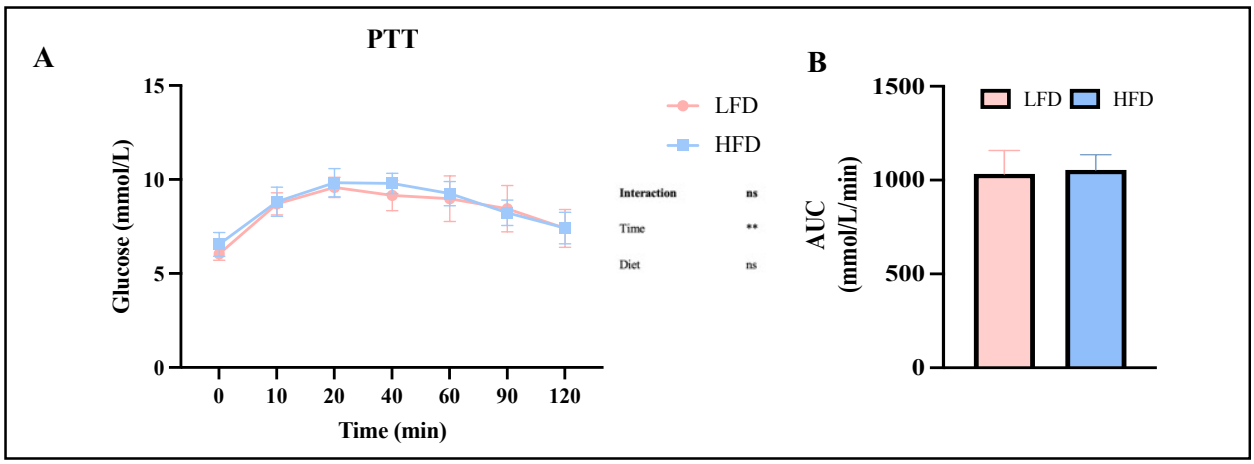

Figure 4.3. Pyruvate tolerance test (PTT) in overnight-fasted LFD and HFD mice. (A) PTT LFD vs HFD (n = 10 / group); (B) PTT area under the curve (AUC). Data expressed as mean ± SEM and analyzed by two-way ANOVA followed by Tukey's post-hoc for the effect of diet and two-tailed t-test for AUC.

4.1.3 Hepatic histology & lipid profile

Histological analysis of hepatic LD showed no changes in the number of LD between the LFD and HFD groups (Figure 4.4C). The average size of LD was smaller in LFD compared to HFD ($p < 0.01$) and the total area covered by LD was lower in LFD ($p < 0.01$) (Figure 4.4B & Figure 4.4D). Hepatic TGs were lower in the LFD group compared to the HFD group ($p < 0.05$) (Table 4.1). No significant differences were seen in hepatic cholesterol concentration or serum non-esterified FA (NEFA) (Table 4.1).

GC analysis of the FA profile of liver total phospholipids and total lipids displayed small changes. Starting with total hepatic lipids (Table 4.2), compared with LFD, HFD trended to have higher polyunsaturated FA (PUFA) content ($p = 0.098$). Total monounsaturated FA (MUFA) and total saturated FA (SFA) were not affected by diet treatment.

To understand the drivers of differences elicited by HFD in the PUFA fractions in liver tissue, FA species were compared. Proportionally higher FA within the PUFA class in HFD included C18:2n-6 ($p < 0.05$), C18:3n-3 ($p < 0.01$) and C20:2 ($p < 0.05$). Two of the omega-3 series were increased in HFD: C22:5n-3 ($p<0.01$) and C20:5n-3 ($p = 0.084$). Within the SFA class, two FA species were higher in HFD: C15:0 ($p <0.05$) and C17:0 ($p = 0.054$). C16:0 trended proportionally lower in HFD compared to LFD ($p = 0.098$). For individual FA within the MUFA class, C17:1 was higher ($p <0.01$) and C18:1n-7 lower in HFD compared to LFD ($p < 0.05$).

For total phospholipids (Table 4.3), the proportions of total SFA, MUFA, and PUFA were not significantly different. The omega-3 series PUFA C18:3n-3 ($p < 0.05$) and C22:5n-3 ($p = 0.072$) were higher in HFD compared to LFD.

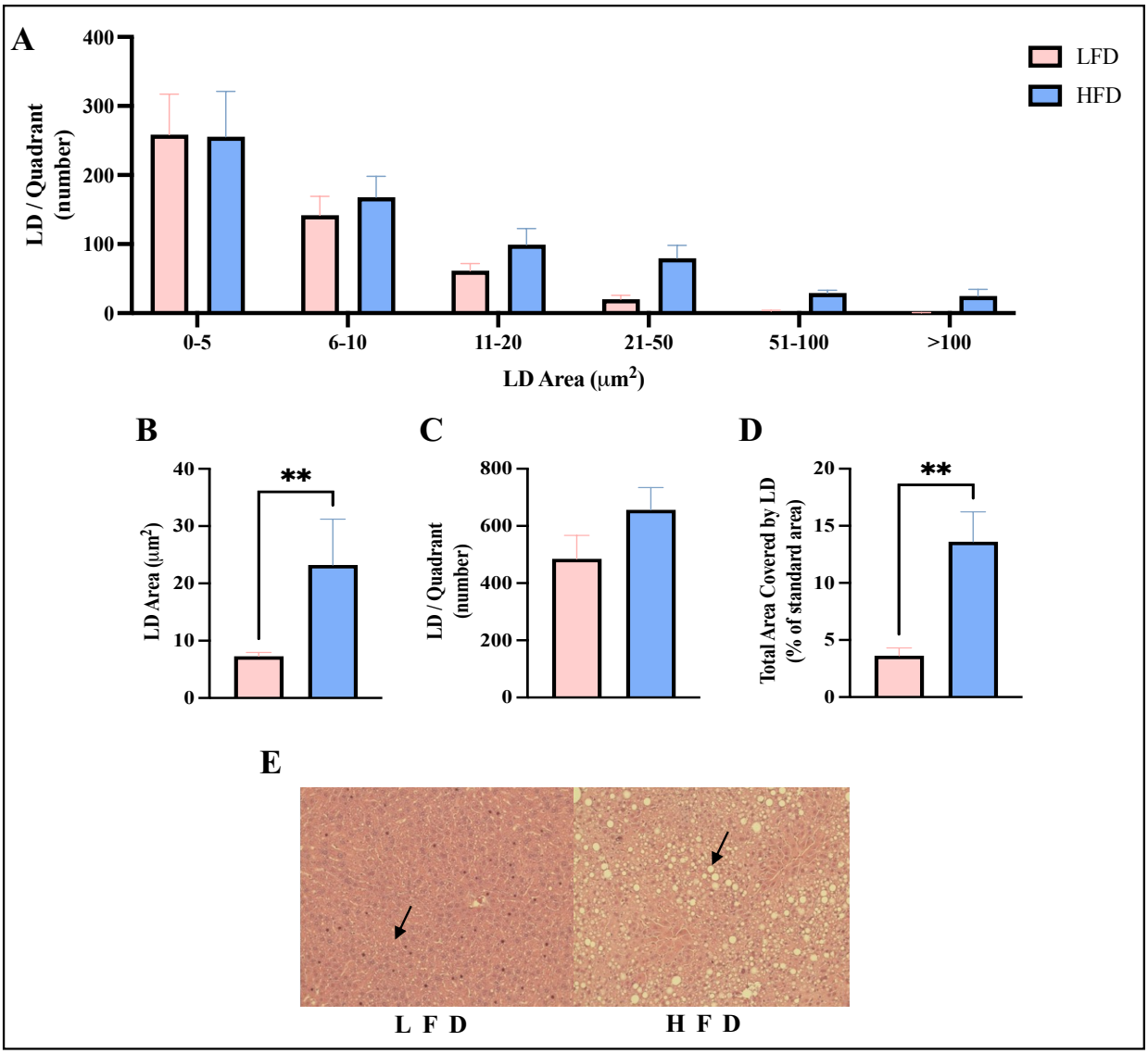

Figure 4.4. Liver histology and morphological characterization in overnight-fasted mice. (A) distribution of lipid droplets by average size and number per quadrant; (B) average area of lipid droplets; (C) average number of lipid droplets per quadrant; (D) percentage of the total area covered by lipid droplets; (E) histological images displaying lipid accumulation in stained liver slides; LD denoted by arrows. Data expressed as mean ± SEM (n = 6 / group) and analyzed by two-tailed t-test. ** Indicates $p < 0.01$. LD, lipid droplet; LFD, low-fat diet; HFD, high-fat diet.

Table 4.2. Total liver lipid content characterization represented as peak area percentage.

	LFD	HFD	*p* - values
SFA			
C14:0	0.54 ± 0.06	0.58 ± 0.06	
C15:0	0.045 ± 0.003	0.061 ± 0.004	$p < 0.05$
C16:0	28.3 ± 0.38	27.2 ± 0.47	$p = 0.098$
C17:0	0.05 ± 0.006	0.08 ± 0.014	$p = 0.054$
C18:0	3.97 ± 0.45	5.00 ± 0.58	
C20:0	0.23 ± 0.03	0.29 ± 0.04	
C24:0	0.01 ± 0.003	0.01 ± 0.002	
∑ SFA (%)	**33.2 ± 0.93**	**33.2 ± 1.17**	
MUFA			
C14:1	0.04 ± 0.008	0.03 ± 0.01	
C15:1	0.02 ± 0.005	0.02 ± 0.005	
C16:1n-7	0.70 ± 0.06	0.71 ± 0.21	
C16:1n-9	5.6 ± 0.58	4.0 ± 0.98	
C17:1	0.07 ± 0.006	0.11 ± 0.01	$p < 0.01$
C18:1n-7	2.8 ± 0.39	1.6 ± 0.18	$p < 0.05$
C18:1n-9	40.5 ± 2.29	35.8 ± 1.88	
C20:1n-6	0.56 ± 0.05	0.45 ± 0.06	
C24:1n-9	0.14 ± 0.03	0.19 ± 0.04	
∑ MUFA (%)	**50.4 ± 3.42**	**42.9 ± 3.38**	

PUFA			
C18:2n-6	8.8 ± 1.42	15.1 ± 1.77	$p < 0.05$
C18:3n-3	0.17 ± 0.03	0.37 ± 0.05	$p < 0.01$
C20:2	0.10 ± 0.02	0.22 ± 0.05	$p < 0.05$
C20:3	0.35 ± 0.06	0.40 ± 0.04	
C20:4	4.6 ± 0.63	4.9 ± 0.84	
C20:5n-3	0.06 ± 0.01	0.09 ± 0.008	$p = 0.084$
C22:5n-3	0.07 ± 0.01	0.16 ± 0.03	$p < 0.01$
C22:6n-3	2.2 ± 0.20	2.6 ± 0.52	
∑ PUFA (%)	**16.4 ± 2.38**	**23.8 ± 3.31**	***p* = 0.098**

Abbreviations: LFD, low-fat diet; HFD, high-fat diet; SFA, saturated fatty acids; MUFA, monounsaturated fatty acids; PUFA, polyunsaturated fatty acids. Data expressed as mean ± SEM (n = 6 / group; fasted), analyzed by two-tailed t-test.

Table 4.3. Total liver phospholipid content characterization represented as peak area percentage.

	LFD	HFD	*p* - values
SFA			
C14:0	0.09 ± 0.01	0.07 ± 0.007	
C15:0	0.07 ± 0.004	0.06 ± 0.004	
C16:0	26.2 ± 0.52	24.7 ± 1.12	
C17:0	0.11 ± 0.004	0.19 ± 0.02	$p < 0.01$
C18:0	16.9 ± 0.70	17.2 ± 0.73	
C20:0	0.27 ± 0.02	0.30 ± 0.007	
C24:0	0.28 ± 0.02	0.16 ± 0.04	$p = 0.063$
∑ SFA (%)	**43.9 ± 1.28**	**42.7 ± 1.93**	
MUFA			
C14:1	0.02 ± 0.003	0.007 ± 0.0007	$p < 0.05$
C15:1	0.02 ± 0.002	0.02 ± 0.002	
C16:1n-7	0.22 ± 0.01	0.19 ± 0.01	
C16:1n-9	1.6 ± 0.22	1.0 ± 0.26	
C17:1	0.06 ± 0.02	0.07 ± 0.02	
C18:1n-7	3.5 ± 0.29	2.1 ± 0.35	$p < 0.05$
C18:1n-9	10.1 ± 0.15	11.5 ± 2.17	
C20:1n-6	0.13 ± 0.02	0.14 ± 0.02	
C24:1n-9	0.65 ± 0.04	0.60 ± 0.03	
∑ MUFA (%)	**16.3 ± 0.76**	**15.6 ± 2.86**	

PUFA			
C18:2n-6	10.0 ± 0.64	13.1 ± 0.73	$p < 0.05$
C18:3n-3	0.05 ± 0.01	0.07 ± 0.008	
C20:2	0.11 ± 0.02	0.20 ± 0.04	$p = 0.064$
C20:3	1.0 ± 0.11	0.94 ± 0.09	
C20:4	18.2 ± 0.51	18.6 ± 0.39	
C20:5n-3	0.11 ± 0.01	0.13 ± 0.01	
C22:5n-3	0.28 ± 0.03	0.38 ± 0.04	$p = 0.053$
C22:6n-3	8.4 ± 0.53	8.1 ± 0.35	
∑ PUFA (%)	**38.2 ± 1.86**	**42.3 ± 1.66**	

Abbreviations: LFD, low-fat diet; HFD, high-fat diet; SFA, saturated fatty acids; MUFA, monounsaturated fatty acids; PUFA, polyunsaturated fatty acids. Data expressed as mean ± SEM (n = 6 / group; fasted), analyzed by two-tailed t-test.

4.1.4 Hepatic lipid metabolism

Hepatic genes within the four arms of lipid metabolism displayed a reduced expression of *Fasn* ($p < 0.01$) and an enhanced expression of *Opa1* ($p < 0.05$) in LFD compared to HFD (Figure 4.5A). Western blot was completed to assess if gene expression differences were continued at the protein level with a summary of the proteins measured displayed in Figure 4.6. There were no significant differences seen between LFD and HFD in FA uptake proteins FABP4 and CD36 (Figure 4.7A, B). Within DNL proteins, acetyl-CoA synthetase (ACS) was significantly higher in HFD compared to LFD ($p < 0.05$) (Figure 4.7C). The ratio of p-ACC/ACC and FAS and abundance was unchanged between LFD and HFD with total ACC trending toward higher abundance in insulin-stimulated LFD compared to HFD ($p = 0.072$) (Figure 4.7E-G). Two-way ANOVA displayed a significant interaction between diet and insulin-stimulation ($p < 0.05$) for ACC.

Within FA oxidation only OXPHOS complex V trended higher in LFD vs HFD ($p = 0.060$) (Figure 4.8E). There were no other differences seen in FA oxidation or FA export proteins between LFD and HFD groups (Figure 4.8 & Figure 4.9). Key regulatory proteins were analyzed within the lipid metabolism arms. p-AMPKα and the ratio of p-AMPKα over total AMPKα trended higher in LFD compared to HFD ($p = 0.070$ & $p = 0.096$ respectively) (Figure 4.10A-C). p-AMPKβ, AMPKβ, and the ratio of p-AMPKβ over total AMPKβ were higher in LFD compared to HFD ($p < 0.05$) (Figure 4.10D-F). PPARγ was significantly higher in LFD compared to HFD ($p < 0.05$) (Figure 4.10G).

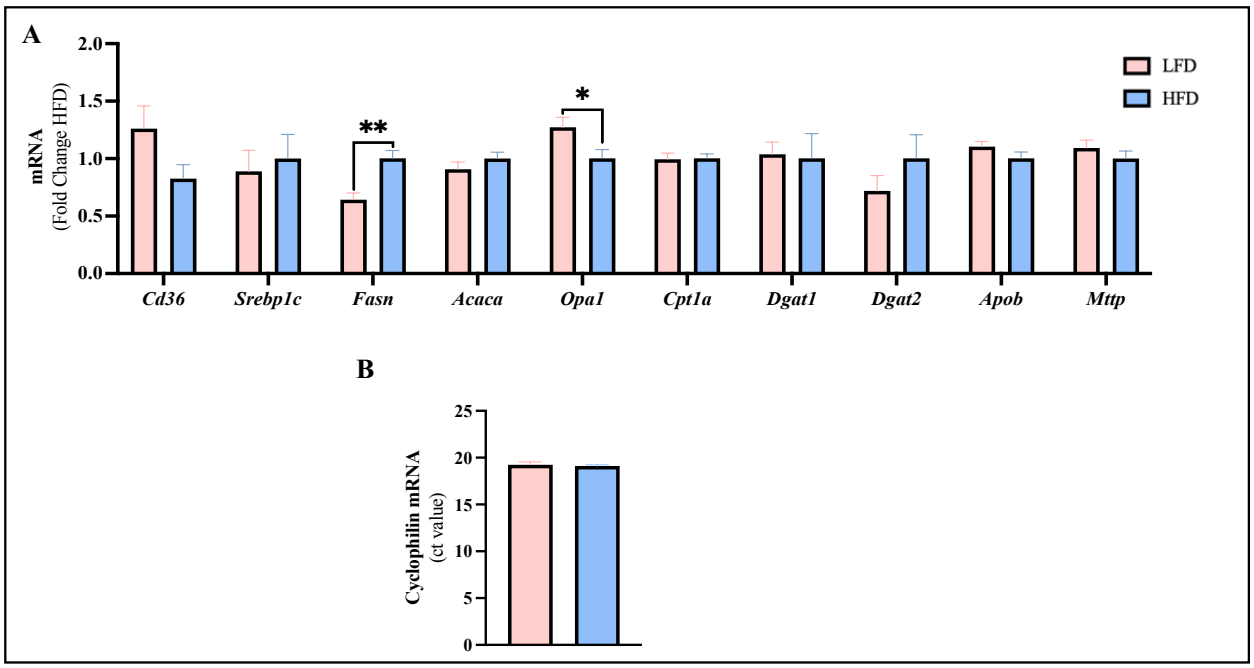

Figure 4.5. Hepatic mRNA expression of genes involved in lipid metabolism in overnight-fasted LFD and HFD groups. (A) LFD vs HFD expression (n = 6 / group). Gene expression was normalized to cyclophilin (B). Data expressed as mean ± SEM and analyzed by two-tailed t-test. * Indicates $p < 0.05$, ** indicates $p < 0.01$.

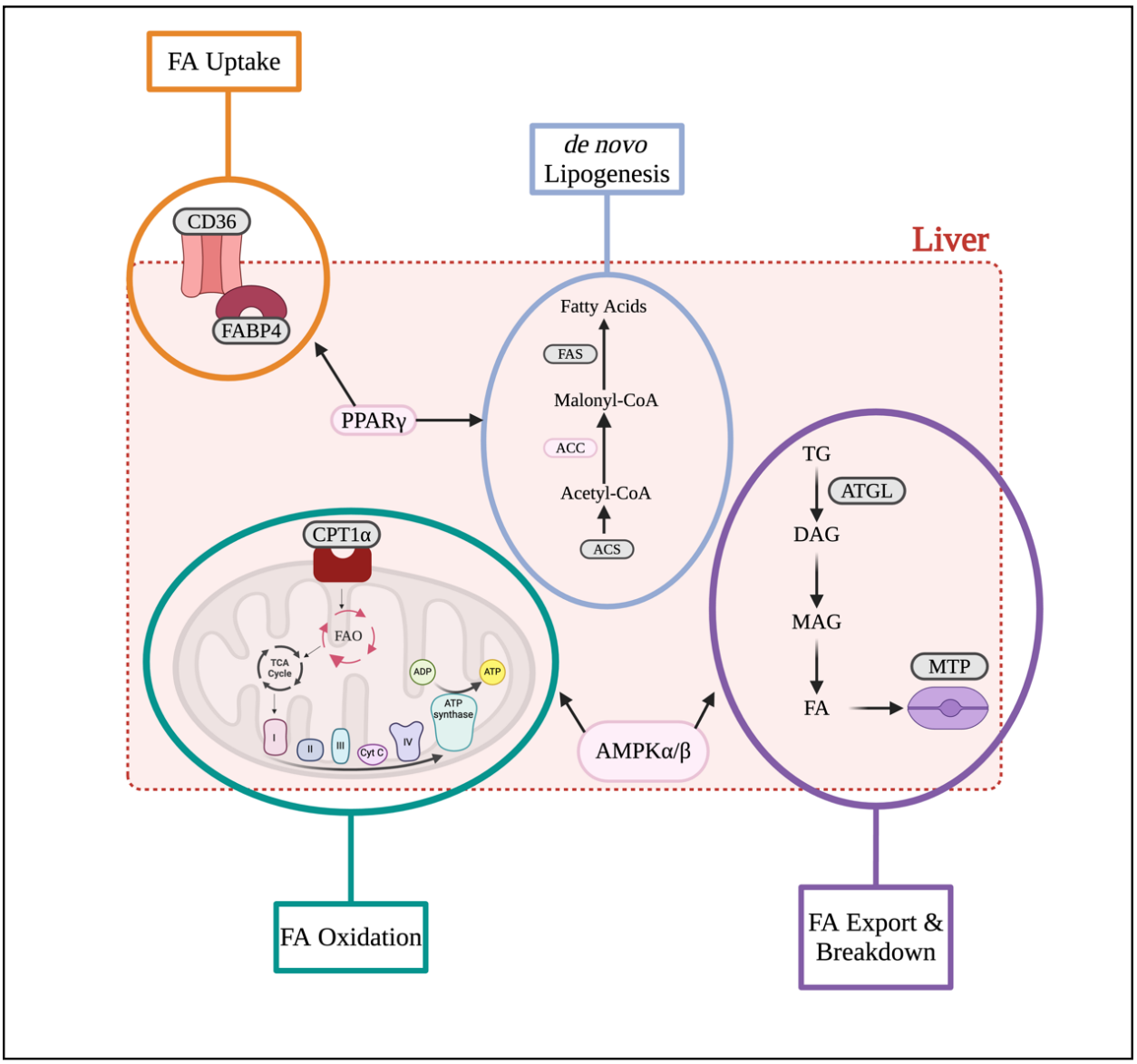

Figure 4.6. Summary of proteins measured within liver lipid metabolism pathways via qPCR and western blot. Proteins coloured grey denote similar abundance between LFD and HFD whereas proteins coloured pink denotes higher abundance in LFD compared to HFD. Created by EB with biorender.com.

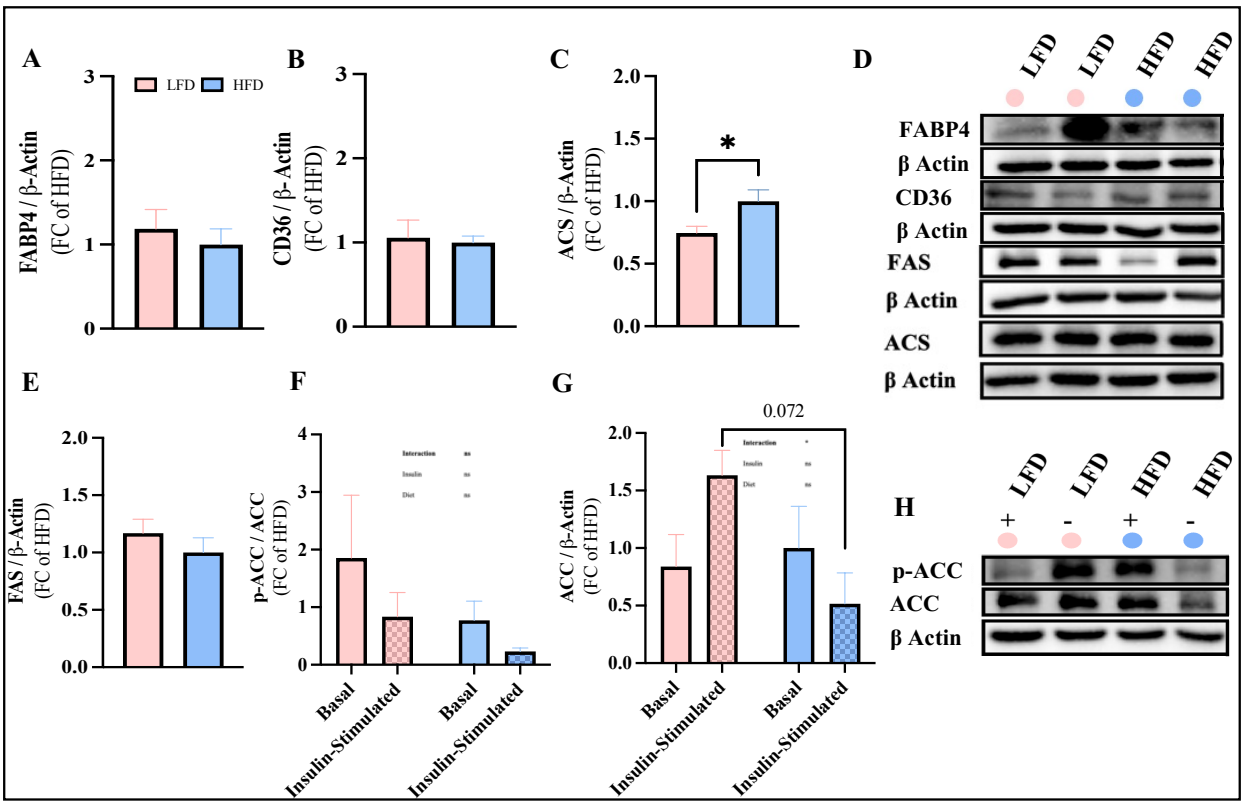

Figure 4.7. Liver lipid transporters and de novo lipogenesis protein abundance in tissue from overnight fasted mice. (A) FABP4, fatty acid binding protein 4; (B) CD36; (C) ACS, acetyl-CoA synthetase; (E) FAS, fatty acid synthase; (F) p-ACC / ACC, acetyl-CoA carboxylase; (G) ACC; (D and H) Representative western blots. Proteins were normalized to β-actin. Data expressed as mean ± SEM. Sample size for A-E was n = 8 / group (combined basal and insulin-stimulated) and for F-G n = 4 / group for basal and n = 4 / group for insulin-stimulated. Data analyzed by two-tailed t-test (A-E) and two-way ANOVA (F-G) followed by Tukey's post-hoc test. * Indicates $p < 0.05$.

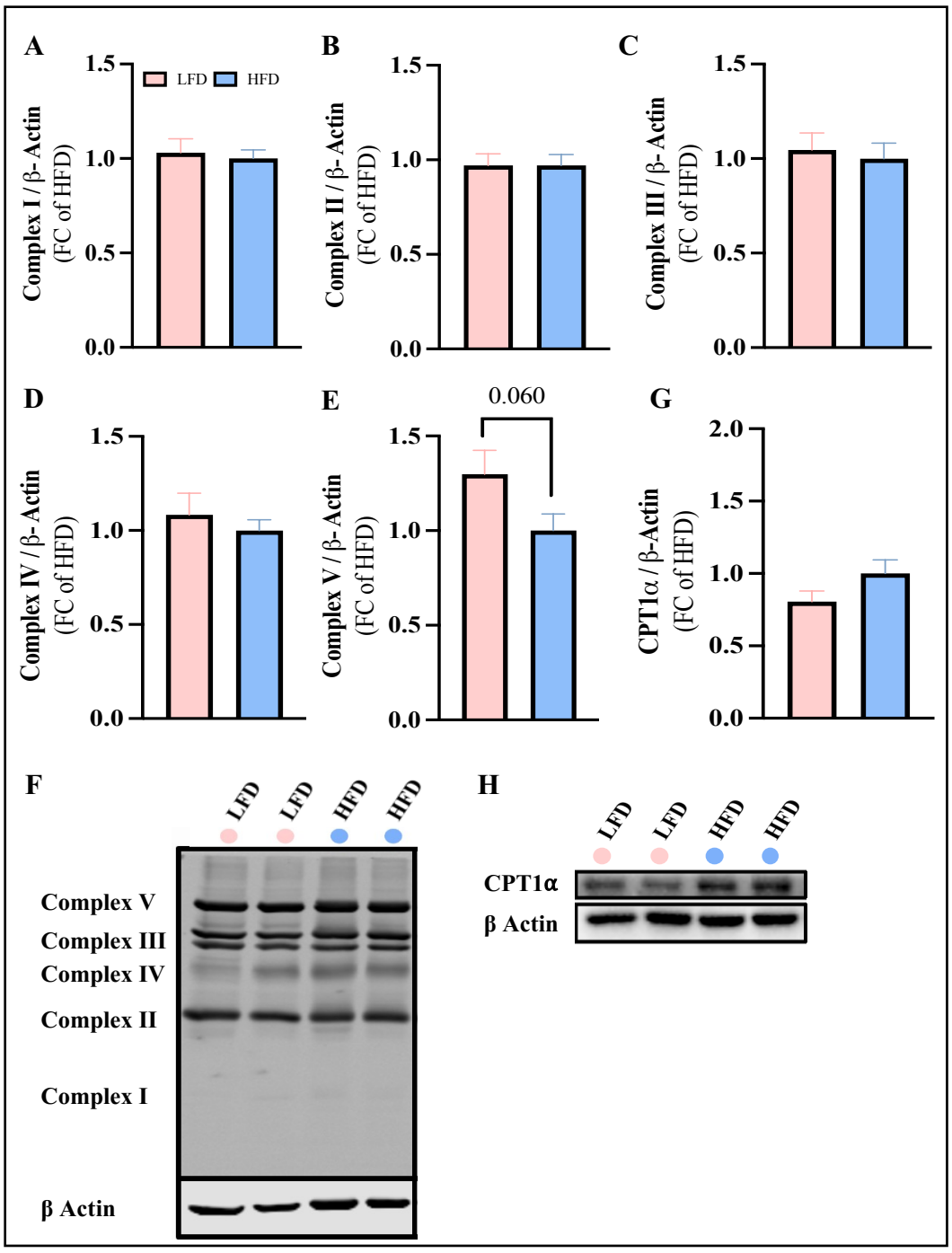

Figure 4.8. Hepatic fatty acid oxidation protein abundance in tissue from overnight fasted mice. (A-E) OXPHOS mitochondrial complexes I-V; (G) CPT1α, carnitine palmitoyltransferase 1α; (F) OXPHOS representative blot; (H) CPT1α representative blot. Data expressed as mean ± SEM (n = 8 / group; combined basal and insulin-stimulated). Data analyzed by two-tailed t-test.

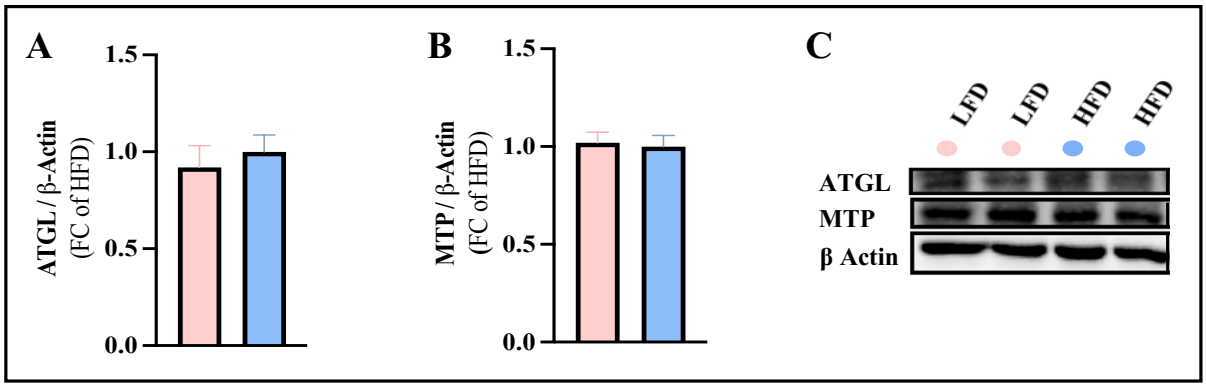

Figure 4.9. Liver lipolysis and export protein abundance in tissue from overnight fasted mice. (A) ATGL, adipose triglyceride lipase; (B) MTP, microsomal triglyceride transfer protein; (C) representative western blot. Proteins were normalized to β-actin. Data expressed as mean ± SEM. Sample size was n = 8 / group (combined basal and insulin-stimulated). Data analyzed by two-tailed t-test.

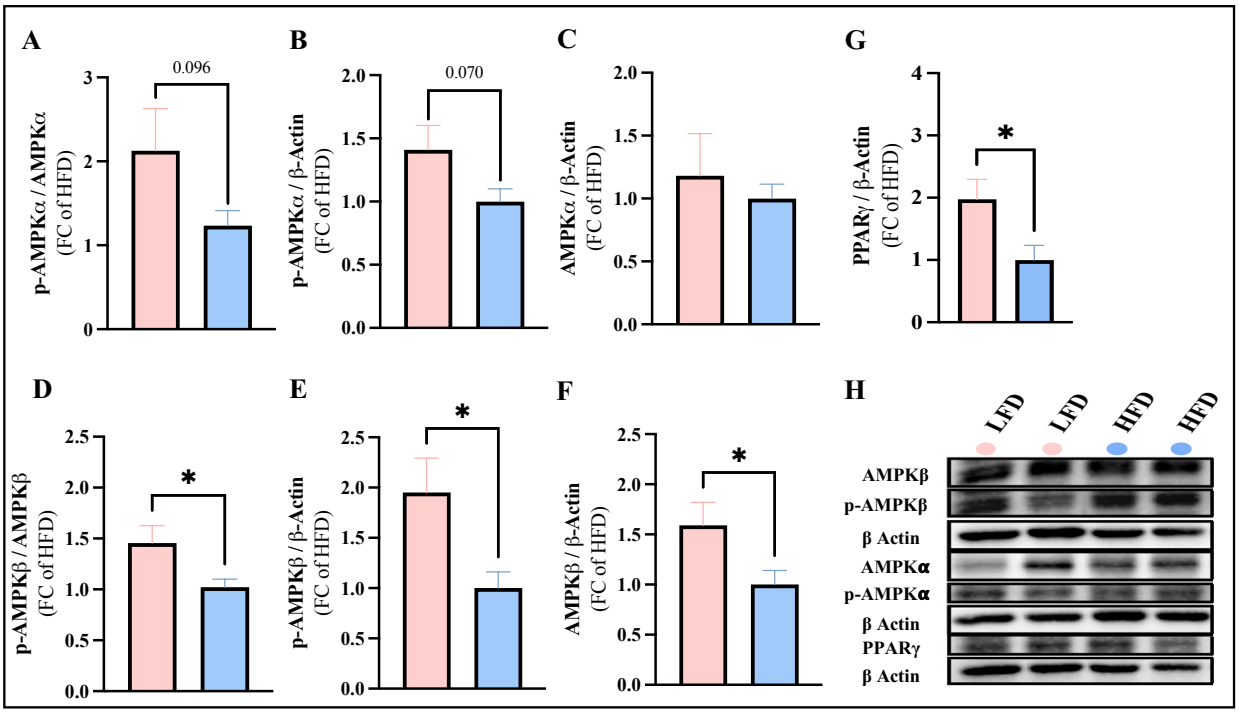

Figure 4.10. Regulators of energy metabolism protein abundance in tissue from overnight fasted mice. (A) p-AMPKα / AMPKα, AMP-activated protein kinase α; (B) AMPKα; (C) PPARγ, peroxisome proliferator-activated receptor gamma; (D) p-AMPKβ / AMPKβ; (E) AMPKβ; (F) representative western blot. Proteins were normalized to β-actin. Data expressed as mean ± SEM. Sample size was n = 8 / group (combined basal and insulin-stimulated). Data analyzed by two-tailed t-test. * Indicates $p < 0.05$.

4.2 Discussion

My first objective aimed to create a model of metabolic dysfunction exhibiting fatty liver using HFD in C57BL/6 mice. The HFD treatment elicited increases in BW and fat mass, mild disturbances in glucose homeostasis, and enhanced hepatic steatosis, consistent with a preclinical phenotype.

Body composition was drastically different between the two groups with HFD displaying significant increases in BW gain, fat mass, and epididymal WAT (eWAT), despite similar food intake. Body composition changes were accompanied by higher four-hour FBG in HFD animals, an indication for mild metabolic disturbance. However significant differences were not seen in the ITT and PTT. This may be due to the inability of ITT to detect subtle changes in insulin sensitivity. In a similar diet study using the same mouse model, ITT was similar between HFD and LFD animals, however data from the hyperinsulinemic-euglycemic clamp displayed a lower glucose infusion rate and higher hepatic glucose production than the LFD group, indicating IR [129].

Hepatic lipid accumulation was enhanced in HFD compared to LFD animals, paired with a higher hepatic TG content. These results follow the literature as HFD ranging from 58-80% fat have induced hepatic steatosis in Sprague-Dawley rats, C57BL/6Ncrj mice, and uncastrated boars [130], [131], [132]. Histological differences in the HFD animals included LD with larger areas and a larger percentage of the liver covered by LD compared to LFD. Larger LDs, also known as macrovesicular steatosis, are enriched with SFA, which has been shown to enhance ER stress, apoptosis, ROS accumulation, and cytotoxicity [133].

Of interest, our diet model to induce metabolic dysfunction presenting with pre-diabetes or MASLD contrasts with models used by other groups. Commonly, HFD with 60% kcal or a

combination of HF (~40% kcal fat) and high sucrose (~27% kcal) are used to induce MASLD over longer intervention periods (12-16 weeks on average) [134], [135], [136]. This could be a reason why there was a lack of fibrosis and immune infiltration in the livers of the HFD animals as seen in a previous study using a similar diet [137], comparable changes in ITT, and similar liver weights between HFD and LFD. However, this model allows us to answer our hypothesis under conditions similar to preclinical disease status in humans, before reaching pronounced IR and MASH, which could be useful in disease prevention. Another potential reason for the absence of MASH characteristics is the temperature in which they were housed as mice require higher ambient temperatures (~29-32 °C) to maintain thermoneutrality [138]. Thus, our mice housed at ~24 °C may be utilizing more energy to maintain their core body temperature, resulting in reductions in weight gain and disease progression.

Molecular pathways were generally unaffected with minimal differences seen in hepatic DNL, FA uptake, oxidation, and export. However, the regulatory proteins, p-AMPKα, p-AMPKβ, and PPARγ, had higher abundance in LFD compared to HFD. AMPK is important in both lipid and glucose metabolism, through the inhibition of DNL and upregulation of FA oxidation and lipolysis [139]. Chronic AMPK activation in transgenic mice elicited reduced DNL, hepatic TG, and hepatic lipid accumulation [140]. Thus, HFD mice may have an impaired ability to adapt to changes in substrate availability and cellular energy; therefore, it will be important in the following studies to examine whether milk treatment mitigates the effect of HFD on AMPK and the enzymes it regulates.

Overall, HFD animals displayed metabolic dysfunction consistent with preclinical T2D and fatty liver. Although molecular changes were modest, key regulatory pathways displayed lower abundance, indicating metabolic dysfunction within crucial metabolic pathways in the

HFD model. The next chapters will outline whether milk supplementation effectively ameliorates HFD effects on metabolism.

Chapter 5: Metabolic outcomes of dairy milk intervention

5.1 Results

5.1.1 Food intake, body composition, and tissue weight

Food intake was similar between groups (Figure 5.1). After 8 weeks of diet intervention, NFM supplementation significantly reduced BW gain when compared to the HFD ($p = 0.031$) and WFM groups ($p = 0.0068$) (Table 5.1). This significance was retained when corrected to baseline BW. Four-hour FBG was not different between groups, however overnight FBG was higher in the WFM group compared to HFD ($p < 0.05$) and the NFM group ($p < 0.01$) (Table 5.1). NFM animals had significantly lower fat mass % compared to the HFD group ($p = 0.029$) and the WFM group ($p = 0.044$) (Table 5.1). The liver weight and eWAT was not different between groups (Table 5.1).

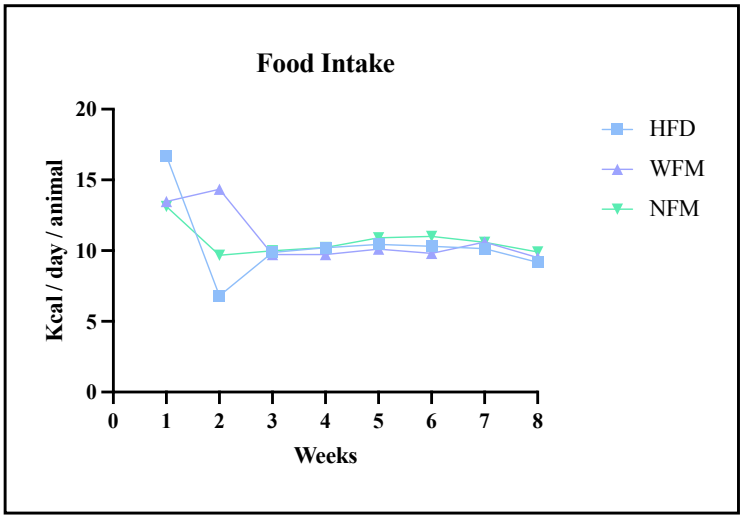

Figure 5.1. Food intake measured as Kcal per day per animal during 8 weeks of NFM and WFM supplementation. Data were expressed as an average per cage with n = 8 mice from 2 cages and analyzed by two-way ANOVA followed by Tukey's post-hoc. HFD, high-fat diet; WFM, whole-fat milk; NFM, non-fat milk.

Table 5.1. Body composition and metabolic profile of NFM and WFM supplemented C57BL/6 mice.

	HFD	WFM	NFM
Body composition			
BW initial (g)	22 ± 0.28	23 ± 0.75	21 ± 0.74
BW final (g)	36 ± 1.0[a]	38 ± 1.7[a, b]	31 ± 1.4[a, c]
BW change (% of Baseline)	61 ± 3.5[a]	68 ± 4.6[a]	46 ± 2.5[B]
Final fat mass (% BW)	34 ± 1.1[a]	35 ± 2.0[a]	28 ± 1.7[B]
Final lean mass (% BW)	58 ± 1.0[a]	57 ± 1.9[a]	64 ± 1.6[B]
Tissue Weight			
Liver (% g/BW)	3.0 ± 0.16	3.2 ± 0.17	3.2 ± 0.12
eWAT (% g/BW)	5.6 ± 0.38	5.9 ± 0.28	5.8 ± 0.33
Plasma (fasting)			
4-hour fasted glucose (mmol/L)	11 ± 0.49	11 ± 0.93	13 ± 0.92
Overnight fasted glucose (mmol/L)	5.9 ± 0.53[a]	7.7 ± 0.35[b]	4.8 ± 0.62[a, C]
NEFA (mEq/L)	0.49 ± 0.04	0.50 ± 0.04	TBD
Liver Content			
TG (mg/g)	71.7 ± 14.4[a]	69.2 ± 16.5[a]	46.0 ± 10.4[b]
Cholesterol (mg/g)	1.40 ± 0.23	1.14 ± 0.22	1.27 ± 0.58

Abbreviations: BW, body weight; eWAT, epididymal white adipose tissue; NEFA, non-esterified fatty acids; TG, triglycerides. Data expressed as mean ± SEM of n = 8 mice / group. Analysis by

one-way ANOVA followed by Tukey's post-hoc test. Different lowercase letters indicate $p < 0.05$ with uppercase letters indicating $p < 0.01$.

5.1.2 ITT, PTT, and FBG

FBG after a four-hour fast was not different between groups (Table 5.1). These values were at time = 0 (baseline) in the ITT. However, WFM animals had higher FBG after an overnight fast compared to HFD ($p < 0.05$) and NFM ($p < 0.01$). These values were time = 0 in the PTT.

Absolute ITT blood glucose concentrations prior to correction were not different, but after correcting for baseline were significantly lower in NFM at the 120-minute time point ($p < 0.05$) (Figure 5.2A, B). ITT AUC values were not different between all groups both prior and after correcting for baseline FBG (Figure 5.2C, D). For PTT, WFM had a higher blood glucose concentration than NFM at the 0-minute and 20-minute time point ($p < 0.05$) and lower blood glucose concentration than NFM at the 120-minute mark ($p < 0.05$) (Figure 5.3A). NFM trended to be lower than HFD at the 40-minute time point ($p = 0.07$). After correction to baseline, WFM presented lower blood glucose concentration compared to HFD at the 40-minute time point ($p < 0.05$) (Figure 5.3B). The PTT AUC was unchanged between groups (Figure 5.3C), but after correction to baseline FBG, NFM was higher than WFM ($p < 0.05$) (Figure 5.3D).

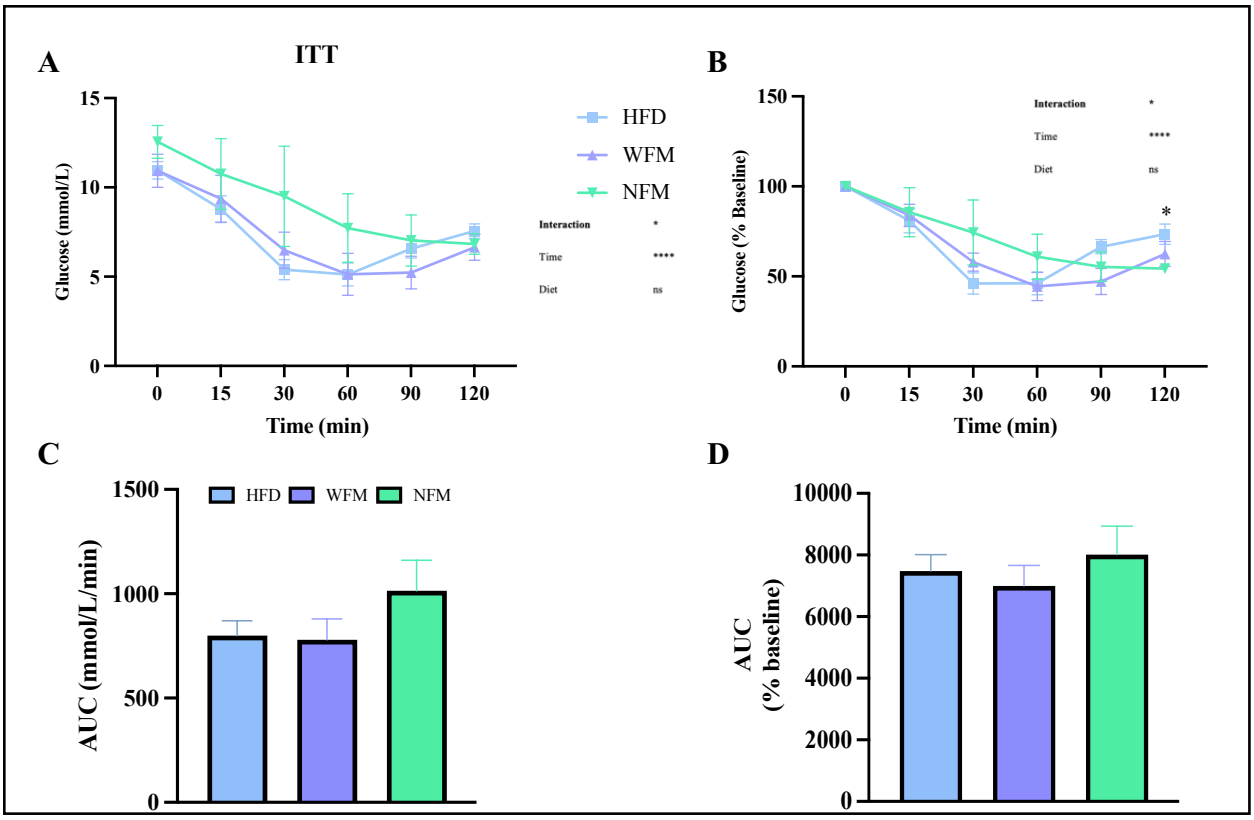

Figure 5.2. Insulin tolerance test (ITT) in 4-hour fasted mice supplemented with WFM and NFM . (A) ITT HFD groups (n = 10 HFD; n = 6 WFM & NFM); (B) ITT as % of baseline fasting blood glucose concentration; (C) ITT area under the curve (AUC) and (D) ITT AUC of baseline corrected curves. Data expressed as mean ± SEM, analyzed by two-way ANOVA (A, B) and one-way ANOVA (C, D) followed by Tukey's post-hoc test, to identify diet effect. * Indicates $p < 0.05$ comparing HFD and NFM.

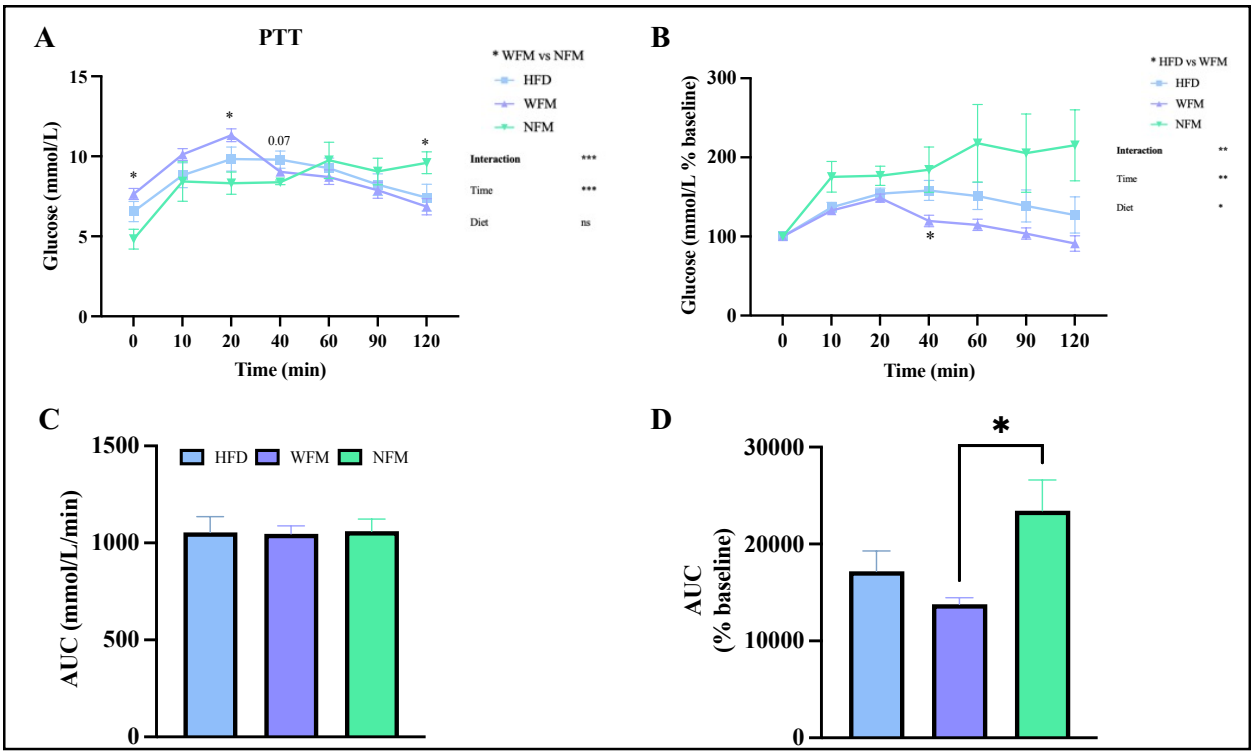

Figure 5.3. Pyruvate tolerance test (PTT) in overnight-fasted mice supplemented with WFM and NFM. (A) PTT HFD groups (n = 10 HFD; n = 6 WFM & NFM); (B) PTT as % of baseline fasting blood glucose concentration; (C) PTT area under the curve (AUC) and (D) PTT AUC of baseline corrected curves. Data expressed as mean ± SEM, analyzed by two-way ANOVA (A, B) and one-way ANOVA (C, D) followed by Tukey's post-hoc test, to identify diet effect. * Indicates $p < 0.05$ comparing WFM and NFM in panel A and HFD and WFM in panel B.

5.1.3 Hepatic histology

Histological analysis of hepatic LD displayed an altered distribution of LD, with an increasing number of larger LD in the HFD group (Figure 5.4A). The average size of LD was not statistically different between HFD groups (Figure 5.4B), however NFM had significantly less LD compared to HFD ($p < 0.05$) (Figure 5.4C). The total area covered by LD was significantly lower in NFM ($p < 0.05$) and strongly trended towards a reduction in WFM ($p = 0.051$) (Figure5.4D). The qualitative analysis of the images reveals a visible reduction in liver fat in the WFM and NFM groups when compared to HFD, shifting towards normalization of lipid accumulation (Figure 5.4E).

Hepatic TG was significantly lower in NFM compared to both HFD and WFM ($p < 0.05$). No significant differences were seen in hepatic cholesterol concentration and serum NEFA. Based on both measures, NFM outperformed WFM, but there is still a suggestion of improvement with WFM, as seen by the representative images.

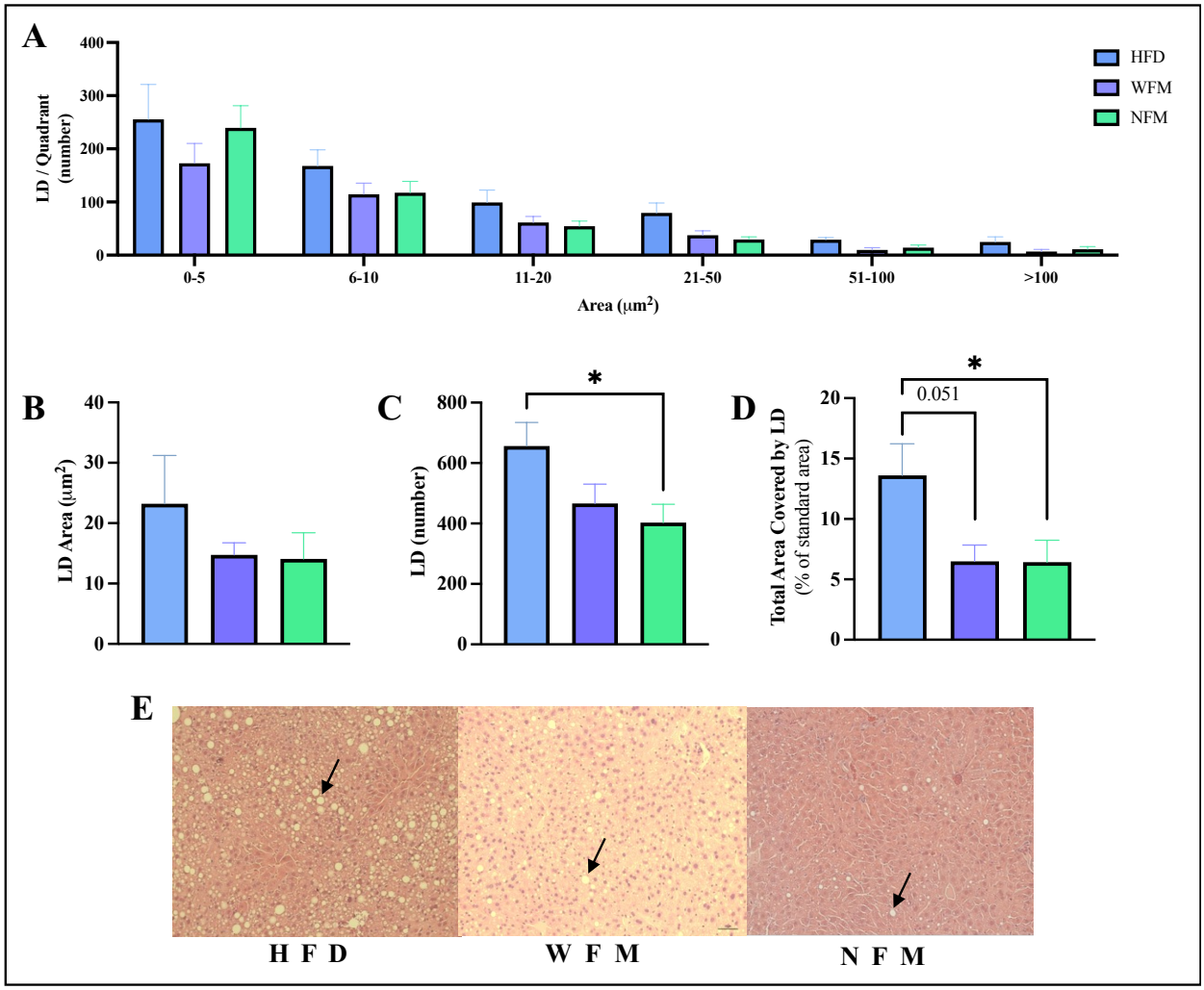

Figure 5.4. Hepatic histology and morphological characterization in tissue from overnight fasted mice. (A) Distribution of LD by average size and number per quadrant; (B) average area of LD; (C) average number of LD per quadrant; (D) percentage of total area covered by LD; (E) histological images displaying lipid accumulation in stained liver slides; LD denoted by arrows. Data expressed as mean ± SEM (n = 6 / group) and analyzed by one-way ANOVA. * Indicates $p < 0.05$. LD, lipid droplet; HFD, high-fat diet; WFM, whole-fat milk; NFM, non-fat milk.

5.1.4 Hepatic lipid profile

GC analysis of the FA profile in liver total phospholipids and total lipids displayed small changes within individual FA, but the overall profile was not statistically different between treatment groups.

Starting with total hepatic lipids (Table 5.2), there were no differences in total MUFA, PUFA, or SFA content between HFD and milk-treated groups. Comparison between groups was completed to uncover possible differences between specific FA species. There was only a single difference between HFD ± milk groups in individual MUFA or PUFA content, with C16:1n-9 trending lower in NFM compared to HFD ($p = 0.088$). For individual FA within the SFA class, NFM animals had higher C17:0 compared to HFD ($p < 0.05$) and WFM ($p = 0.053$), higher C18:0 compared to WFM ($p = 0.086$), and lower C14:0 compared to HFD ($p = 0.073$). WFM animals had higher C16:0 compared to NFM ($p < 0.05$).

For total phospholipids (Table 5.3), WFM exhibited lower MUFA in phospholipids compared to HFD ($p = 0.095$). Total SFA and PUFA content was not significantly different between any of the groups. Within the MUFA class, FA accounting for the reduction in WFM included C16:1n-9 ($p = 0.067$). For NFM, C16:1n-9 ($p = 0.052$) and C18:1n-9 ($p = 0.076$) were lower whereas C24:1n-9 trended higher compared to WFM ($p = 0.057$). Of interest within the SFA class were FA considered to be biomarkers of dairy intake. However, no clear pattern emerged as C15:0 was lower in WFM compared to NFM ($p < 0.05$) while C17:0 was similar between groups. C20:2 trended higher in NFM compared to WFM ($p = 0.065$).

Table 5.2. Total liver lipid content characterization represented as peak area percentage.

	HFD	WFM	NFM
SFA			
C14:0	0.58 ± 0.06	0.46 ± 0.06	0.39 ± 0.04[#]
C15:0	0.06 ± 0.003	0.06 ± 0.004	0.07 ± 0.003
C16:0	27.2 ± 0.47[a, b]	28.1 ± 0.51[a]	26.5 ± 0.43[b]
C17:0	0.08 ± 0.014[a]	0.08 ± 0.01[a]	0.12 ± 0.01[b]
C18:0	5.00 ± 0.58	4.2 ± 0.65	6.8 ± 1.03[#]
C20:0	0.29 ± 0.04	0.29 ± 0.03	0.37 ± 0.05
C24:0	0.01 ± 0.002	0.01 ± 0.002	0.02 ± 0.003
∑ SFA (%)	**33.2 ± 1.17**	**33.2 ± 1.27**	**34.3 ± 1.57**
MUFA			
C14:1	0.04 ± 0.008	0.02 ± 0.009	0.01 ± 0.003
C15:1	0.02 ± 0.005	0.01 ± 0.04	0.02 ± 0.002
C16:1n-7	0.70 ± 0.06	0.93 ± 0.16	0.66 ± 0.06
C16:1n-9	5.6 ± 0.58	3.3 ± 0.32	2.3 ± 0.26[#]
C17:1	0.07 ± 0.006	0.13 ± 0.02	0.11 ± 0.01
C18:1n-7	2.8 ± 0.39	1.7 ± 0.25	1.7 ± 0.18
C18:1n-9	35.8 ± 1.88	35.7 ± 2.01	29.5 ± 2.71
C20:1n-6	0.45 ± 0.06	0.45 ± 0.05	0.38 ± 0.05
C24:1n-9	0.19 ± 0.04	0.20 ± 0.01	0.28 ± 0.03
∑ MUFA (%)	**42.9 ± 3.38**	**42.4 ± 2.87**	**35.0 ± 3.31**

PUFA			
C18:2n-6	15.1 ± 1.77	15.4 ± 1.37	18.2 ± 0.86
C18:3n-3	0.37 ± 0.05	0.34 ± 0.06	0.37 ± 0.04
C20:2	0.22 ± 0.05	0.19 ± 0.03	0.24 ± 0.02
C20:3	0.40 ± 0.04	0.46 ± 0.03	0.45 ± 0.03
C20:4	4.9 ± 0.84	4.8 ± 0.76	7.4 ± 1.30
C20:5n-3	0.09 ± 0.008	0.12 ± 0.02	0.13 ± 0.02
C22:5n-3	0.16 ± 0.03	0.24 ± 0.03	0.25 ± 0.03
C22:6n-3	2.6 ± 0.52	2.3 ± 0.09	3.8 ± 0.61
∑ PUFA (%)	**23.8 ± 3.31**	**23.9 ± 2.39**	**30.8 ± 2.91**

Abbreviations: LFD, low-fat diet; HFD, high-fat diet; WFM, whole-fat milk; NFM, non-fat milk; SFA, saturated fatty acids; MUFA, monounsaturated fatty acids; PUFA, polyunsaturated fatty acids. Data expressed as mean ± SEM (n = 6 / group; fasted), analyzed by one-way ANOVA followed by Tukey's post-hoc test. Different lowercase letters indicate $p < 0.05$ and $^{\#}$ represents a trend of $0.05 < p < 0.1$.

Table 5.3. Total liver phospholipid content characterization represented as peak area percentage.

	HFD	WFM	NFM
SFA			
C14:0	0.07 ± 0.007	0.06 ± 0.01	0.11 ± 0.03
C15:0	0.06 ± 0.004[a, b]	0.05 ± 0.003[a]	0.06 ± 0.002[b]
C16:0	24.7 ± 1.12	25.5 ± 1.0	25.9 ± 0.25
C17:0	0.19 ± 0.02	0.18 ± 0.01	0.21 ± 0.01
C18:0	17.2 ± 0.73	17.5 ± 1.1	18.4 ± 0.49
C20:0	0.30 ± 0.007	0.29 ± 0.02	0.32 ± 0.03
C24:0	0.16 ± 0.04	0.21 ± 0.02	0.27 ± 0.02
∑ SFA (%)	**42.7 ± 1.93**	**43.8 ± 2.16**	**45.3 ± 0.83**
MUFA			
C14:1	0.007 ± 0.0007	0.01 ± 0.006	0.007 ± 0.001
C15:1	0.02 ± 0.002	0.017 ± 0.002	0.016 ± 0.001
C16:1n-7	0.19 ± 0.01	0.16 ± 0.01	0.18 ± 0.01
C16:1n-9	1.0 ± 0.26	0.60 ± 0.02[#]	0.59 ± 0.04[#]
C17:1	0.07 ± 0.02	0.08 ± 0.02	0.10 ± 0.01
C18:1n-7	2.1 ± 0.35	1.6 ± 0.22	1.6 ± 0.15
C18:1n-9	11.5 ± 2.17	8.0 ± 0.31	7.9 ± 0.37[#]
C20:1n-6	0.14 ± 0.02	0.12 ± 0.01	0.13 ± 0.01
C24:1n-9	0.60 ± 0.03	0.53 ± 0.02	0.66 ± 0.05[#]
∑ MUFA (%)	**15.6 ± 2.86**	**11.1 ± 0.62[#]**	**11.2 ± 0.64**

PUFA			
C18:2n-6	13.1 ± 0.73	13.3 ± 1.79	13.8 ± 0.36
C18:3n-3	0.07 ± 0.008	0.06 ± 0.02	0.06 ± 0.008
C20:2	0.20 ± 0.04	0.17 ± 0.03	0.26 ± 0.02[#]
C20:3	0.94 ± 0.09	0.82 ± 0.10	0.72 ± 0.06
C20:4	18.6 ± 0.39	19.2 ± 1.0	19.8 ± 0.58
C20:5n-3	0.13 ± 0.01	0.10 ± 0.01	0.11 ± 0.01
C22:5n-3	0.38 ± 0.04	0.31 ± 0.04	0.35 ± 0.04
C22:6n-3	8.1 ± 0.35	8.3 ± 0.64	8.5 ± 0.23
∑ PUFA (%)	**42.3 ± 1.66**	**42.3 ± 3.63**	**43.6 ± 1.31**

Abbreviations: HFD, high-fat diet; WFM, whole-fat milk; NFM, non-fat milk; SFA, saturated fatty acids; MUFA, monounsaturated fatty acids; PUFA, polyunsaturated fatty acids. Data expressed as mean ± SEM (n = 6 / group; fasted), analyzed by one-way ANOVA followed by Tukey's post-hoc test. Different lowercase letters indicate $p < 0.05$ and [#] represents a trend of $0.05 < p < 0.1$.

5.2 Discussion

Dairy consumption reduces the risk and incidence of MASLD, however, the mechanism of action has yet to be elucidated and is likely to vary depending on the dairy product [88]. In this chapter, in which I used the model of metabolic dysfunction described in Chapter 4, I provided data consistent with my hypothesis that a low dose (equivalent to less than half a serving) of NFM supplementation significantly reduces BW gain and body fat mass and, importantly, reduces hepatic lipid accumulation without changes in food intake. In contrast, WFM treatment did not improve body composition and only partially mitigated hepatic steatosis. This suggests that NFM is superior to WFM in mitigating hepatic steatosis perhaps secondary to reduced BW gain and fat mass, which are known risk factors for metabolic dysfunction. Similarly, feeding skim milk powder to obese Sprague-Dawley rats significantly reduced weight gain and body fat %, pointing to a benefit of skim milk over WFM [100].

Moreover, observational research in an elderly Mediterranean population demonstrated an inverse relationship between low-fat milk consumption and risk of MetS, with no association seen with WFM [141]. Previously discussed studies found similar results, with an increased intake of low-fat milk inversely associated with T2D and MASLD risk in various adult populations [89], [142]. The data from this study can serve to support dietary recommendations for those at risk of metabolic dysfunction and contribute to resolving the controversy between WFM and NFM. However, this is not to propose that there are no metabolic benefits of WFM as mild mitigation of hepatic steatosis was demonstrated, but to a lesser extent than NFM, which suggests that NFM has a greater therapeutic benefit.

Overnight FBG was reduced in NFM compared to WFM, suggesting a healthier metabolic phenotype. However, AUC for PTT corrected to baseline displayed significant

elevation in the NFM group compared to WFM, consistent with altered control of gluconeogenesis. In a RCT of adult participants, consumption of 3.3 servings of either WFM or NFM per day resulted in a reduction of the Matsuda insulin sensitivity index and an increased HOMA-IR, suggesting that increased dairy intake impairs glucose tolerance compared to limited dairy controls [143]. Further, WFM displayed reduced oral disposition index, pointing towards impaired β-cell insulin secretion, a relationship not indicated in the NFM group. NFM consumption with a fat-containing meal in male adults enhanced post-prandial insulin secretion, pointing to blunted hyperglycemia, and promoted lipid metabolism by NFM compared to a milk protein only drink [144]. Overall, more research is required to determine the effect of NFM over WFM as my data supports a beneficial role post-prandially. The fasting data are equivocal because FBG was reduced but a possible increased capacity for hepatic gluconeogenesis was indicated in the PTT.

Hepatic lipid content and accumulation were different between groups, displaying morphological and metabolic differences in lipid metabolism. In NFM-fed mice, the reduction in hepatic steatosis was evidenced by a reduction in the number and total area of hepatic parenchyma covered by LDs, and lower hepatic TG compared to HFD. WFM treatment did not reduce LD numbers but tended to reduce the area covered by LDs. Similar results to NFM were observed in C57BL/6 mice supplemented with phospholipid-rich dairy milk [95]. Dairy phospholipids are mainly found on the MFGM in WFM and membranous material in NFM, and phosphatidylethanolamines (PE) are the most abundant PL in milk fat [145]. PE comprises several distinct FAs, among which C16:0, C18:0, C18:1n-9, and C18:2n-6 constitute the largest proportion, with differences present when looking at MFGM in isolation versus WFM [146]. SFA and MUFA have various implications on metabolic health, with positive associations found

between plasma phospholipids C16:0 and C18:0 and T2D, and enhanced C18:1n-9 and C18:2n-6 seen in human NASH hepatocytes [147], [148].

However, our analysis of hepatic lipid profiles displayed only small differences between individual FA in the WFM and NFM groups. In obese patients with MASLD, overall hepatic PUFA lipid content was lower with individual FA 20:4n-6, 22:5n-3, and 22:6n-3 reduced when compared to controls [149]. Docosapentaenoic acid (DPA, 22:5n-3) and docosahexaenoic acid (DHA, 22:6n-3) are commonly known as beneficial omega-3 FA, with their consumption resulting in improvements demonstrated in heart rate, blood pressure, circulating lipids, and anti-inflammatory effects [150]. Arachidonic acid (20:4n-6) affects lipid metabolism, with supplementation for 7 weeks in California yellowtail juveniles resulting in improved blood cortisol and FBG, and enhanced expression of hepatic β-oxidation enzyme *Cpt1a* and reduced expression of *Fas* [151]. Although not statistically significant, NFM increased overall PUFA content by almost 23% compared to HFD, with DPA increased by 36%, DHA increased by 32%, and arachidonic acid by 31%. This may reflect a healthier metabolic phenotype in the total lipid pool compared to HFD groups, complementing the human and animal findings within the literature.

Considering the significant difference in hepatic morphology, metabolic parameters, and liver content, our next step was to determine the mechanism of action by which NFM, and WFM to a lesser extent, prevented hepatic steatosis and promoted a healthier metabolic phenotype. Based on the phenotypic data, I predict that the molecular effects in the liver will be more pronounced in the NFM group.

Chapter 6: Molecular mechanisms of dairy milk interventions

6.1 Results

Of hepatic genes within the four arms of lipid metabolism only *Opa1* ($p < 0.05$) was higher in WFM compared to HFD and a trend towards enhanced expression of *Mttp* in WFM was noted compared to HFD ($p = 0.07$) and NFM ($p = 0.06$) (Figure 6.2). Western blot was completed to assess if gene expression patterns were continued or altered at the protein level with a summary of the proteins measured displayed in Figure 6.1.

6.1.1 Liver lipid transporters and *de novo* lipogenesis

FA transporter CD36 was unchanged between groups (Figure 6.3A) but a regulator of FA uptake, FABP4 trended towards enhanced abundance in the WFM group compared to NFM (Figure 6.3B, $p = 0.059$). FAS, the rate limiting enzyme for DNL, was significantly higher in WFM compared to NFM ($p < 0.05$) (Figure 6.3C) but there was no difference between groups in ACS abundance (Figure 6.3D). p-ACC had altered responses to diet (two-way ANOVA, $p < 0.05$). There was higher abundance in the insulin-stimulated WFM group compared to NFM, where it was nearly undetectable in many samples ($p = 0.069$) (Figure 6.3E). Also, total ACC trended towards higher abundance in insulin-stimulated WFM compared to NFM ($p = 0.097$) (Figure 6.3F). In addition, two-way ANOVA revealed a significant diet x insulin-stimulation interaction for p-ACL ($p < 0.05$) and a significant effect of diet ($p < 0.05$). The ratio of p-ACL / ACL also displayed significant diet x insulin stimulation interaction, with insulin increasing versus decreasing p-ACL in NFM versus WFM ($p < 0.05$) and a similar trend for NFM compared to HFD ($p = 0.060$). There were also independent effects of diet and insulin ($p = 0.0013$, $p <$

0.0001 respectively) (Figure 6.3G). There was no difference in total ACL between groups (Figure 6.3H).

6.1.2 Liver fatty acid oxidation

Within the OXPHOS complexes, there were consistent increases in Complex I (Figure 6.4A, $p = 0.088$), Complex II (Figure 6.4B, $p < 0.05$) and Complex IV (Figure 6.4D, $p < 0.05$) in NFM compared to WFM ($p = 0.088$), although Complexes III (Figure 6.4C) and V (Figure 6.4E) were not different between groups. The enzyme that catalyzes acyl-carnitine production and transport into the mitochondria, CPT1α was significantly higher in WFM compared to HFD ($p < 0.05$) (Figure 6.4G).

6.1.3 Liver lipogenesis and export

With FA synthesis and export proteins, there were no differences between groups for ATGL (Figure 6.5A). MTP trended towards higher abundance in NFM compared to WFM ($p = 0.076$) with no difference between any other groups (Figure 6.5B).

6.1.4 Liver lipid metabolism modulators

Western blots were also completed for key regulatory proteins within the lipid metabolism arms. PPARγ trended towards higher abundance in NFM compared to HFD ($p = 0.068$) (Figure 6.6G). There were no differences seen between groups for p-AMPKα, AMPKα, p-AMPKα / AMPKα, p-AMPKβ, AMPKβ, and p-AMPKβ / AMPKβ (Figure 6.6A-F).

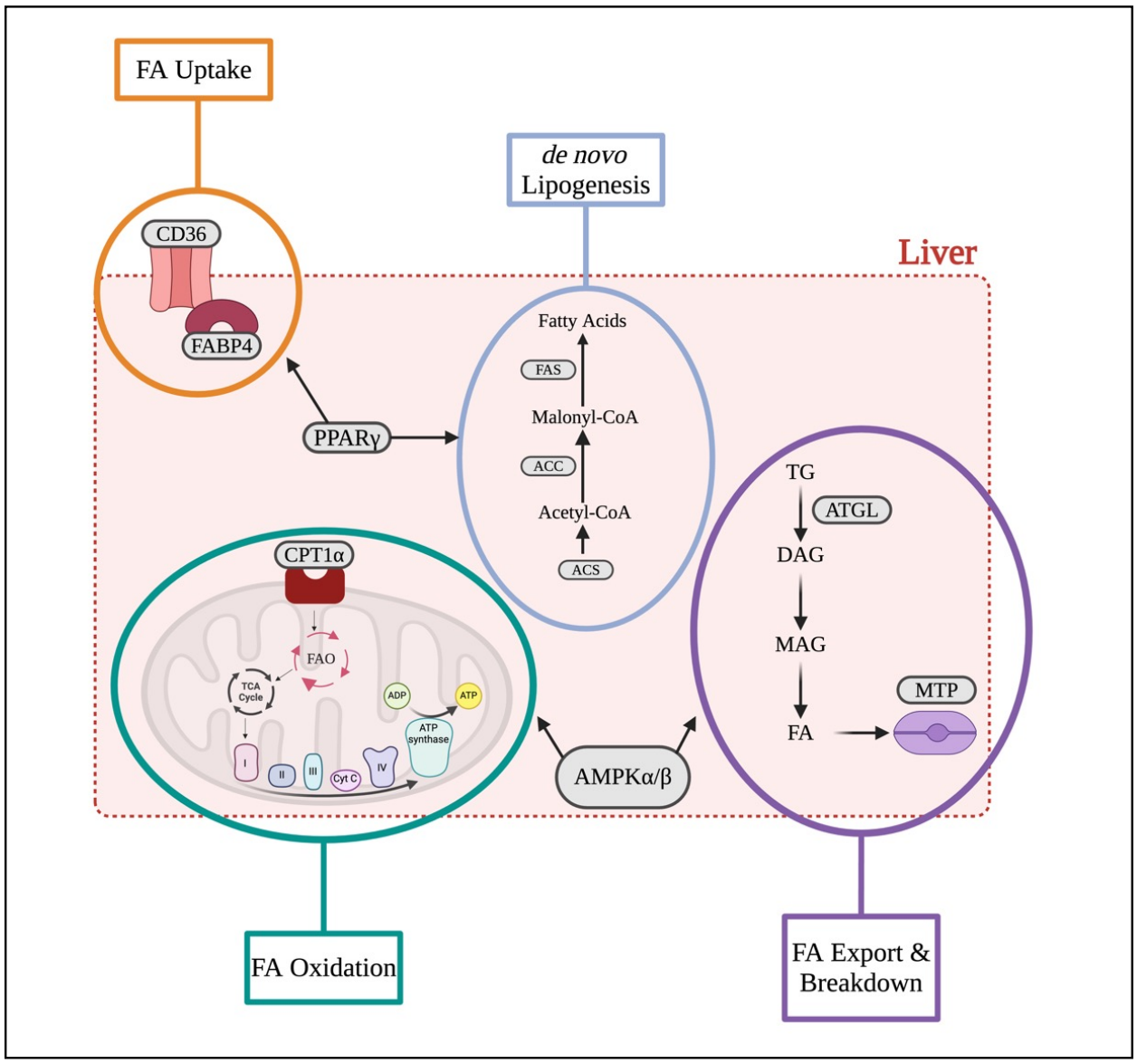

Figure 6.1. Summary of proteins within lipid metabolism measured by qPCR and western blot within milk-supplemented groups. Proteins coloured grey denote proteins of interest. Created by EB with biorender.com.

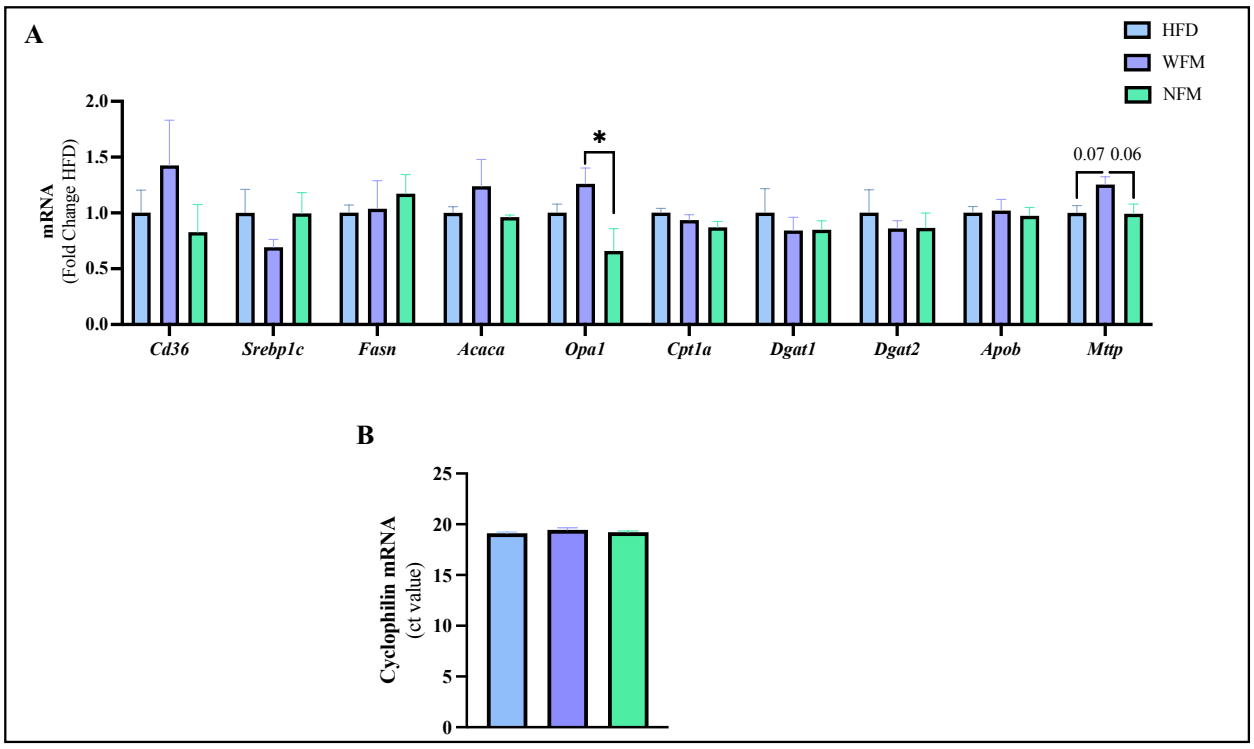

Figure 6.2. Hepatic mRNA expression of lipid metabolism genes in overnight fasted mice.

(A) Comparison of HFD groups (n = 6 / group). Gene expression was normalized to cyclophilin (B). Data analyzed by one-way ANOVA followed by Tukey's post-hoc test. * Indicates $p < 0.05$.

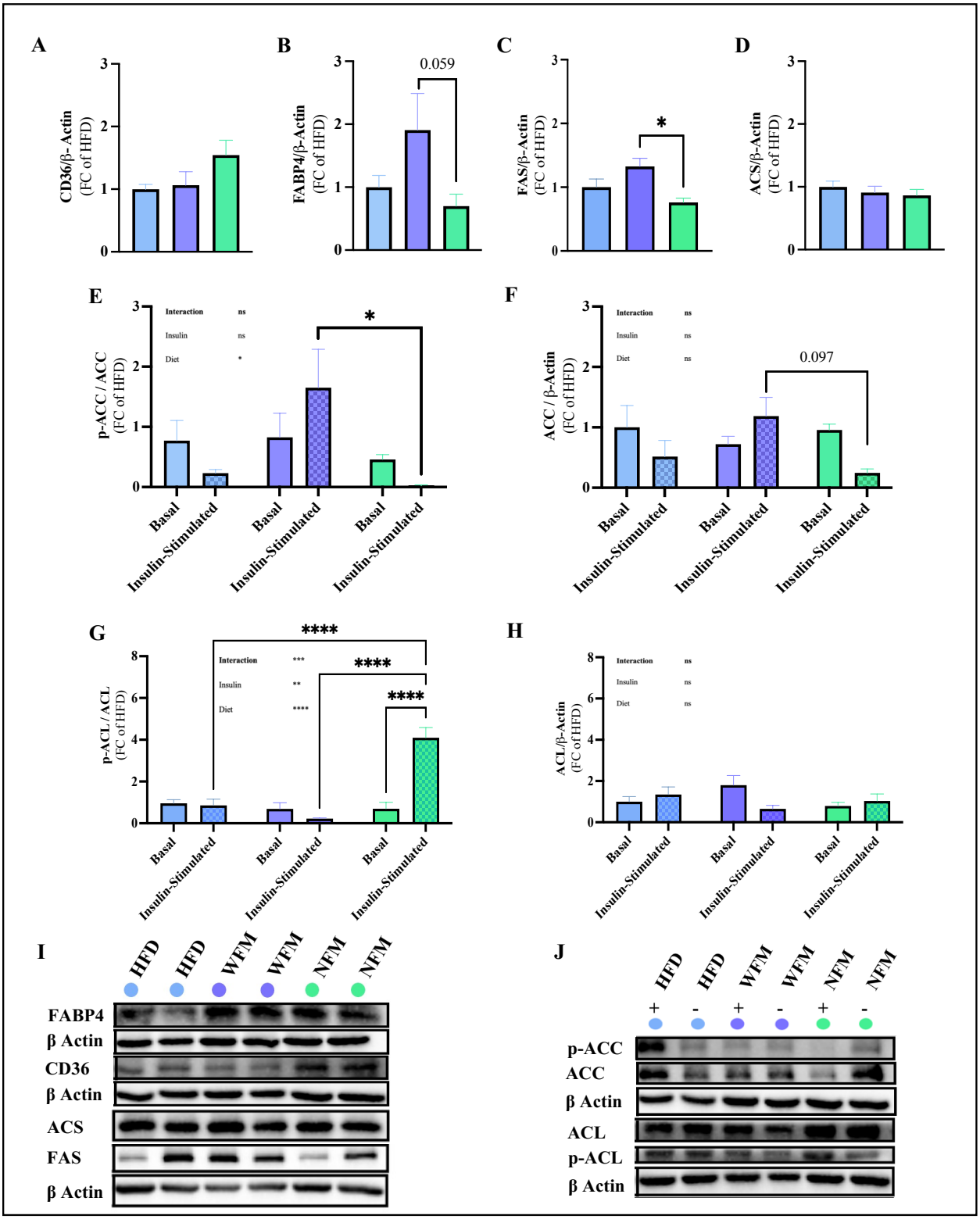

Figure 6.3. Liver lipid transporters and de novo lipogenesis enzyme abundance in tissue from overnight fasted mice. (A) CD36; (B) FABP4, fatty acid binding protein 4; (C) FAS, fatty

acid synthase; (D) ACS, acetyl-CoA synthetase; (E) p-ACC / ACC, acetyl-CoA carboxylase; (F) ACC; (G) p-ACL / ACL, ATP-citrate lyase; (H) ACL; (I, J) representative western blots. Proteins were normalized to β-actin. Data expressed as mean ± SEM. Sample size for A-D was n = 8 (combined basal and insulin-stimulated) and for E-H n = 4 for basal and n = 4 for insulin-injected. Data analyzed by one-way ANOVA (A-D), and two-way ANOVA (E-H) followed by Tukey's post-hoc test for effect of diet and insulin. * Indicates $p < 0.05$, **** indicates $p < 0.0001$.

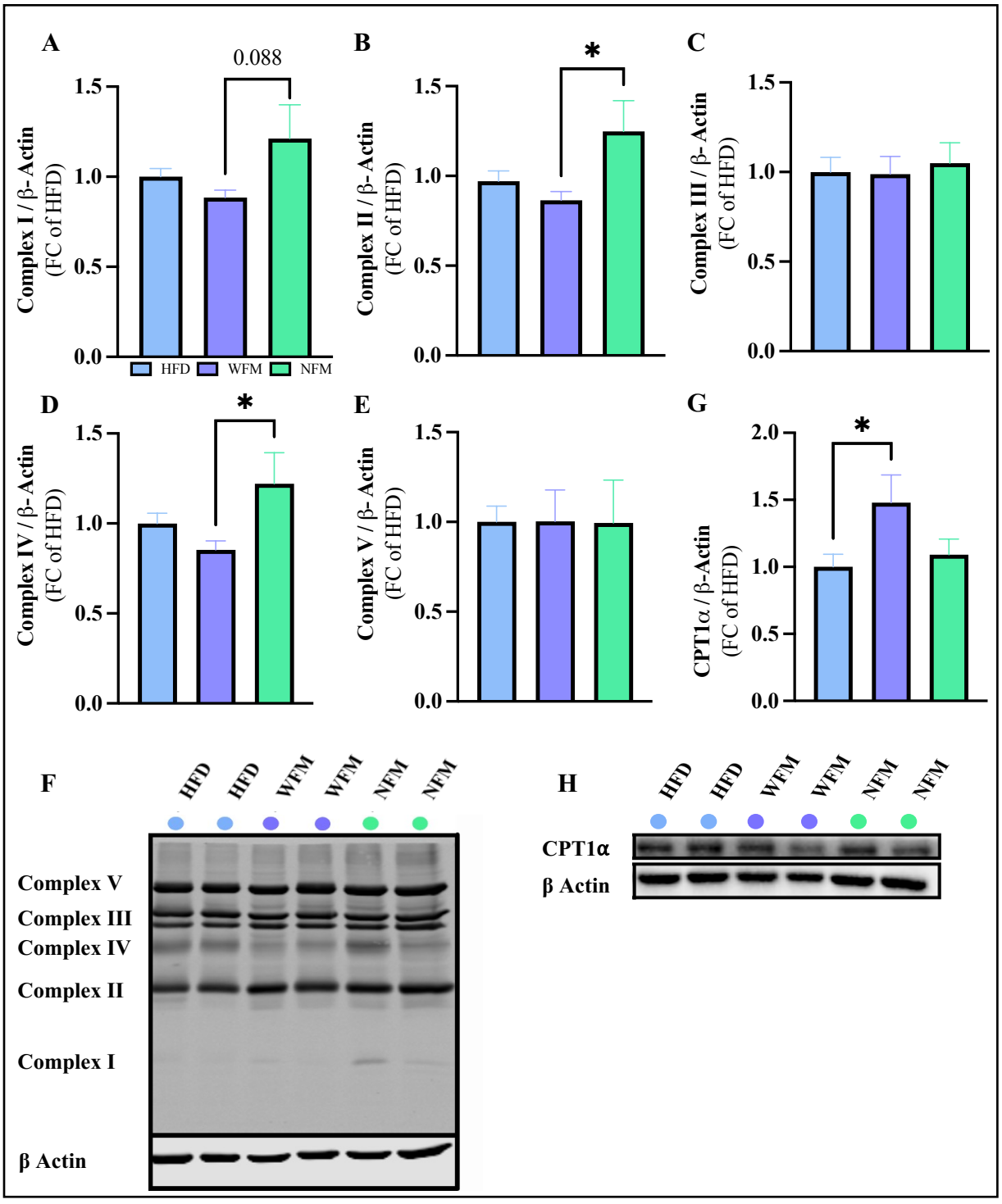

Figure 6.4. Liver fatty acid oxidation protein abundance in tissue from overnight fasted mice. (A-E) OXPHOS mitochondrial complexes I-V; (F) OXPHOS representative western blot; (G) CPT1α, carnitine palmitoyltransferase 1α; (H) CPT1α representative western blot. Proteins

were normalized to β-actin. Data expressed as mean ± SEM (n = 8 / group; combined basal and insulin-stimulated). Data analyzed by one-way ANOVA followed by Tukey's post-hoc test. * Indicates $p < 0.05$.

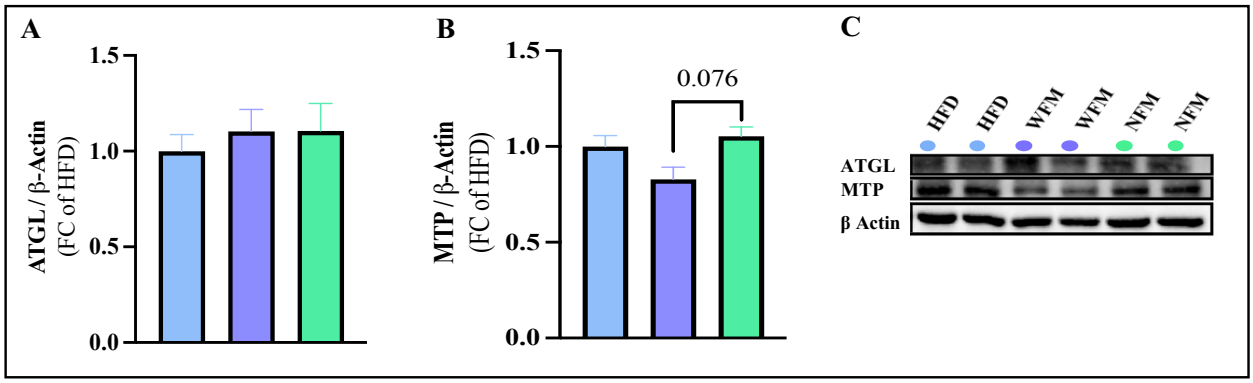

Figure 6.5. Liver lipogenesis and export protein abundance in tissue from overnight fasted mice. (A) ATGL, adipose triglyceride lipase; (B) MTP, microsomal triglyceride transfer protein; (C) representative western blot. Proteins were normalized to β-actin. Data expressed as mean ± SEM. Sample size was n = 8 (combined basal and insulin-stimulated). Data analyzed by one-way ANOVA followed by Tukey's post-hoc test.

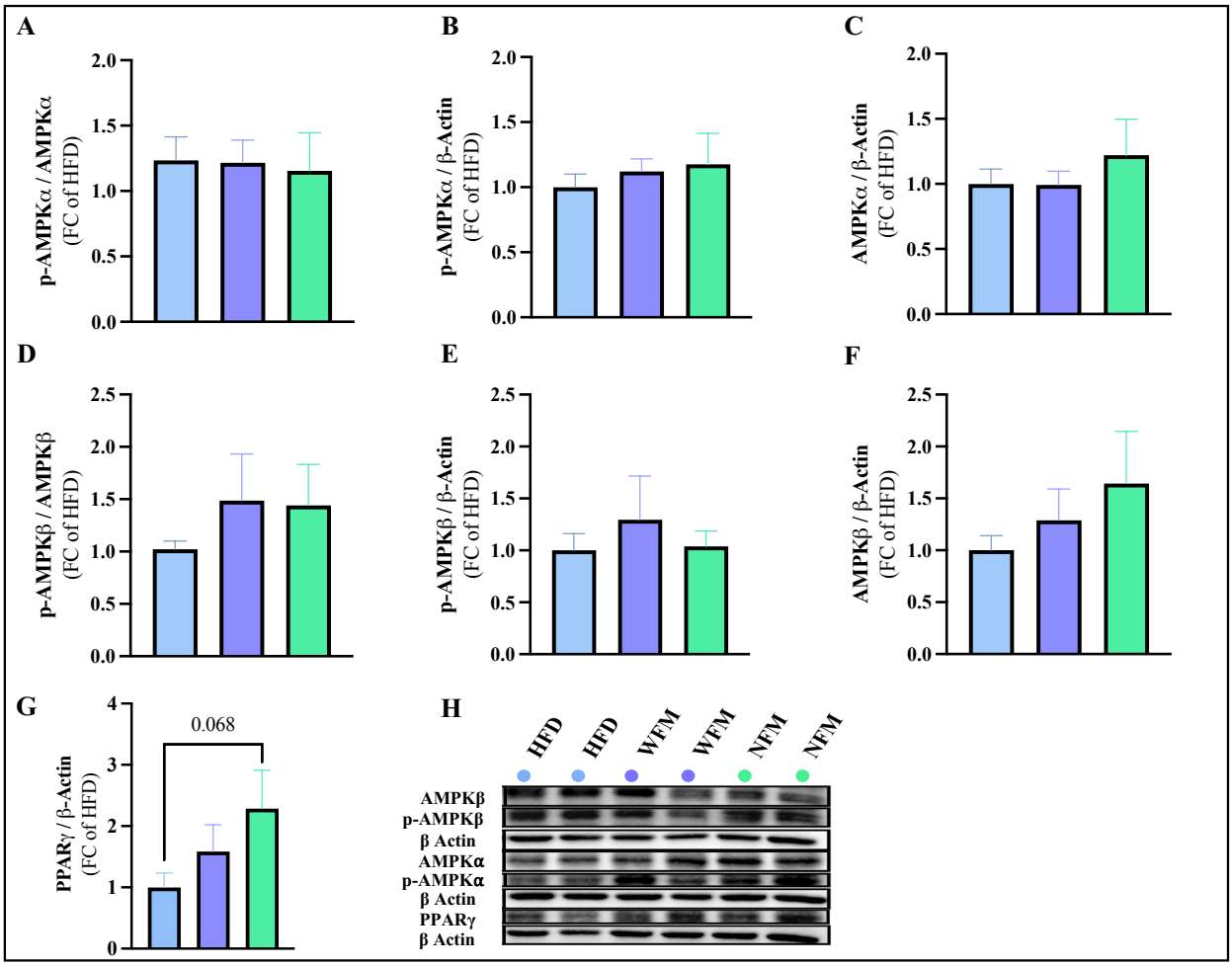

Figure 6.6. Liver lipid metabolism regulatory protein abundance in tissue from overnight fasted mice. (A) p-AMPKα / AMPKα, AMP-activated protein kinase α; (B) p-AMPKα; (C) AMPKα; (D) p-AMPKβ / AMPKβ; (E) p-AMPKβ; (F) AMPKβ; (G) PPARγ, peroxisome proliferator-activated receptor γ; (H) representative western blot. Proteins were normalized to β-actin. Sample size was n = 8 (combined basal and insulin-stimulated). Data analyzed by one-way ANOVA followed by Tukey's post-hoc test.

6.2 Discussion

The objective of this chapter was to characterize and compare regulation of hepatic lipid metabolic pathway(s) by NFM and WFM. Based on the results in Chapter 5, showing that NFM was more effective in reducing liver fat, I hypothesized that NFM would induce metabolic pathways associated with increased fat oxidation and/or export. Overall, my data supports the hypothesis, with NFM increasing proteins of the mitochondrial oxidative phosphorylation complexes while also reducing some enzymes that regulate DNL. Whereas the WFM effects on lipid metabolic enzymes would be predicted to increase FA uptake and possibly DNL. Neither milk product reversed the decrease in AMPK or p-AMPK noted in HFD mouse livers (Chapter 4).

FA oxidation is the process by which FA are transported into the mitochondrial matrix by the rate-limiting enzyme CPT1α and targeted to undergo β-oxidation and oxidative phosphorylation [152], [153]. Mitochondrial dysfunction is intricately linked to MASLD progression, as chronic activation of FA oxidation in the presence of elevated plasma and hepatic TGs can result in increased ROS, ATP depletion, and mitochondrial apoptosis [154]. WFM increased the abundance of CPT1α compared to HFD, which could promote shuttling of FA into the mitochondrial matrix. However, complexes I, II, and IV were higher than HFD in NFM and not WFM, suggesting a greater oxidative phosphorylation capacity. Supplementation of the milk protein whey in Sprague Dawley rats yielded reduced hepatic oxidative stress and restoration of complex I, II, and IV activity [155], and in a T2D model whey lowered hepatocyte oxidative stress, enhanced mitochondrial function, and sustained ATP production *in vitro* [156]. This may suggest a potential bioactive role of milk protein, however the difference between protein content

in the overall diet of our animals was less than 1 mg, indicating a difference of less than 0.2 mg of whey intake solely from the NFM versus WFM.

Regarding lipid uptake, I found weak evidence for increased capacity with non-significant increases for FABP4 abundance in WFM group compared with HFD ($p < 0.1$), and ~50% increase in CD36 abundance in NFM versus WFM. Although gene expression of the DNL enzymes *Fasn* and *Acaca* were similar between groups, FAS protein abundance was enhanced in WFM. FAS catalyzes the synthesis of *de novo* FA from malonyl-CoA, acetyl-CoA, and NADPH, suggesting increased lipogenic capacity in this group compared to NFM [157]. However, the ratio of p-ACC to total ACC was significantly higher in the WFM group. p-ACC is the inactive form of the enzyme and signifies a lack of substrate availability for FAS. Overall, the histology, direct measurement of TG, and molecular results support the hypothesis of reduced hepatic lipid production in the NFM group whereas WFM results are equivocal. Neither NFM nor WFM altered AMPK proteins or their phosphorylation relative to HFD. Thus, the ability of hepatocytes to switch from fat to carbohydrate metabolism or respond to low energy availability may still be impaired [158].

As the metabolic and molecular results from the liver displayed alterations in the NFM group compared to WFM and HFD, and because of the inter-organ crosstalk described in Chapter 1, I questioned whether these effects on lipid or glucose metabolism would be evident elsewhere to promote a healthier metabolic phenotype. I hypothesized that skeletal muscle may play a protective role in reducing lipid and glucose metabolic dysfunction, as it is essential to both glucose storage and utilization as well as being a key consumer of FA [159]. NFM also displayed an enhancement of lean muscle mass % and a reduction of BW gain, suggesting an

altered metabolic phenotype compared to WFM. Thus, the next chapter will outline findings in skeletal muscle in LFD, HFD, NFM, and WFM groups.

Chapter 7: Alterations in skeletal muscle metabolism

7.1 Results

7.1.1 Skeletal muscle glucose metabolism

When comparing the LFD and HFD groups, there were no notable variances observed in central regulatory proteins of glucose metabolism, AMPKα, AMPKβ, or Akt, including the ratio of phosphorylated to total protein (Figure 7.1). Similarly, the NFM and WFM groups displayed no significant differences in the three proteins of interest when compared to HFD. However, there was a notable trend towards higher levels of p-Akt / Akt within the NFM group, indicating a potential augmentation of insulin-dependent glucose uptake (Figure 7.2).

7.1.2 Skeletal muscle lipid metabolism

Within key lipid pathway proteins, LFD had higher abundance of SIRT1 compared to HFD ($p < 0.05$), with no significant differences seen in CD36, PGC1α, or CPT1α (Figure 7.3). NFM and WFM displayed lower abundance of CD36 compared to HFD ($p < 0.01$ and $p < 0.05$ respectively), suggesting a reduction in FA uptake (Figure 7.4). WFM had higher abundance of SIRT1 compared to NFM ($p < 0.05$) and HFD ($p = 0.079$), suggesting a higher utilization of FA present in the muscle tissue. There were no other differences between the HFD groups for PGC1α or CPT1α.

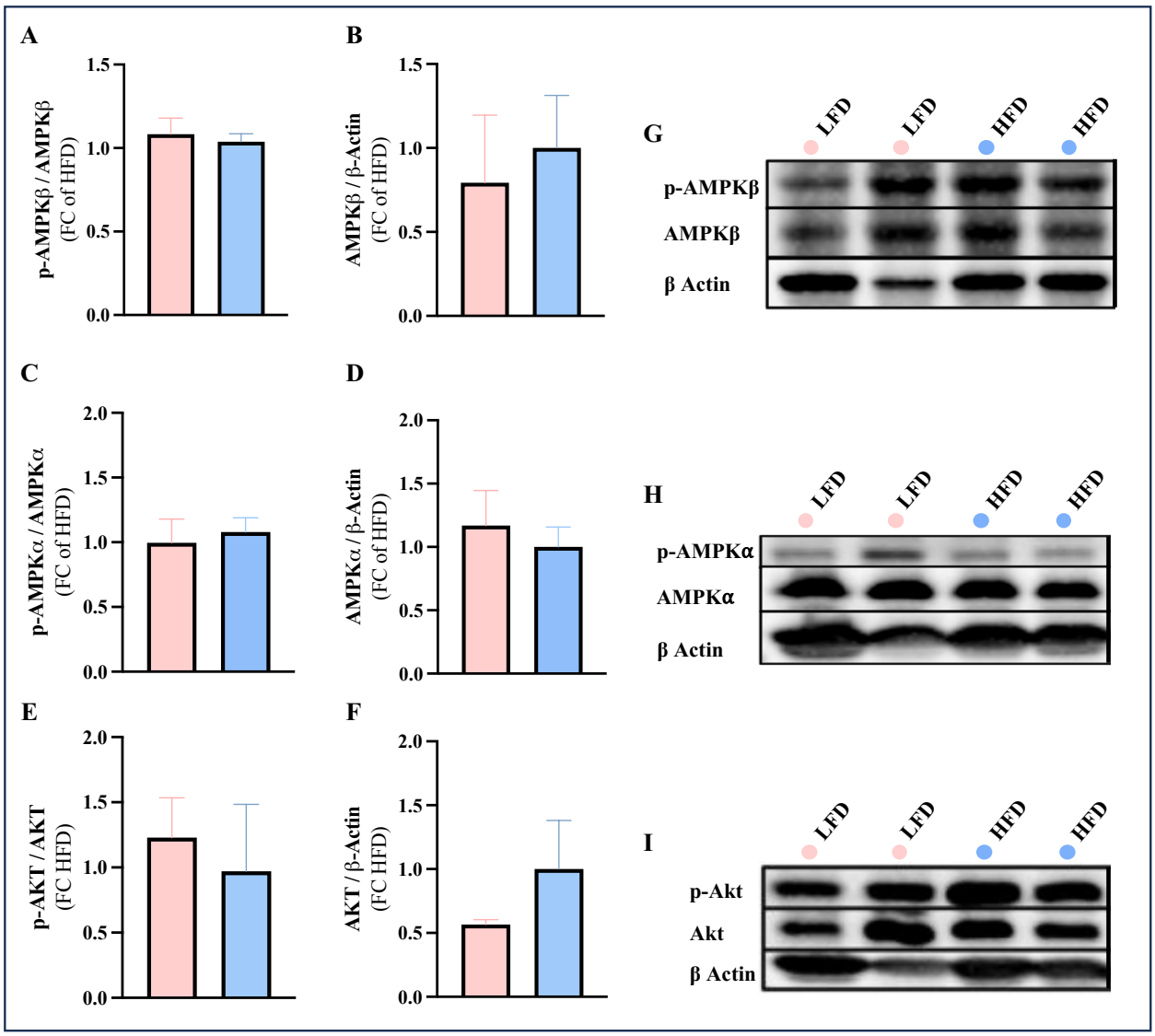

Figure 7.1. Skeletal muscle glucose metabolism protein abundance for LFD and HFD in tissue from overnight fasted mice. (A) p-AMPKβ / AMPKβ; (B) AMPKβ; (C) p-AMPKα / AMPKα; (D) AMPKα; (E) p-Akt / Akt; (F) Akt; (G-I) representative western blots. Sample size for A-D was n = 8 (combined basal and insulin-stimulated), E-F was n = 4 (insulin-stimulated). Data analyzed by two-tailed t-test.

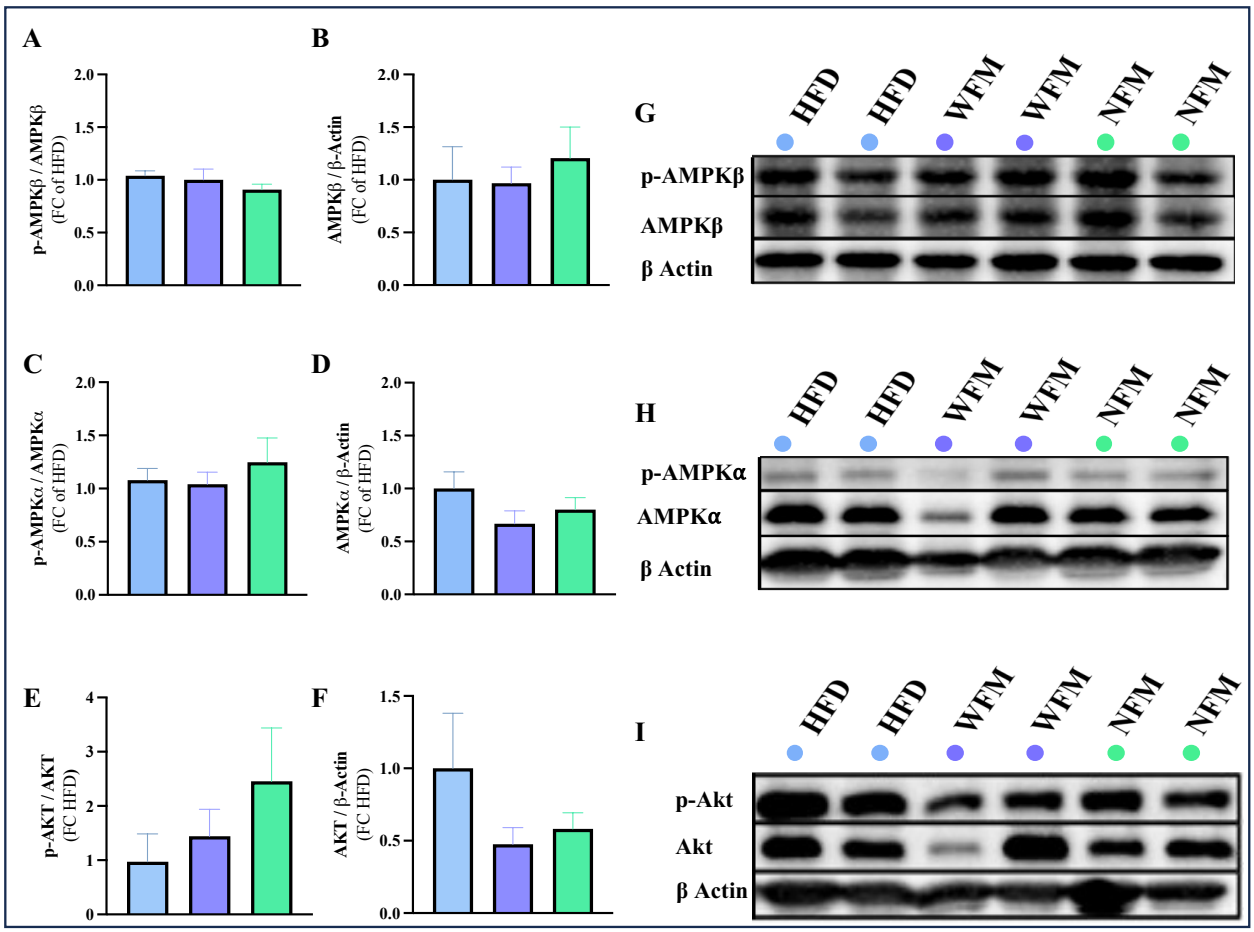

Figure 7.2. Skeletal muscle glucose metabolism protein abundance for NFM and WFM supplemented mice in tissue from overnight fasted mice. (A) p-AMPKβ / AMPKβ; (B) AMPKβ; (C) p-AMPKα / AMPKα; (D) AMPKα; (E) p-Akt / Akt; (F) Akt; (G-I) representative western blots. All proteins normalized to β-Actin. Sample size for A,B,C,D was n = 8 (combined basal and insulin-stimulated); E,F sample size was n = 4 (insulin-stimulated). Data analyzed by one-way ANOVA.

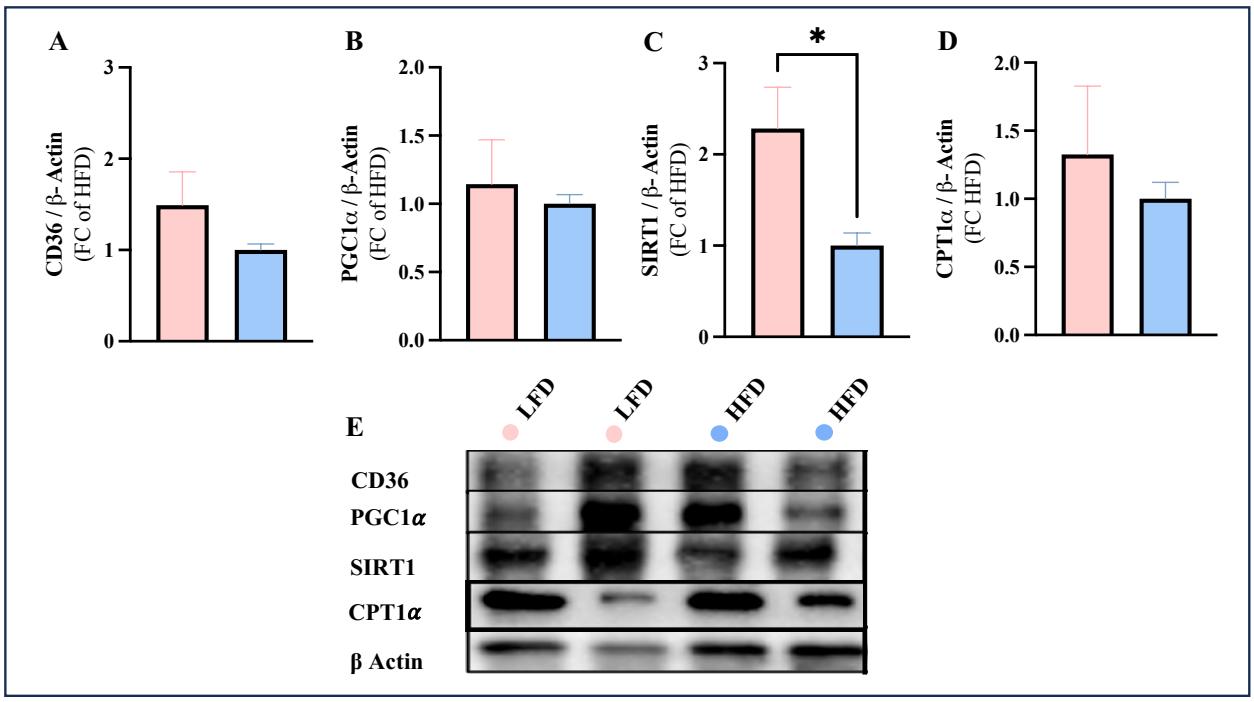

Figure 7.3. Skeletal muscle lipid metabolism protein abundance for overnight-fasted LFD and HFD mice. (A) CD36; (B) PGC1α; (C) SIRT1; (D) CPT1α (E) representative western blot. All proteins normalized to β-Actin. Sample size for A, C was n = 4 (basal). Sample size for B, D was n = 8 (combined basal and insulin-stimulated). Data analyzed by two-tailed t-test. * Indicates $p < 0.05$.

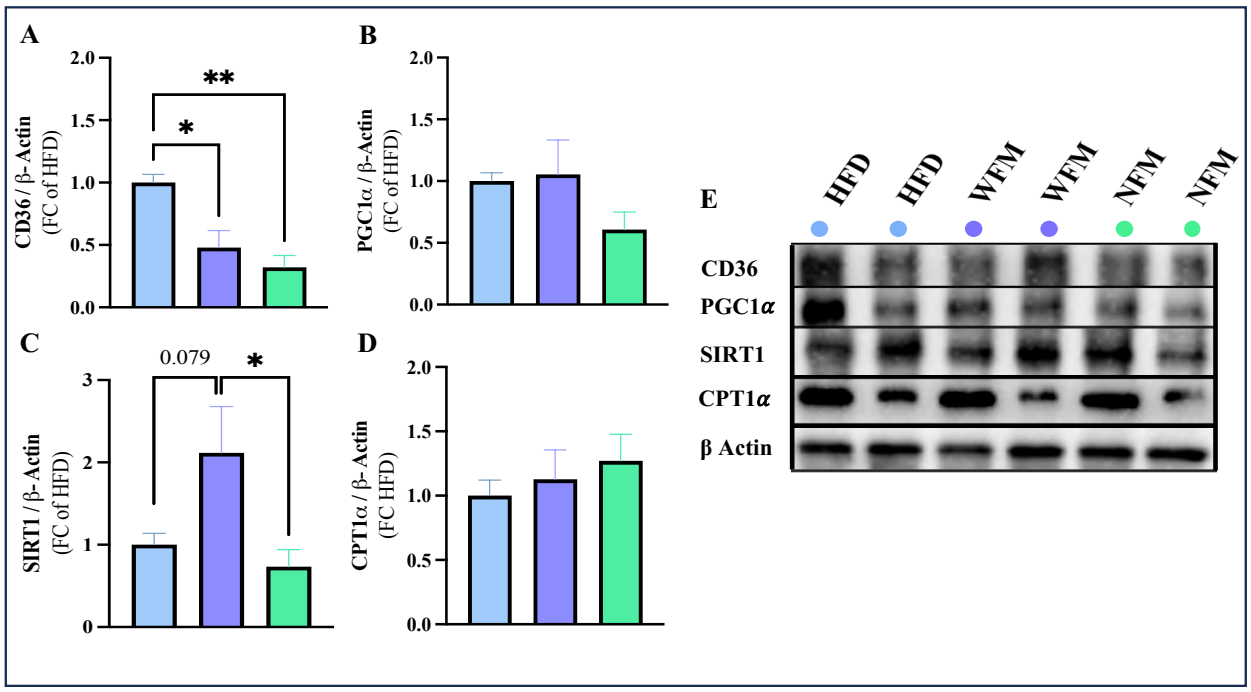

Figure 7.4. Skeletal muscle lipid metabolism protein abundance for overnight fasted mice. (A) CD36; (B) PGC1α; (C) SIRT1; (D) CPT1α (E) representative western blot. All proteins normalized to β-Actin. Sample size for A, C was n = 4 (basal). Sample size for B, D was n = 8 (combined basal and insulin-stimulated). Data analyzed by one-way ANOVA. * Indicates $p < 0.05$, ** indicates $p < 0.01$.

7.2 Discussion

Skeletal muscle plays an integral role in maintaining glucose and lipid homeostasis, and I hypothesized that NFM would more effectively enhance glucose and lipid metabolism in the skeletal muscle than WFM. Such an outcome would have the potential to reduce the load on the liver and promote a healthier metabolic profile. However, this hypothesis was refuted as glucose metabolism regulators Akt and AMPK displayed no significant abundance changes with milk supplementation, with only a trend to increased abundance in p-Akt / Akt after NFM treatment. However, these results should be interpreted with caution because the Akt and AMPK pathways were not altered by HFD compared with LFD; thus, marked effects of milk treatment might not be expected.

On the other hand, lipid metabolism showed the opposite results as expected as CD36 abundance was lower in both WFM and NFM compared to HFD, and SIRT1 abundance, which is important for FA oxidation, was higher in the WFM compared to NFM, which essentially returned SIRT1 to a similar level as observed in the LFD group.

Other studies found that more severe MASH in C57BL/6N mice results in the overexpression of skeletal muscle microRNA-34a (miR-34a), a microRNA that inhibits SIRT1 and AMPK, and skeletal muscle SIRT1 and p-AMPK abundance were reduced [160]. Our HFD results are consistent with the SIRT1 but not the p-AMPK profile, suggesting that the latter develops later in the pathogenesis of MASLD. SIRT1 also plays a role in mediating inflammation in the skeletal muscle, with enhanced abundance mitigating muscle atrophy, inflammatory cytokine production and enhancing ROS scavenging [161], [162]. This may provide an alternate pathway WFM may be acting and be a future direction for further research.

IMCL in skeletal muscle can have contradictory effects, with enhanced abundance associated with IR and chronic metabolic dysfunction, while also providing essential fuel during periods of activity [163], [164]. Although I was unable to run TG assays and histological analysis on the skeletal muscle in this study, a previous RCT in adults found that high-protein, low-fat skimmed milk drinks reduced IMCL compared with low-protein, high-fat diets [165]. T2D and prediabetes have both been associated with an increase in IMCL, suggesting that an attenuation of IMCL accumulation by dairy may provide a therapeutic benefit for metabolic disorders [166]. This is a future gap that could be assessed.

MASLD and skeletal muscle are intricately linked as evidenced by a 7-year longitudinal study of ten thousand individuals without and 3000 with MASLD that showed an inverse relationship between relative muscle mass and MASLD incidence [167]. Muscle mass was also positively associated with the resolution of MASLD, suggesting that there is a protective factor. Dairy intake attenuated sarcopenia, loss of skeletal muscle mass, in a RCT studying adults over 60 years of age [168]. In adult female LCR rats, milk protein supplementation reduced fat mass %, and LDL content and enhanced mitochondrial biogenesis in the plantaris muscle [169]. This animal trial was conducted over 21 weeks, potentially highlighting a limitation in the short duration of our study in replicating the beneficial effects in skeletal muscle. This may also indicate that the muscle mass of our animals was not enhanced to the point of altered metabolic function, highlighting a future research area.

Chapter 8: General discussion and conclusion

8.1 Summary of hypothesis and main findings

The global incidence and prevalence of MASLD, in association with T2D, MetS, and obesity are increasing rapidly, each acting as their own global epidemic. Functional foods, such as dairy products, have demonstrated significant beneficial effects in reducing the progression of MASLD and the incidence of concurrent metabolic disorders, providing a possible therapeutic that can reduce the burden of MASLD while pharmacological treatments are still in development [13]. Moreover, foods that reduce fatty liver could be used preventatively before therapeutic agents are prescribed. In this study, I hypothesized that both NFM and WFM would significantly improve diet-induced hepatic lipid accumulation and prevent the initiation of early-stage MASLD in C57BL/6 mice but via different mechanisms. Overall, the data support the hypothesis, but with NFM being superior to WFM. NFM significantly reduced BW gain and fat mass %, hepatic lipid accumulation and TG, and enhanced the abundance of enzymes involved in FA oxidation.

Interestingly, while not improving body composition, WFM did elicit a strong trend to reduced hepatic lipid accumulation but enhanced both hepatic DNL and FA oxidation protein abundance, which would be predicted to have antagonistic effects. Further investigation into the skeletal muscle did not support our hypothesis of a potential protective role of the skeletal muscle as there was a reduction in the capacity for FA uptake, and no consistent changes in enzyme pathways that might contribute to glucose uptake or lipid oxidation in either WFM or NFM tissues. This suggests that the skeletal muscle is not playing the role I proposed and leaves open future directions into other organs involved in MASLD such as the adipose tissue, pancreas, and gut.

8.2 Impacts of dairy and its components on hepatic lipid metabolism

Dairy consumption reduces the risk and incidence of MASLD, however, the mechanism of action has yet to be elucidated and is likely to vary depending on the dairy product [88]. In this study, I demonstrated that a low dose (equivalent to a third of a human serving) of NFM significantly reduces hepatic lipid accumulation, as evidenced by a reduction in the number and total area of hepatic parenchyma covered by LDs, and lower hepatic TG compared to HFD. Whereas WFM treatment did not reduce LD numbers but tended to reduce the area covered by LDs.

Milk as a functional food has certain nutrients and bioactive molecules that could contribute to reducing hepatosteatosis. Choline, which is vital for the synthesis of cell membranes and neurotransmission, is associated with MASLD, with higher intake associated with lower incidence risk [110], [111]. Choline may prevent hepatic lipid accumulation, because choline-deficient bovine hepatic cells display significantly larger LD, hepatocyte TG content, and FAS [112]. Other studies demonstrate normalization of HFD-induced weight gain in a mouse model and enhanced FA oxidation with choline supplementation *in vitro* [113], [114]. Dairy products are a common source of choline in the diet with both NFM and WFM containing 16 mg and 14 mg respectively in 100g of milk [111]. The dosage in each of these mouse studies ranged from 0.3-1 mg/day of total choline supplementation, compared with < 0.1mg/day in our study. The differences in choline between milk groups in our study are minimal (0.02 mg/day), and only represent 2-3% of the total choline intake from chow and milk combined, therefore I speculate this difference may not be enough by itself to result in the morphological and molecular changes seen. However, in combination with other elements of the dairy matrix, it is possible that choline plays a role. Choline in the chow is present as a salt, whereas choline in

milk segregates largely in the MFGM in the form of phospholipids, i.e. phosphatidylcholine. As previously described, phospholipids from dairy are implicated in improving cardiovascular risk, and research shows that diets enriched in phosphatidylcholine, but not free choline reduces atherosclerotic plaque formation and lowered circulating VLDL [106], [107], [170]. A mix of lipid-soluble choline forms fed to dams also reduced inflammatory cytokine production in gut-derived immune cells from their female offspring while a mix of free choline and phosphatidylcholine reduced gut permeability in inflammatory cytokines in a HFD rat model [171]. Thus, a role for choline cannot be completely ruled out and could be a potential future direction of study.

Calcium is another potential nutrient that is rich in milk and is involved in endoplasmic reticulum (ER) stress, and mitochondrial dysfunction in cells [115]. Calcium enhances the activity of Complex I and IV *in vitro* to facilitate oxidative phosphorylation [116]. Calcium supplementation of approximately 0.1 mg/day in C57BL/6 mice reduced hepatic steatosis, liver TG, epididymal fat, and enhanced hepatic ATGL activity [172]. As the calcium per dose in the NFM group is only 0.03 mg/day more than WFM and 1.6% of total calcium intake from chow and milk combined, it may not play a primary role in the differential molecular changes seen within the mitochondrial oxidative capacity and hepatic lipid accumulation in our study. However, as with choline, combining calcium with other elements of the dairy matrix, such as vitamin D, has demonstrated lower hepatic lipid accumulation, adiposity, and elevation of HDL-C in male Wistar rats [173]. This further supports our reasoning that the dairy matrix elements are acting in an additive factor rather than one single element in isolation causing these pronounced metabolic effects.

Milk protein is also a potential player in the modified lipid metabolism as the NFM diet contains 0.6 mg/day more milk protein compared to WFM. Casein and whey are major proteins in dairy milk with each displaying therapeutic properties, some of which have been described above [174]. Casein supplementation reduces BW gain, hepatic steatosis, and FAS activity in Sprague-Dawley rats and Leiden male mice [101], [102]. However, the Sprague-Dawley rats were supplemented with approximately 30 mg/day of casein and the Leiden mice were supplemented with approximately 9 mg/day, which is drastically higher than the difference between our milk groups. Whey intake of 7 mg/day also reduces hepatic TG, lipid accumulation, and DNL while enhancing FA oxidation in a mouse model [175]. As such, milk protein may contribute to eliciting the morphological and molecular changes seen in our study, but again, the additive effects of protein with the other bioactive components may be playing a larger role.

As our study focuses on the dairy matrix as a whole and not the individual components, it is important to understand that although the above studies remarked on the beneficial effects of certain molecules in isolation, other studies were unable to replicate the same benefits or instead found opposing effects. An increase in hepatotoxicity and inflammatory biomarkers was seen in male Wistar rats supplemented with whey whereas complete dairy supplementation improved BW and HOMA-IR in Sprague-Dawley rats compared to whey and casein supplementation alone [100], [120]. The additive effects of each bioactive molecule and nutrient such as choline, calcium, and milk proteins within the dairy matrix may be potentiating the benefits seen in our study.

8.3 Impacts of dairy on skeletal muscle glucose and lipid metabolism

Milk-derived nutrients may have direct effects on hepatic metabolism, or effects on other organs may elicit secondary improvement in liver steatosis. Skeletal muscle is one of the key players in glucose metabolism, responsible for approximately 80% of postprandial glucose uptake [176]. It is intricately linked with the adipose tissue and liver to balance glucose and lipid homeostasis. When this balance is disrupted by an excess of circulating glucose and lipids, as seen in MASLD, myosteatosis can develop, resulting in dysfunctional muscle tissue, atrophy, and worsened systemic IR [177]. Reduced skeletal muscle mass, known as sarcopenia, is positively associated with the development of MASLD, while sarcopenic obesity is associated with an even higher risk of MASLD [178]. Milk consumption positively associates with increased skeletal muscle mass, mitigating the risk of sarcopenia [179]. Although NFM mice in this study did not have more fat-free mass, which includes skeletal muscle, than WFM or HFD groups, it was higher as a percentage of total BW, which may confer some metabolic advantage.

I measured activation of two regulatory proteins of glucose uptake important in skeletal muscle, Akt and AMPK. No significant alterations of Akt were seen. However, I did see a 2-fold higher abundance of p-Akt / Akt in NFM ($p > 0.05$), suggesting enhanced capacity for glucose uptake through insulin-dependent pathways. In future studies, it may be beneficial to study Akt phosphorylation using a fasting-refeeding paradigm, which is more physiological than injecting animals with supraphysiological doses of insulin that could mask mild or moderate differences. AMPKα/β abundance and phosphorylation were similar across all groups, indicating a lack of enhancement of insulin-independent glucose uptake that may have mitigated the elevation of 4-hour FBG. Contrasting results have been seen in the literature as treatment with milk casein hydrolysate significantly increased p-AMPK in skeletal muscle cells grown in similar

environments and milk-fat globule supplementation up-regulated p-Akt in sarcopenic rats injected daily with D-galactose, promoting an increase in muscle glucose uptake [180], [181].

8.4 Impacts of dairy on a pre-disease state and clinical relevance

The central aim of this project was to determine dairy milk efficacy as an early intervention tool to mitigate the initiation of metabolic dysfunction and alleviate the burden of chronic disease. Almost 762 million individuals were diagnosed with prediabetes in 2021 and 35% of adults in North American have MASLD, highlighting the importance of preventative methods to attenuate progression [5], [34]. In the Lifelines Cohort Study, 112, 086 Dutch adults completed food frequency questionnaires and donated blood [182]. Out of the total number of participants, 25, 549 had pre-diabetes and low-fat dairy consumption was inversely associated with incident T2D. In an Australian adult population, a higher intake of high-fat dairy was associated with a lower risk of prediabetes following a 12-year longitudinal study [183]. Results from the Korean Genome and Epidemiology study display an inverse association with dairy-rich diets and MASLD risk [184].

These studies within human populations display the clinical relevance of proper dietary counselling and intervention. Current recommendations by Obesity Canada for providers suggest calorie-restriction diets, the Mediterranean diet, and low-glycemic index diets as the top three medical nutrition therapies [185]. These often require a complete overhaul of a patient's current diet practices and may have low adherence. However, at the end of the list of recommendations are dairy foods, although no specificity to which dairy products to add or limit to promote metabolic health. Diabetes Canada also outlines lifestyle management, with a quick nutrition guide outlining health options including low-fat milk with meals [186]. This study may help to

clarify and specify to patients why milk, in particular, can be a beneficial addition to their diets and that it may not require high consumption, but rather approximately 75 mL of milk daily.

8.5 Overall energy metabolism impacts of milk

The impacts of NFM on hepatic lipid metabolism may be mediated by its effects on overall energy metabolism and mitigation of weight gain, rather than direct effects on the liver. As seen in Table 5.1, NFM had significantly less weight gain than both HFD and WFM. Unpublished work in our lab focusing on the impacts of high-dose supplementation of NFM (equivalent to 2 human servings) in a similar experimental model, demonstrated a greater capacity for diet-induced thermogenesis (DIT) within BAT through enhanced abundance of UCP-1, SIRT1, and PGC1α. Additionally, whey intake in 23 lean humans increased DIT and cumulative fat oxidation compared to casein, soy, and high-carbohydrate controls [187]. DIT refers to an increase in energy expenditure postprandially, and is associated with digestion, absorption, utilization, and storage of dietary components [188].

BAT is integral for shivering and non-shivering thermogenesis to increase energy expenditure and maintain body temperature and weight, respectively. Reduced BAT activity was demonstrated in 29 MASLD participants and was associated with greater hepatic fat content [189]. BAT activation through CNS-stimulated hypothalamic circuits in male mice led to enhanced expression of UCP-1 and inhibited hepatic steatosis [190]. BAT activation through dietary measures, such as milk, may effectively reduce BW gain, mitigate hepatic steatosis, and result in a healthier metabolic phenotype. As obesity is a main risk factor for and consequence of MASLD, increasing energy expenditure through DIT could act as a potential therapeutic for both chronic diseases. NFM may be acting in this route to reduce dyslipidemia, mitigate weight gain,

and attenuate the metabolic load on the liver, resulting in the beneficial morphological and metabolic effects seen in this study.

8.6 Limitations & future directions

This is the first study elucidating the mechanistic differences between NFM and WFM to mitigate the progression of HFD-induced MASLD. Further research is still needed to fully understand the crosstalk between the liver, skeletal muscle, and adipose tissue. However, compared with WFM, NFM supplementation has superior potential to mitigate the effects of HFD-induced MASLD through reduced hepatic lipid accumulation and enhanced FA uptake and oxidation mediated by increased mitochondrial capacity. This would result in a reduction of DNL and an enhanced usage of dietary fats to mitigate the progression of early-stage MASLD, highlighting an important intervention window. Although I utilized a low dosage of NFM and WFM, most adults do not consume the recommended 2-3 servings per day, with multiple studies citing average adult dairy consumption around 1-2 servings per day [89], [191], [192]. As such, an equivalent dosage as was provided to the mice, is easily attainable in by encouraging a small increase in daily dairy consumption in people with low dairy consumption and increased risk of MASLD [88].

This study has limitations as I did not achieve full IR as indicated by the ITT and phosphorylation of Akt, thus I cannot assume similar effects would be seen in an overtly insulin resistant MASLD model. However, this is also a benefit to our study as I can determine the impacts of dietary changes before full disease progression, allowing insights into the preventative impacts of dietary modifications. Exploration of the adipose tissue was not investigated, leaving a future route into possible alterations in adipogenesis and thermogenesis. A

final limitation is the lack of statistical power for my insulin-stimulated groups as the sample size was four, leaving room for improvement.

8.7 Conclusion

To conclude, while both NFM and WFM improved morphological characteristics of MASLD, NFM had a greater beneficial effect in reducing liver TG and enhancing capacity for mitochondrial oxidative phosphorylation. WFM treatment on the other hand yielded a potential enhancement in β-oxidation that may be partially negated by enhanced DNL and accumulation of liver TG in comparison with NFM. Therefore, NFM demonstrates a greater protective effect in mitigating hepatic steatosis and preventing the progression of MASLD. A summary depicting the proposed mechanisms of action of both NFM and can be seen in Figure 8.1.

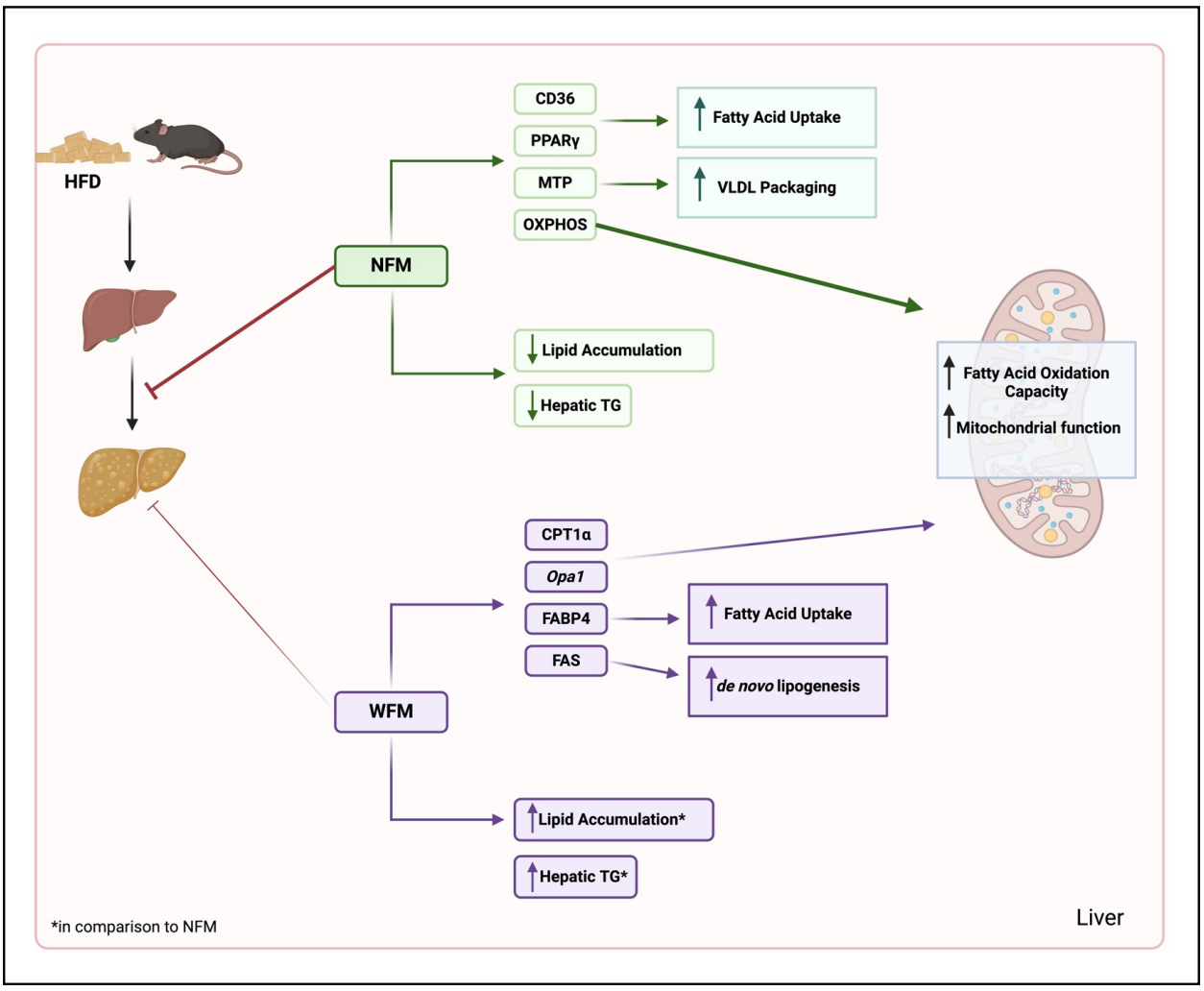

Figure 8.1. Summary of the mechanisms of action impacted by NFM and WFM. HFD, high-fat diet; NFM, non-fat milk; WFM, whole-fat milk; PPARγ, proliferator activated receptor gamma; MTP, microsomal transport protein; OXPHOS, oxidative phosphorylation complexes; TG, triglycerides; CPT1α, carnitine palmitoyl transferase 1α; Opa1, optic atrophy 1; FABP4, fatty acid binding protein 4; FAS, fatty acid synthase; VLDL, very low density lipoprotein. Created by EB with Biorender.com.

References:

[1] R. N. Haththotuwa, C. N. Wijeyaratne, and U. Senarath, "Worldwide epidemic of obesity," in *Obesity and Obstetrics*, Elsevier, 2020, pp. 3–8. doi: 10.1016/B978-0-12-817921-5.00001-1.

[2] G. A. Gregory *et al.*, "Global incidence, prevalence, and mortality of type 1 diabetes in 2021 with projection to 2040: a modelling study," *Lancet Diabetes Endocrinol*, vol. 10, no. 10, pp. 741–760, Oct. 2022, doi: 10.1016/S2213-8587(22)00218-2.

[3] K. L. Ong *et al.*, "Global, regional, and national burden of diabetes from 1990 to 2021, with projections of prevalence to 2050: a systematic analysis for the Global Burden of Disease Study 2021," *The Lancet*, vol. 402, no. 10397, pp. 203–234, Jul. 2023, doi: 10.1016/S0140-6736(23)01301-6.

[4] M. Gierach, J. Gierach, M. Ewertowska, A. Arndt, and R. Junik, "Correlation between Body Mass Index and Waist Circumference in Patients with Metabolic Syndrome," *ISRN Endocrinol*, vol. 2014, pp. 1–6, Mar. 2014, doi: 10.1155/2014/514589.

[5] M. H. Le *et al.*, "2019 Global NAFLD Prevalence: A Systematic Review and Meta-analysis," *Clinical Gastroenterology and Hepatology*, vol. 20, no. 12, pp. 2809-2817.e28, Dec. 2022, doi: 10.1016/j.cgh.2021.12.002.

[6] Y. Handelsman *et al.*, "Early intervention and intensive management of patients with diabetes, cardiorenal, and metabolic diseases," *J Diabetes Complications*, vol. 37, no. 2, p. 108389, Feb. 2023, doi: 10.1016/j.jdiacomp.2022.108389.

[7] M. G. Saklayen, "The Global Epidemic of the Metabolic Syndrome," *Curr Hypertens Rep*, vol. 20, no. 2, p. 12, Feb. 2018, doi: 10.1007/s11906-018-0812-z.

[8] Y. Reznik *et al.*, "The use of an automated insulin delivery system is associated with a reduction in diabetes distress and improvement in quality of life in people with type 1 diabetes," *Diabetes Obes Metab*, Jan. 2024, doi: 10.1111/dom.15462.

[9] A. Y. Patel, P. Shah, and J. H. Flaherty, "Number of medications is associated with outcomes in the elderly patient with metabolic syndrome.," *J Geriatr Cardiol*, vol. 9, no. 3, pp. 213–9, Sep. 2012, doi: 10.3724/SP.J.1263.2011.12011.

[10] L. Lipscombe *et al.*, "Pharmacologic Glycemic Management of Type 2 Diabetes in Adults: 2020 Update," *Can J Diabetes*, vol. 44, no. 7, pp. 575–591, Oct. 2020, doi: 10.1016/j.jcjd.2020.08.001.

[11] N. E. Bonekamp *et al.*, "Long-term lifestyle change and risk of mortality and Type 2 diabetes in patients with cardiovascular disease," *Eur J Prev Cardiol*, vol. 31, no. 2, pp. 205–213, Jan. 2024, doi: 10.1093/eurjpc/zwad316.

[12] M. M. Ghahfarrokhi, H. Shirvani, M. Rahimi, B. Bazgir, A. Shamsadini, and V. Sobhani, "Feasibility and preliminary efficacy of different intensities of functional training in elderly type 2 diabetes patients with cognitive impairment: a pilot randomised controlled trial," *BMC Geriatr*, vol. 24, no. 1, p. 71, Jan. 2024, doi: 10.1186/s12877-024-04698-8.

[13] S. Oh *et al.*, "Weight-loss-independent benefits of exercise on liver steatosis and stiffness in Japanese men with NAFLD," *JHEP Reports*, vol. 3, no. 3, p. 100253, Jun. 2021, doi: 10.1016/j.jhepr.2021.100253.

[14] R. de la Iglesia, V. Loria-Kohen, M. Zulet, J. Martinez, G. Reglero, and A. Ramirez de Molina, "Dietary Strategies Implicated in the Prevention and Treatment of Metabolic Syndrome," *Int J Mol Sci*, vol. 17, no. 11, p. 1877, Nov. 2016, doi: 10.3390/ijms17111877.

[15] Y. Gepner *et al.*, “Effect of Distinct Lifestyle Interventions on Mobilization of Fat Storage Pools,” *Circulation*, vol. 137, no. 11, pp. 1143–1157, Mar. 2018, doi: 10.1161/CIRCULATIONAHA.117.030501.
[16] A. R. G. Look, “Long-term Effects of a Lifestyle Intervention on Weight and Cardiovascular Risk Factors in Individuals With Type 2 Diabetes Mellitus,” *Arch Intern Med*, vol. 170, no. 17, Sep. 2010, doi: 10.1001/archinternmed.2010.334.
[17] M. E. J. Lean *et al.*, “Durability of a primary care-led weight-management intervention for remission of type 2 diabetes: 2-year results of the DiRECT open-label, cluster-randomised trial,” *Lancet Diabetes Endocrinol*, vol. 7, no. 5, pp. 344–355, May 2019, doi: 10.1016/S2213-8587(19)30068-3.
[18] J. Guo *et al.*, “The Impact of Dairy Products in the Development of Type 2 Diabetes: Where Does the Evidence Stand in 2019?,” *Advances in Nutrition*, vol. 10, no. 6, pp. 1066–1075, Nov. 2019, doi: 10.1093/advances/nmz050.
[19] S. J. Moftah, “Comparison of cheese, yogurt, and milk effects on glucose homeostasis and liver lipid accumulation in mice fed high-fat diet.,” MSc Thesis, University of Alberta, Edmonton, 2022.
[20] T. S. Han and M. E. J. Lean, “Metabolic syndrome,” *Medicine*, vol. 43, no. 2, pp. 80–87, Feb. 2015, doi: 10.1016/j.mpmed.2014.11.006.
[21] Z. Punthakee, R. Goldenberg, and P. Katz, “Definition, Classification and Diagnosis of Diabetes, Prediabetes and Metabolic Syndrome,” *Can J Diabetes*, vol. 42, pp. S10–S15, Apr. 2018, doi: 10.1016/j.jcjd.2017.10.003.
[22] Canadian Mental Health Measures Survey, “Metabolic syndrome in adults, 2012-2013,” 2014.
[23] E. McCracken, M. Monaghan, and S. Sreenivasan, “Pathophysiology of the metabolic syndrome,” *Clin Dermatol*, vol. 36, no. 1, pp. 14–20, Jan. 2018, doi: 10.1016/j.clindermatol.2017.09.004.
[24] G. Fahed *et al.*, “Metabolic Syndrome: Updates on Pathophysiology and Management in 2021,” *Int J Mol Sci*, vol. 23, no. 2, p. 786, Jan. 2022, doi: 10.3390/ijms23020786.
[25] U. Galicia-Garcia *et al.*, “Pathophysiology of Type 2 Diabetes Mellitus,” *Int J Mol Sci*, vol. 21, no. 17, p. 6275, Aug. 2020, doi: 10.3390/ijms21176275.
[26] J. F. Ndisang, A. Vannacci, and S. Rastogi, “Insulin Resistance, Type 1 and Type 2 Diabetes, and Related Complications 2017,” *J Diabetes Res*, vol. 2017, pp. 1–3, 2017, doi: 10.1155/2017/1478294.
[27] R. A. DeFronzo, “From the Triumvirate to the Ominous Octet: A New Paradigm for the Treatment of Type 2 Diabetes Mellitus,” *Diabetes*, vol. 58, no. 4, pp. 773–795, Apr. 2009, doi: 10.2337/db09-9028.
[28] W.-K. Chan, K.-H. Chuah, R. B. Rajaram, L.-L. Lim, J. Ratnasingam, and S. R. Vethakkan, “Metabolic Dysfunction-Associated Steatotic Liver Disease (MASLD): A State-of-the-Art Review.,” *J Obes Metab Syndr*, vol. 32, no. 3, pp. 197–213, Sep. 2023, doi: 10.7570/jomes23052.
[29] A. L. Hill *et al.*, “Global liver transplantation: emerging trends and ethical challenges,” *Langenbecks Arch Surg*, vol. 408, no. 1, p. 418, Oct. 2023, doi: 10.1007/s00423-023-03144-4.
[30] J. Quek *et al.*, “Global prevalence of non-alcoholic fatty liver disease and non-alcoholic steatohepatitis in the overweight and obese population: a systematic review and meta-

analysis," *Lancet Gastroenterol Hepatol*, vol. 8, no. 1, pp. 20–30, Jan. 2023, doi: 10.1016/S2468-1253(22)00317-X.
[31] Z. M. Younossi *et al.*, "The global epidemiology of NAFLD and NASH in patients with type 2 diabetes: A systematic review and meta-analysis," *J Hepatol*, vol. 71, no. 4, pp. 793–801, Oct. 2019, doi: 10.1016/j.jhep.2019.06.021.
[32] I. L. K. Nalbantoglu and E. M. Brunt, "Role of liver biopsy in nonalcoholic fatty liver disease.," *World J Gastroenterol*, vol. 20, no. 27, pp. 9026–37, Jul. 2014, doi: 10.3748/wjg.v20.i27.9026.
[33] V. A. Piazzolla and A. Mangia, "Noninvasive Diagnosis of NAFLD and NASH," *Cells*, vol. 9, no. 4, p. 1005, Apr. 2020, doi: 10.3390/cells9041005.
[34] M. R. Rooney *et al.*, "Global Prevalence of Prediabetes," *Diabetes Care*, vol. 46, no. 7, pp. 1388–1394, Jul. 2023, doi: 10.2337/dc22-2376.
[35] M. Z. Banday, A. S. Sameer, and S. Nissar, "Pathophysiology of diabetes: An overview," *Avicenna J Med*, vol. 10, no. 04, pp. 174–188, Oct. 2020, doi: 10.4103/ajm.ajm_53_20.
[36] P. V Dludla *et al.*, "Pancreatic β-cell dysfunction in type 2 diabetes: Implications of inflammation and oxidative stress," *World J Diabetes*, vol. 14, no. 3, pp. 130–146, Mar. 2023, doi: 10.4239/wjd.v14.i3.130.
[37] G. Targher, K. E. Corey, C. D. Byrne, and M. Roden, "The complex link between NAFLD and type 2 diabetes mellitus — mechanisms and treatments," *Nat Rev Gastroenterol Hepatol*, vol. 18, no. 9, pp. 599–612, Sep. 2021, doi: 10.1038/s41575-021-00448-y.
[38] Z. M. Younossi *et al.*, "The global epidemiology of NAFLD and NASH in patients with type 2 diabetes: A systematic review and meta-analysis," *J Hepatol*, vol. 71, no. 4, pp. 793–801, Oct. 2019, doi: 10.1016/j.jhep.2019.06.021.
[39] P. V Röder, B. Wu, Y. Liu, and W. Han, "Pancreatic regulation of glucose homeostasis.," *Exp Mol Med*, vol. 48, no. 3, p. e219, Mar. 2016, doi: 10.1038/emm.2016.6.
[40] L. Chen, B. Tuo, and H. Dong, "Regulation of Intestinal Glucose Absorption by Ion Channels and Transporters," *Nutrients*, vol. 8, no. 1, p. 43, Jan. 2016, doi: 10.3390/nu8010043.
[41] M. M. Adeva-Andany, N. Pérez-Felpete, C. Fernández-Fernández, C. Donapetry-García, and C. Pazos-García, "Liver glucose metabolism in humans," *Biosci Rep*, vol. 36, no. 6, Dec. 2016, doi: 10.1042/BSR20160385.
[42] L. Rui, "Energy metabolism in the liver.," *Compr Physiol*, vol. 4, no. 1, pp. 177–97, Jan. 2014, doi: 10.1002/cphy.c130024.
[43] E. A. Melkonian, E. Asuka, and M. P. Schury, *Physiology, Gluconeogenesis*. StatPearls Publishing, 2024.
[44] R. Carnagarin, A. M. Dharmarajan, and C. R. Dass, "Molecular aspects of glucose homeostasis in skeletal muscle – A focus on the molecular mechanisms of insulin resistance," *Mol Cell Endocrinol*, vol. 417, pp. 52–62, Dec. 2015, doi: 10.1016/j.mce.2015.09.004.
[45] P. L. Evans, S. L. McMillin, L. A. Weyrauch, and C. A. Witczak, "Regulation of Skeletal Muscle Glucose Transport and Glucose Metabolism by Exercise Training," *Nutrients*, vol. 11, no. 10, p. 2432, Oct. 2019, doi: 10.3390/nu11102432.
[46] K. E. Merz and D. C. Thurmond, "Role of Skeletal Muscle in Insulin Resistance and Glucose Uptake," in *Comprehensive Physiology*, Wiley, 2020, pp. 785–809. doi: 10.1002/cphy.c190029.

[47] E. O. Ojuka *et al.*, “Regulation of GLUT4 biogenesis in muscle: evidence for involvement of AMPK and Ca,” *American Journal of Physiology-Endocrinology and Metabolism*, vol. 282, no. 5, pp. E1008–E1013, May 2002, doi: 10.1152/ajpendo.00512.2001.
[48] N. Patil, O. Howe, P. Cahill, and H. J. Byrne, “Monitoring and modelling the dynamics of the cellular glycolysis pathway: A review and future perspectives,” *Mol Metab*, vol. 66, p. 101635, Dec. 2022, doi: 10.1016/j.molmet.2022.101635.
[49] E. V. Prochownik and H. Wang, “The Metabolic Fates of Pyruvate in Normal and Neoplastic Cells,” *Cells*, vol. 10, no. 4, p. 762, Mar. 2021, doi: 10.3390/cells10040762.
[50] M. Dashty, “A quick look at biochemistry: Carbohydrate metabolism,” *Clin Biochem*, vol. 46, no. 15, pp. 1339–1352, Oct. 2013, doi: 10.1016/j.clinbiochem.2013.04.027.
[51] J. Jensen, P. I. Rustad, A. J. Kolnes, and Y.-C. Lai, “The Role of Skeletal Muscle Glycogen Breakdown for Regulation of Insulin Sensitivity by Exercise,” *Front Physiol*, vol. 2, 2011, doi: 10.3389/fphys.2011.00112.
[52] M. P. Czech, “Insulin action and resistance in obesity and type 2 diabetes,” *Nat Med*, vol. 23, no. 7, pp. 804–814, Jul. 2017, doi: 10.1038/nm.4350.
[53] M. C. Petersen, D. F. Vatner, and G. I. Shulman, “Regulation of hepatic glucose metabolism in health and disease,” *Nat Rev Endocrinol*, vol. 13, no. 10, pp. 572–587, Oct. 2017, doi: 10.1038/nrendo.2017.80.
[54] K. Kato, Y. Takeshita, H. Misu, Y. Zen, S. Kaneko, and T. Takamura, “Liver steatosis is associated with insulin resistance in skeletal muscle rather than in the liver in <scp>J</scp> apanese patients with non-alcoholic fatty liver disease,” *J Diabetes Investig*, vol. 6, no. 2, pp. 158–163, Mar. 2015, doi: 10.1111/jdi.12271.
[55] J. Miao *et al.*, “Hepatic insulin receptor deficiency impairs the SREBP-2 response to feeding and statins,” *J Lipid Res*, vol. 55, no. 4, pp. 659–667, Apr. 2014, doi: 10.1194/jlr.M043711.
[56] K. Bouzakri *et al.*, “siRNA-based gene silencing reveals specialized roles of IRS-1/Akt2 and IRS-2/Akt1 in glucose and lipid metabolism in human skeletal muscle,” *Cell Metab*, vol. 4, no. 1, pp. 89–96, Jul. 2006, doi: 10.1016/j.cmet.2006.04.008.
[57] M. Brownlee, “The Pathobiology of Diabetic Complications,” *Diabetes*, vol. 54, no. 6, pp. 1615–1625, Jun. 2005, doi: 10.2337/diabetes.54.6.1615.
[58] W. T. Cade, “Diabetes-Related Microvascular and Macrovascular Diseases in the Physical Therapy Setting,” *Phys Ther*, vol. 88, no. 11, pp. 1322–1335, Nov. 2008, doi: 10.2522/ptj.20080008.
[59] N. A. Abumrad and N. O. Davidson, “Role of the Gut in Lipid Homeostasis,” *Physiol Rev*, vol. 92, no. 3, pp. 1061–1085, Jul. 2012, doi: 10.1152/physrev.00019.2011.
[60] C.-W. Ko, J. Qu, D. D. Black, and P. Tso, “Regulation of intestinal lipid metabolism: current concepts and relevance to disease,” *Nat Rev Gastroenterol Hepatol*, vol. 17, no. 3, pp. 169–183, Mar. 2020, doi: 10.1038/s41575-019-0250-7.
[61] M. M. Hussain, “Intestinal lipid absorption and lipoprotein formation,” *Curr Opin Lipidol*, vol. 25, no. 3, pp. 200–206, Jun. 2014, doi: 10.1097/MOL.0000000000000084.
[62] P. Nguyen *et al.*, “Liver lipid metabolism,” *J Anim Physiol Anim Nutr (Berl)*, vol. 92, no. 3, pp. 272–283, Jun. 2008, doi: 10.1111/j.1439-0396.2007.00752.x.
[63] M. Alves-Bezerra and D. E. Cohen, “Triglyceride Metabolism in the Liver.,” *Compr Physiol*, vol. 8, no. 1, pp. 1–8, Dec. 2017, doi: 10.1002/cphy.c170012.

[64] F. Ameer, L. Scandiuzzi, S. Hasnain, H. Kalbacher, and N. Zaidi, “De novo lipogenesis in health and disease,” *Metabolism*, vol. 63, no. 7, pp. 895–902, Jul. 2014, doi: 10.1016/j.metabol.2014.04.003.
[65] J.-M. Schwarz, P. Linfoot, D. Dare, and K. Aghajanian, “Hepatic de novo lipogenesis in normoinsulinemic and hyperinsulinemic subjects consuming high-fat, low-carbohydrate and low-fat, high-carbohydrate isoenergetic diets,” *Am J Clin Nutr*, vol. 77, no. 1, pp. 43–50, Jan. 2003, doi: 10.1093/ajcn/77.1.43.
[66] P. E. Morales, J. L. Bucarey, and A. Espinosa, “Muscle Lipid Metabolism: Role of Lipid Droplets and Perilipins,” *J Diabetes Res*, vol. 2017, pp. 1–10, 2017, doi: 10.1155/2017/1789395.
[67] M. Bosma, “Lipid droplet dynamics in skeletal muscle,” *Exp Cell Res*, vol. 340, no. 2, pp. 180–186, Jan. 2016, doi: 10.1016/j.yexcr.2015.10.023.
[68] A.-M. Lundsgaard, A. M. Fritzen, and B. Kiens, “Molecular Regulation of Fatty Acid Oxidation in Skeletal Muscle during Aerobic Exercise,” *Trends in Endocrinology & Metabolism*, vol. 29, no. 1, pp. 18–30, Jan. 2018, doi: 10.1016/j.tem.2017.10.011.
[69] B. Kiens, T. H. M. Roemen, and G. J. van der Vusse, “Muscular long-chain fatty acid content during graded exercise in humans,” *American Journal of Physiology-Endocrinology and Metabolism*, vol. 276, no. 2, pp. E352–E357, Feb. 1999, doi: 10.1152/ajpendo.1999.276.2.E352.
[70] M. Lee and S. Park, “Myosteatosis: a potential missing link between hypertension and metabolic disorder in the Asian population,” *Hypertension Research*, vol. 46, no. 6, pp. 1603–1605, Jun. 2023, doi: 10.1038/s41440-023-01270-6.
[71] Y.-L. Fang, H. Chen, C.-L. Wang, and L. Liang, “Pathogenesis of non-alcoholic fatty liver disease in children and adolescence: From ‘two hit theory’ to ‘multiple hit model,’” *World J Gastroenterol*, vol. 24, no. 27, pp. 2974–2983, Jul. 2018, doi: 10.3748/wjg.v24.i27.2974.
[72] H. Tilg, T. E. Adolph, and A. R. Moschen, “Multiple Parallel Hits Hypothesis in Nonalcoholic Fatty Liver Disease: Revisited After a Decade,” *Hepatology*, vol. 73, no. 2, pp. 833–842, Feb. 2021, doi: 10.1002/hep.31518.
[73] H. A. Ferris and C. R. Kahn, “Unraveling the Paradox of Selective Insulin Resistance in the Liver: the Brain–Liver Connection,” *Diabetes*, vol. 65, no. 6, pp. 1481–1483, Jun. 2016, doi: 10.2337/dbi16-0010.
[74] S. B. Biddinger *et al.*, “Hepatic Insulin Resistance Is Sufficient to Produce Dyslipidemia and Susceptibility to Atherosclerosis,” *Cell Metab*, vol. 7, no. 2, pp. 125–134, Feb. 2008, doi: 10.1016/j.cmet.2007.11.013.
[75] T. Scherer *et al.*, “Insulin Regulates Hepatic Triglyceride Secretion and Lipid Content via Signaling in the Brain,” *Diabetes*, vol. 65, no. 6, pp. 1511–1520, Jun. 2016, doi: 10.2337/db15-1552.
[76] K. Pafili and M. Roden, “Nonalcoholic fatty liver disease (NAFLD) from pathogenesis to treatment concepts in humans,” *Mol Metab*, vol. 50, p. 101122, Aug. 2021, doi: 10.1016/j.molmet.2020.101122.
[77] K. Fujita *et al.*, “Dysfunctional very-low-density lipoprotein synthesis and release is a key factor in nonalcoholic steatohepatitis pathogenesis,” *Hepatology*, vol. 50, no. 3, pp. 772–780, Sep. 2009, doi: 10.1002/hep.23094.
[78] E. Piragine, D. Petri, A. Martelli, V. Calderone, and E. Lucenteforte, “Adherence to Oral Antidiabetic Drugs in Patients with Type 2 Diabetes: Systematic Review and Meta-Analysis,” *J Clin Med*, vol. 12, no. 5, p. 1981, Mar. 2023, doi: 10.3390/jcm12051981.

[79] W. S. Bibeau, H. Fu, A. D. Taylor, and A. Y. M. Kwan, “Impact of Out-of-Pocket Pharmacy Costs on Branded Medication Adherence Among Patients with Type 2 Diabetes,” *J Manag Care Spec Pharm*, vol. 22, no. 11, pp. 1338–1347, Nov. 2016, doi: 10.18553/jmcp.2016.22.11.1338.
[80] S. A. Harrison *et al.*, “A Phase 3, Randomized, Controlled Trial of Resmetirom in NASH with Liver Fibrosis,” *New England Journal of Medicine*, vol. 390, no. 6, pp. 497–509, Feb. 2024, doi: 10.1056/NEJMoa2309000.
[81] Y. Shao, S. Chen, L. Han, and J. Liu, “Pharmacotherapies of NAFLD: updated opportunities based on metabolic intervention,” *Nutr Metab (Lond)*, vol. 20, no. 1, p. 30, Jul. 2023, doi: 10.1186/s12986-023-00748-x.
[82] A. L. Sberna *et al.*, “European Association for the Study of the Liver (EASL), European Association for the Study of Diabetes (EASD) and European Association for the Study of Obesity (EASO) clinical practice recommendations for the management of non-alcoholic fatty liver disease: evaluation of their application in people with Type 2 diabetes,” *Diabetic Medicine*, vol. 35, no. 3, pp. 368–375, Mar. 2018, doi: 10.1111/dme.13565.
[83] D. Gallardo-Gómez *et al.*, “Optimal Dose and Type of Physical Activity to Improve Glycemic Control in People Diagnosed With Type 2 Diabetes: A Systematic Review and Meta-analysis,” *Diabetes Care*, vol. 47, no. 2, pp. 295–303, Feb. 2024, doi: 10.2337/dc23-0800.
[84] M. E. Lean *et al.*, “Primary care-led weight management for remission of type 2 diabetes (DiRECT): an open-label, cluster-randomised trial,” *The Lancet*, vol. 391, no. 10120, pp. 541–551, Feb. 2018, doi: 10.1016/S0140-6736(17)33102-1.
[85] S. L. Hocking, T. P. Markovic, C. M. Y. Lee, T. J. Picone, K. E. Gudorf, and S. Colagiuri, “Intensive Lifestyle Intervention for Remission of Early Type 2 Diabetes in Primary Care in Australia: DiRECT-Aus,” *Diabetes Care*, vol. 47, no. 1, pp. 66–70, Jan. 2024, doi: 10.2337/dc23-0781.
[86] S. Katsaridis *et al.*, “Low Reported Adherence to the 2019 American Diabetes Association Nutrition Recommendations among Patients with Type 2 Diabetes Mellitus, Indicating the Need for Improved Nutrition Education and Diet Care,” *Nutrients*, vol. 12, no. 11, p. 3516, Nov. 2020, doi: 10.3390/nu12113516.
[87] K. B. Comerford, G. D. Miller, A. C. Boileau, S. N. Masiello Schuette, J. C. Giddens, and K. A. Brown, “Global Review of Dairy Recommendations in Food-Based Dietary Guidelines,” *Front Nutr*, vol. 8, May 2021, doi: 10.3389/fnut.2021.671999.
[88] E. Yuzbashian, D. N. Fernando, M. Pakseresht, D. T. Eurich, and C. B. Chan, “Dairy product consumption and risk of non-alcoholic fatty liver disease: A systematic review and meta-analysis of observational studies,” *Nutrition, Metabolism and Cardiovascular Diseases*, vol. 33, no. 8, pp. 1461–1471, Aug. 2023, doi: 10.1016/j.numecd.2023.04.018.
[89] E. Yuzbashian, G. Asghari, P. Mirmiran, C. B. Chan, and F. Azizi, “Changes in dairy product consumption and subsequent type 2 diabetes among individuals with prediabetes: Tehran Lipid and Glucose Study,” *Nutr J*, vol. 20, no. 1, p. 88, Dec. 2021, doi: 10.1186/s12937-021-00745-x.
[90] S. Jin and Y. Je, “Dairy Consumption and Risk of Metabolic Syndrome: Results from Korean Population and Meta-Analysis,” *Nutrients*, vol. 13, no. 5, p. 1574, May 2021, doi: 10.3390/nu13051574.
[91] C. E. Dugan, D. Aguilar, Y.-K. Park, J.-Y. Lee, and M. L. Fernandez, “Dairy Consumption Lowers Systemic Inflammation and Liver Enzymes in Typically Low-Dairy Consumers

with Clinical Characteristics of Metabolic Syndrome," *J Am Coll Nutr*, vol. 35, no. 3, pp. 255–261, Apr. 2016, doi: 10.1080/07315724.2015.1022637.
[92] M. C. Sawh *et al.*, "Dairy Fat Intake, Plasma Pentadecanoic Acid, and Plasma Iso-heptadecanoic Acid Are Inversely Associated With Liver Fat in Children," *J Pediatr Gastroenterol Nutr*, vol. 72, no. 4, Apr. 2021, doi: 10.1097/MPG.0000000000003040.
[93] B. Bhavadharini *et al.*, "Association of dairy consumption with metabolic syndrome, hypertension and diabetes in 147 812 individuals from 21 countries," *BMJ Open Diabetes Res Care*, vol. 8, no. 1, p. e000826, Apr. 2020, doi: 10.1136/bmjdrc-2019-000826.
[94] J. Mitri *et al.*, "Effect of dairy consumption and its fat content on glycemic control and cardiovascular disease risk factors in patients with type 2 diabetes: a randomized controlled study," *Am J Clin Nutr*, vol. 112, no. 2, pp. 293–302, Aug. 2020, doi: 10.1093/ajcn/nqaa138.
[95] E. Wat *et al.*, "Dietary phospholipid-rich dairy milk extract reduces hepatomegaly, hepatic steatosis and hyperlipidemia in mice fed a high-fat diet," *Atherosclerosis*, vol. 205, no. 1, pp. 144–150, Jul. 2009, doi: 10.1016/j.atherosclerosis.2008.12.004.
[96] X. Sun and M. B. Zemel, "Calcium and Dairy Products Inhibit Weight and Fat Regain during Ad Libitum Consumption Following Energy Restriction in Ap2-Agouti Transgenic Mice," *J Nutr*, vol. 134, no. 11, pp. 3054–3060, Nov. 2004, doi: 10.1093/jn/134.11.3054.
[97] H. B. Yamin, M. Barnea, Y. Genzer, N. Chapnik, and O. Froy, "Long-term commercial cow's milk consumption and its effects on metabolic parameters associated with obesity in young mice," *Mol Nutr Food Res*, vol. 58, no. 5, pp. 1061–1068, May 2014, doi: 10.1002/mnfr.201300650.
[98] T. K. Thorning *et al.*, "Whole dairy matrix or single nutrients in assessment of health effects: current evidence and knowledge gaps ," *Am J Clin Nutr*, vol. 105, no. 5, pp. 1033–1045, May 2017, doi: 10.3945/ajcn.116.151548.
[99] D. R. Hill and D. S. Newburg, "Clinical applications of bioactive milk components," *Nutr Rev*, vol. 73, no. 7, pp. 463–476, Jul. 2015, doi: 10.1093/nutrit/nuv009.
[100] L. K. Eller and R. A. Reimer, "Dairy Protein Attenuates Weight Gain in Obese Rats Better Than Whey or Casein Alone," *Obesity*, vol. 18, no. 4, pp. 704–711, Apr. 2010, doi: 10.1038/oby.2009.300.
[101] S.-P. Xu, X.-Y. Mao, X. Cheng, and B. Chen, "Ameliorating effects of casein glycomacropeptide on obesity induced by high-fat diet in male Sprague-Dawley rats," *Food and Chemical Toxicology*, vol. 56, pp. 1–7, Jun. 2013, doi: 10.1016/j.fct.2013.01.027.
[102] M. H. Schoemaker *et al.*, "A casein hydrolysate based formulation attenuates obesity and associated non-alcoholic fatty liver disease and atherosclerosis in LDLr-/-.Leiden mice," *PLoS One*, vol. 12, no. 7, p. e0180648, Jul. 2017, doi: 10.1371/journal.pone.0180648.
[103] K. Wang *et al.*, "Whey protein hydrolysate alleviated atherosclerosis and hepatic steatosis by regulating lipid metabolism in apoE-/- mice fed a Western diet," *Food Research International*, vol. 157, p. 111419, Jul. 2022, doi: 10.1016/j.foodres.2022.111419.
[104] M. U. Ijaz *et al.*, "Beef, Casein, and Soy Proteins Differentially Affect Lipid Metabolism, Triglycerides Accumulation and Gut Microbiota of High-Fat Diet-Fed C57BL/6J Mice," *Front Microbiol*, vol. 9, Sep. 2018, doi: 10.3389/fmicb.2018.02200.
[105] A. L. Zhou and R. E. Ward, "Milk polar lipids modulate lipid metabolism, gut permeability, and systemic inflammation in high-fat-fed C57BL/6J ob/ob mice, a model of

severe obesity," *J Dairy Sci*, vol. 102, no. 6, pp. 4816–4831, Jun. 2019, doi: 10.3168/jds.2018-15949.
[106] Q. Yuan, B. Zhan, M. Du, R. Chang, T. Li, and X. Mao, "Dietary milk fat globule membrane regulates JNK and PI3K/Akt pathway and ameliorates type 2 diabetes in mice induced by a high-fat diet and streptozotocin," *J Funct Foods*, vol. 60, p. 103435, Sep. 2019, doi: 10.1016/j.jff.2019.103435.
[107] F. Rosqvist *et al.*, "Potential role of milk fat globule membrane in modulating plasma lipoproteins, gene expression, and cholesterol metabolism in humans: a randomized study," *Am J Clin Nutr*, vol. 102, no. 1, pp. 20–30, Jul. 2015, doi: 10.3945/ajcn.115.107045.
[108] X. Wang, A. England, C. Sinclair, F. Merkosky, and C. B. Chan, "Trans-11 vaccenic acid improves glucose homeostasis in a model of type 2 diabetes by promoting insulin secretion via GPR40," *J Funct Foods*, vol. 60, p. 103410, Sep. 2019, doi: 10.1016/j.jff.2019.06.012.
[109] W.-C. Fu *et al.*, "Pentadecanoic acid promotes basal and insulin-stimulated glucose uptake in C2C12 myotubes," *Food Nutr Res*, vol. 65, Jan. 2021, doi: 10.29219/fnr.v65.4527.
[110] D. Yu *et al.*, "Higher Dietary Choline Intake Is Associated with Lower Risk of Nonalcoholic Fatty Liver in Normal-Weight Chinese Women," *J Nutr*, vol. 144, no. 12, pp. 2034–2040, Dec. 2014, doi: 10.3945/jn.114.197533.
[111] K. Y. Patterson, S. A. Bhagwat, J. R. Williams, J. C. Howe, and J. M. Holden, "USDA Database for the Choline Content of Common Foods: Release Two," Baltimore, Jan. 2008.
[112] W. Lu *et al.*, "Effects of choline deficiency and supplementation on lipid droplet accumulation in bovine primary liver cells in vitro," *J Dairy Sci*, vol. 106, no. 12, pp. 9868–9878, Dec. 2023, doi: 10.3168/jds.2023-23452.
[113] J. Shen, B. Sun, C. Yu, Y. Cao, C. Cai, and J. Yao, "Choline and methionine regulate lipid metabolism via the AMPK signaling pathway in hepatocytes exposed to high concentrations of nonesterified fatty acids," *J Cell Biochem*, vol. 121, no. 8–9, pp. 3667–3678, Aug. 2020, doi: 10.1002/jcb.29494.
[114] J. Nam *et al.*, "Choline prevents fetal overgrowth and normalizes placental fatty acid and glucose metabolism in a mouse model of maternal obesity," *J Nutr Biochem*, vol. 49, pp. 80–88, Nov. 2017, doi: 10.1016/j.jnutbio.2017.08.004.
[115] C.-C. Chen, L.-W. Hsu, K.-D. Chen, K.-W. Chiu, C.-L. Chen, and K.-T. Huang, "Emerging Roles of Calcium Signaling in the Development of Non-Alcoholic Fatty Liver Disease," *Int J Mol Sci*, vol. 23, no. 1, p. 256, Dec. 2021, doi: 10.3390/ijms23010256.
[116] B. Glancy, W. T. Willis, D. J. Chess, and R. S. Balaban, "Effect of Calcium on the Oxidative Phosphorylation Cascade in Skeletal Muscle Mitochondria," *Biochemistry*, vol. 52, no. 16, pp. 2793–2809, Apr. 2013, doi: 10.1021/bi3015983.
[117] W. S. Blaner, "Vitamin A signaling and homeostasis in obesity, diabetes, and metabolic disorders," *Pharmacol Ther*, vol. 197, pp. 153–178, May 2019, doi: 10.1016/j.pharmthera.2019.01.006.
[118] S. E. Trasino, X. -H. Tang, J. Jessurun, and L. J. Gudas, "Retinoic acid receptor β2 agonists restore glycaemic control in diabetes and reduce steatosis," *Diabetes Obes Metab*, vol. 18, no. 2, pp. 142–151, Feb. 2016, doi: 10.1111/dom.12590.
[119] J. Amengual, P. Petrov, M. L. Bonet, J. Ribot, and A. Palou, "Induction of carnitine palmitoyl transferase 1 and fatty acid oxidation by retinoic acid in HepG2 cells," *Int J*

Biochem Cell Biol, vol. 44, no. 11, pp. 2019–2027, Nov. 2012, doi: 10.1016/j.biocel.2012.07.026.
[120] S. Gürgen, A. Yücel, A. Karakuş, D. Çeçen, G. Özen, and S. Koçtürk, "Usage of whey protein may cause liver damage via inflammatory and apoptotic responses," *Hum Exp Toxicol*, vol. 34, no. 7, pp. 769–779, Jul. 2015, doi: 10.1177/0960327114556787.
[121] J. E. Ayala *et al.*, "Standard operating procedures for describing and performing metabolic tests of glucose homeostasis in mice," *Dis Model Mech*, vol. 3, no. 9–10, pp. 525–534, Sep. 2010, doi: 10.1242/dmm.006239.
[122] C. C. Hughey, D. H. Wasserman, R. S. Lee-Young, and L. Lantier, "Approach to assessing determinants of glucose homeostasis in the conscious mouse," *Mammalian Genome*, vol. 25, no. 9–10, pp. 522–538, Oct. 2014, doi: 10.1007/s00335-014-9533-z.
[123] F. Jahandideh *et al.*, "Egg white hydrolysate enhances insulin sensitivity in high-fat diet-induced insulin-resistant rats via Akt activation," *British Journal of Nutrition*, vol. 122, no. 1, pp. 14–24, Jul. 2019, doi: 10.1017/S0007114519000837.
[124] J. FOLCH, M. LEES, and G. H. SLOANE STANLEY, "A simple method for the isolation and purification of total lipides from animal tissues.," *J Biol Chem*, vol. 226, no. 1, pp. 497–509, May 1957.
[125] C. Cruz-Hernandez *et al.*, "Methods for Analysis of Conjugated Linoleic Acids and trans-18:1 Isomers in Dairy Fats by Using a Combination of Gas Chromatography, Silver-Ion Thin-Layer Chromatography/Gas Chromatography, and Silver-Ion Liquid Chromatography," *J AOAC Int*, vol. 87, no. 2, pp. 545–562, Mar. 2004, doi: 10.1093/jaoac/87.2.545.
[126] C. J. Field, E. A. Ryan, A. B. Thomson, and M. T. Clandinin, "Dietary fat and the diabetic state alter insulin binding and the fatty acyl composition of the adipocyte plasma membrane," *Biochemical Journal*, vol. 253, no. 2, pp. 417–424, Jul. 1988, doi: 10.1042/bj2530417.
[127] J. Schindelin *et al.*, "Fiji: an open-source platform for biological-image analysis." pp. 676–682, Jul. 28, 2012. doi: 10.1038/nmeth.2019.
[128] A. Ferdouse, R. R. Agrawal, M. A. Gao, H. Jiang, W. S. Blaner, and R. D. Clugston, "Alcohol induced hepatic retinoid depletion is associated with the induction of multiple retinoid catabolizing cytochrome P450 enzymes," *PLoS One*, vol. 17, no. 1, p. e0261675, Jan. 2022, doi: 10.1371/journal.pone.0261675.
[129] S. C. de Campos Zani *et al.*, "An Egg White-Derived Peptide Enhances Systemic Insulin Sensitivity and Modulates Markers of Non-Alcoholic Fatty Liver Disease in Obese, Insulin Resistant Mice," *Metabolites*, vol. 13, no. 2, p. 174, Jan. 2023, doi: 10.3390/metabo13020174.
[130] P. Wang, Z. Lu, M. He, B. Shi, X. Lei, and A. Shan, "The Effects of Endoplasmic-Reticulum-Resident Selenoproteins in a Nonalcoholic Fatty Liver Disease Pig Model Induced by a High-Fat Diet," *Nutrients*, vol. 12, no. 3, p. 692, Mar. 2020, doi: 10.3390/nu12030692.
[131] M. Inoue *et al.*, "Increased expression of PPARγ in high fat diet-induced liver steatosis in mice," *Biochem Biophys Res Commun*, vol. 336, no. 1, pp. 215–222, Oct. 2005, doi: 10.1016/j.bbrc.2005.08.070.
[132] R. Meli *et al.*, "High Fat Diet Induces Liver Steatosis and Early Dysregulation of Iron Metabolism in Rats," *PLoS One*, vol. 8, no. 6, p. e66570, Jun. 2013, doi: 10.1371/journal.pone.0066570.

[133] H. Alamri *et al.*, “Mapping the triglyceride distribution in NAFLD human liver by MALDI imaging mass spectrometry reveals molecular differences in micro and macro steatosis,” *Anal Bioanal Chem*, vol. 411, no. 4, pp. 885–894, Feb. 2019, doi: 10.1007/s00216-018-1506-8.
[134] L. Recena Aydos, L. Aparecida do Amaral, R. Serafim de Souza, A. C. Jacobowski, E. Freitas dos Santos, and M. L. Rodrigues Macedo, “Nonalcoholic Fatty Liver Disease Induced by High-Fat Diet in C57bl/6 Models,” *Nutrients*, vol. 11, no. 12, p. 3067, Dec. 2019, doi: 10.3390/nu11123067.
[135] T. M. Demaria, L. D. Crepaldi, E. Costa-Bartuli, J. R. Branco, P. Zancan, and M. Sola-Penna, “Once a week consumption of Western diet over twelve weeks promotes sustained insulin resistance and non-alcoholic fat liver disease in C57BL/6 J mice,” *Sci Rep*, vol. 13, no. 1, p. 3058, Feb. 2023, doi: 10.1038/s41598-023-30254-2.
[136] T. Chiba, K. Noji, S. Shinozaki, S. Suzuki, K. Umegaki, and K. Shimokado, “Diet-induced non-alcoholic fatty liver disease affects expression of major cytochrome P450 genes in a mouse model,” *Journal of Pharmacy and Pharmacology*, vol. 68, no. 12, pp. 1567–1576, Nov. 2016, doi: 10.1111/jphp.12646.
[137] S. C. de Campos Zani *et al.*, “IRW improves diet-induced non-alcoholic fatty liver disease by reducing steatosis associated with increased capacity for oxidative phosphorylation,” *J Funct Foods*, vol. 112, p. 105976, Jan. 2024, doi: 10.1016/j.jff.2023.105976.
[138] R. J. Seeley and O. A. MacDougald, “Mice as experimental models for human physiology: when several degrees in housing temperature matter,” *Nat Metab*, vol. 3, no. 4, pp. 443–445, Mar. 2021, doi: 10.1038/s42255-021-00372-0.
[139] C. Fang *et al.*, “The AMPK pathway in fatty liver disease,” *Front Physiol*, vol. 13, Aug. 2022, doi: 10.3389/fphys.2022.970292.
[140] A. Woods *et al.*, “Liver-Specific Activation of AMPK Prevents Steatosis on a High-Fructose Diet,” *Cell Rep*, vol. 18, no. 13, pp. 3043–3051, Mar. 2017, doi: 10.1016/j.celrep.2017.03.011.
[141] N. Babio *et al.*, “Consumption of Yogurt, Low-Fat Milk, and Other Low-Fat Dairy Products Is Associated with Lower Risk of Metabolic Syndrome Incidence in an Elderly Mediterranean Population,” *J Nutr*, vol. 145, no. 10, pp. 2308–2316, Oct. 2015, doi: 10.3945/jn.115.214593.
[142] W. Dai *et al.*, “Dairy product consumption was associated with a lower likelihood of non-alcoholic fatty liver disease: A systematic review and meta-analysis,” *Front Nutr*, vol. 10, Feb. 2023, doi: 10.3389/fnut.2023.1119118.
[143] K. A. Schmidt *et al.*, “The impact of diets rich in low-fat or\ full-fat dairy on glucose tolerance and its determinants: a randomized controlled trial,” *Am J Clin Nutr*, vol. 113, no. 3, pp. 534–547, Mar. 2021, doi: 10.1093/ajcn/nqaa301.
[144] L. E. C. van Meijl and R. P. Mensink, “Effects of milk and milk constituents on postprandial lipid and glucose metabolism in overweight and obese men,” *British Journal of Nutrition*, vol. 110, no. 3, pp. 413–419, Aug. 2013, doi: 10.1017/S0007114512005314.
[145] G. Contarini and M. Povolo, “Phospholipids in Milk Fat: Composition, Biological and Technological Significance, and Analytical Strategies,” *Int J Mol Sci*, vol. 14, no. 2, pp. 2808–2831, Jan. 2013, doi: 10.3390/ijms14022808.
[146] F. Sánchez-Juanes, J. M. Alonso, L. Zancada, and P. Hueso, “Distribution and fatty acid content of phospholipids from bovine milk and bovine milk fat globule membranes,” *Int Dairy J*, vol. 19, no. 5, pp. 273–278, May 2009, doi: 10.1016/j.idairyj.2008.11.006.

[147] B. Jenkins, J. West, and A. Koulman, “A Review of Odd-Chain Fatty Acid Metabolism and the Role of Pentadecanoic Acid (C15:0) and Heptadecanoic Acid (C17:0) in Health and Disease,” *Molecules*, vol. 20, no. 2, pp. 2425–2444, Jan. 2015, doi: 10.3390/molecules20022425.
[148] F. Chiappini *et al.*, “Metabolism dysregulation induces a specific lipid signature of nonalcoholic steatohepatitis in patients,” *Sci Rep*, vol. 7, no. 1, p. 46658, Apr. 2017, doi: 10.1038/srep46658.
[149] L. Hodson, F. Rosqvist, and S. A. Parry, “The influence of dietary fatty acids on liver fat content and metabolism,” *Proceedings of the Nutrition Society*, vol. 79, no. 1, pp. 30–41, Feb. 2020, doi: 10.1017/S0029665119000569.
[150] O. A. Byelashov, A. J. Sinclair, and G. Kaur, “Dietary sources, current intakes, and nutritional role of omega-3 docosapentaenoic acid,” *Lipid Technol*, vol. 27, no. 4, pp. 79–82, Apr. 2015, doi: 10.1002/lite.201500013.
[151] B. C. Araújo *et al.*, “Dietary Arachidonic Acid (20:4n-6) Levels and Its Effect on Growth Performance, Fatty Acid Profile, Gene Expression for Lipid Metabolism, and Health Status of Juvenile California Yellowtail (Seriola dorsalis),” *Fishes*, vol. 7, no. 4, p. 185, Jul. 2022, doi: 10.3390/fishes7040185.
[152] M. Guzmán and M. J. H. Geelen, “Regulation of fatty acid oxidation in mammalian liver,” *Biochimica et Biophysica Acta (BBA) - Lipids and Lipid Metabolism*, vol. 1167, no. 3, pp. 227–241, Apr. 1993, doi: 10.1016/0005-2760(93)90224-W.
[153] S. C. Lim *et al.*, “Loss of the Mitochondrial Fatty Acid β-Oxidation Protein Medium-Chain Acyl-Coenzyme A Dehydrogenase Disrupts Oxidative Phosphorylation Protein Complex Stability and Function,” *Sci Rep*, vol. 8, no. 1, p. 153, Jan. 2018, doi: 10.1038/s41598-017-18530-4.
[154] K. Begriche, J. Massart, M.-A. Robin, F. Bonnet, and B. Fromenty, “Mitochondrial adaptations and dysfunctions in nonalcoholic fatty liver disease,” *Hepatology*, vol. 58, no. 4, pp. 1497–1507, Oct. 2013, doi: 10.1002/hep.26226.
[155] B. Aydın, A. Oğuz, V. Şekeroğlu, and Z. Atlı Şekeroğlu, “Whey protein protects liver mitochondrial function against oxidative stress in rats exposed to acrolein,” *Archives of Industrial Hygiene and Toxicology*, vol. 73, no. 3, pp. 200–206, Sep. 2022, doi: 10.2478/aiht-2022-73-3640.
[156] E. Martino *et al.*, “Whey Improves In Vitro Endothelial Mitochondrial Function and Metabolic Redox Status in Diabetic State,” *Antioxidants*, vol. 12, no. 6, p. 1311, Jun. 2023, doi: 10.3390/antiox12061311.
[157] A. P. L. Jensen-Urstad and C. F. Semenkovich, “Fatty acid synthase and liver triglyceride metabolism: housekeeper or messenger?,” *Biochim Biophys Acta*, vol. 1821, no. 5, pp. 747–53, May 2012, doi: 10.1016/j.bbalip.2011.09.017.
[158] C. Fang *et al.*, “The AMPK pathway in fatty liver disease,” *Front Physiol*, vol. 13, Aug. 2022, doi: 10.3389/fphys.2022.970292.
[159] A. M. Fritzen, A.-M. Lundsgaard, and B. Kiens, “Tuning fatty acid oxidation in skeletal muscle with dietary fat and exercise,” *Nat Rev Endocrinol*, vol. 16, no. 12, pp. 683–696, Dec. 2020, doi: 10.1038/s41574-020-0405-1.
[160] A. L. Simão *et al.*, “Skeletal muscle miR-34a/SIRT1:AMPK axis is activated in experimental and human non-alcoholic steatohepatitis,” *J Mol Med*, vol. 97, no. 8, pp. 1113–1126, Aug. 2019, doi: 10.1007/s00109-019-01796-8.

[161] J. Tonkin, F. Villarroya, P. L. Puri, and M. Vinciguerra, “SIRT1 signaling as potential modulator of skeletal muscle diseases,” *Curr Opin Pharmacol*, vol. 12, no. 3, pp. 372–376, Jun. 2012, doi: 10.1016/j.coph.2012.02.010.
[162] S. Stein and C. M. Matter, “Protective roles of SIRT1 in atherosclerosis,” *Cell Cycle*, vol. 10, no. 4, pp. 640–647, Feb. 2011, doi: 10.4161/cc.10.4.14863.
[163] Y. Li, S. Xu, X. Zhang, Z. Yi, and S. Cichello, “Skeletal intramyocellular lipid metabolism and insulin resistance,” *Biophys Rep*, vol. 1, no. 2, pp. 90–98, Oct. 2015, doi: 10.1007/s41048-015-0013-0.
[164] S. Kakehi *et al.*, “Increased intramyocellular lipid/impaired insulin sensitivity is associated with altered lipid metabolic genes in muscle of high responders to a high-fat diet,” *American Journal of Physiology-Endocrinology and Metabolism*, vol. 310, no. 1, pp. E32–E40, Jan. 2016, doi: 10.1152/ajpendo.00220.2015.
[165] A. Surowska *et al.*, “Effects of Dietary Protein and Fat Content on Intrahepatocellular and Intramyocellular Lipids during a 6-Day Hypercaloric, High Sucrose Diet: A Randomized Controlled Trial in Normal Weight Healthy Subjects,” *Nutrients*, vol. 11, no. 1, p. 209, Jan. 2019, doi: 10.3390/nu11010209.
[166] L. S. Kiefer *et al.*, “Distribution patterns of intramyocellular and extramyocellular fat by magnetic resonance imaging in subjects with diabetes, prediabetes and normoglycaemic controls,” *Diabetes Obes Metab*, vol. 23, no. 8, pp. 1868–1878, Aug. 2021, doi: 10.1111/dom.14413.
[167] G. Kim *et al.*, “Relationship Between Relative Skeletal Muscle Mass and Nonalcoholic Fatty Liver Disease: A 7-Year Longitudinal Study,” *Hepatology*, vol. 68, no. 5, pp. 1755–1768, Nov. 2018, doi: 10.1002/hep.30049.
[168] H. Aleman-Mateo, A. C. Gallegos Aguilar, V. Ramirez Carreon, L. Macias, H. Astiazaran Garcia, and J. R. Ramos Enriquez, “Nutrient-rich dairy proteins improve appendicular skeletal muscle mass and physical performance, and attenuate the loss of muscle strength in older men and women subjects: a single-blind randomized clinical trial,” *Clin Interv Aging*, p. 1517, Sep. 2014, doi: 10.2147/CIA.S67449.
[169] S. Lensu *et al.*, “Beneficial effects of running and milk protein supplements on Sirtuins and risk factors of metabolic disorders in rats with low aerobic capacity,” *Metabol Open*, vol. 4, p. 100019, Dec. 2019, doi: 10.1016/j.metop.2019.100019.
[170] P. Aldana-Hernández *et al.*, “Dietary phosphatidylcholine supplementation reduces atherosclerosis in Ldlr male mice2,” *J Nutr Biochem*, vol. 92, p. 108617, Jun. 2021, doi: 10.1016/j.jnutbio.2021.108617.
[171] J. Azarcoya-Barrera *et al.*, “The Lipid-Soluble Forms of Choline Enhance Ex Vivo Responses from the Gut-Associated Immune System in Young Female Rat Offspring,” *J Nutr*, vol. 152, no. 11, pp. 2604–2614, Nov. 2022, doi: 10.1093/jn/nxac180.
[172] Z. Zhang *et al.*, “Calcium supplementation relieves high-fat diet-induced liver steatosis by reducing energy metabolism and promoting lipolysis,” *J Nutr Biochem*, vol. 94, p. 108645, Aug. 2021, doi: 10.1016/j.jnutbio.2021.108645.
[173] S. Shojaei Zarghani, H. Soraya, and M. Alizadeh, “Calcium and vitamin D3 combinations improve fatty liver disease through AMPK-independent mechanisms,” *Eur J Nutr*, vol. 57, no. 2, pp. 731–740, Mar. 2018, doi: 10.1007/s00394-016-1360-4.
[174] S. H. Davoodi *et al.*, “Health-Related Aspects of Milk Proteins.,” *Iran J Pharm Res*, vol. 15, no. 3, pp. 573–591, 2016.

[175] K. Wang *et al.*, “Whey protein hydrolysate alleviated atherosclerosis and hepatic steatosis by regulating lipid metabolism in apoE-/- mice fed a Western diet,” *Food Research International*, vol. 157, p. 111419, Jul. 2022, doi: 10.1016/j.foodres.2022.111419.
[176] K. E. Merz and D. C. Thurmond, “Role of Skeletal Muscle in Insulin Resistance and Glucose Uptake,” in *Comprehensive Physiology*, Wiley, 2020, pp. 785–809. doi: 10.1002/cphy.c190029.
[177] S. Altajar and G. Baffy, “Skeletal Muscle Dysfunction in the Development and Progression of Nonalcoholic Fatty Liver Disease,” *J Clin Transl Hepatol*, vol. 8, no. 4, pp. 1–10, Dec. 2020, doi: 10.14218/JCTH.2020.00065.
[178] D. Gan *et al.*, “Low muscle mass and low muscle strength associate with nonalcoholic fatty liver disease,” *Clinical Nutrition*, vol. 39, no. 4, pp. 1124–1130, Apr. 2020, doi: 10.1016/j.clnu.2019.04.023.
[179] J.-H. Lee, H. S. Lee, H. Kim, Y.-J. Kwon, and J.-W. Lee, “Association of milk consumption frequency on muscle mass and strength: an analysis of three representative Korean population studies,” *Eur J Nutr*, vol. 59, no. 7, pp. 3257–3267, Oct. 2020, doi: 10.1007/s00394-019-02164-5.
[180] M. Iwasa, S. Takezoe, N. Kitaura, T. Sutani, H. Miyazaki, and W. Aoi, “A milk casein hydrolysate-derived peptide enhances glucose uptake through the AMP-activated protein kinase signalling pathway in skeletal muscle cells,” *Exp Physiol*, vol. 106, no. 2, pp. 496–505, Feb. 2021, doi: 10.1113/EP088770.
[181] H. Li, R. Wang, L. Wang, L. Li, Y. Ma, and S. Zhou, “Bovine Milk Fat Globule Epidermal Growth Factor VIII activates PI3K/Akt signaling pathway and attenuates sarcopenia in rat model induced by d-galactose,” *Food Biosci*, vol. 40, p. 100847, Apr. 2021, doi: 10.1016/j.fbio.2020.100847.
[182] E. M. Brouwer-Brolsma, D. Sluik, C. M. Singh-Povel, and E. J. M. Feskens, “Dairy product consumption is associated with pre-diabetes and newly diagnosed type 2 diabetes in the Lifelines Cohort Study,” *British Journal of Nutrition*, vol. 119, no. 4, pp. 442–455, Feb. 2018, doi: 10.1017/S0007114517003762.
[183] I. AL. Slurink, L. Chen, D. J. Magliano, N. Kupper, T. Smeets, and S. S. Soedamah-Muthu, “Dairy Product Consumption and Incident Prediabetes in the Australian Diabetes, Obesity, and Lifestyle Study With 12 Years of Follow-Up,” *J Nutr*, vol. 153, no. 6, pp. 1742–1752, Jun. 2023, doi: 10.1016/j.tjnut.2023.03.032.
[184] J. H. Lee, H. S. Lee, S. Jeon, J.-H. Lee, and Y.-J. Kwon, “Association between dairy-rich dietary pattern and metabolic dysfunction-associated steatotic liver disease: Findings from the Korean Genome and Epidemiology Study,” *Digestive and Liver Disease*, Feb. 2024, doi: 10.1016/j.dld.2024.01.200.
[185] J. Brown, C. Clarke, C. Johnson Stoklossa, and J. Sievenpiper, “Medical Nutrition Therapy in Obesity Management,” Oct. 2022.
[186] Diabetes Canada, “Just the basics,” Diabetes Canada Practical Guidelines.
[187] K. J. Acheson *et al.*, “Protein choices targeting thermogenesis and metabolism,” *Am J Clin Nutr*, vol. 93, no. 3, pp. 525–534, Mar. 2011, doi: 10.3945/ajcn.110.005850.
[188] P.-C. Chan and P.-S. Hsieh, “The Role and Regulatory Mechanism of Brown Adipose Tissue Activation in Diet-Induced Thermogenesis in Health and Diseases,” *Int J Mol Sci*, vol. 23, no. 16, p. 9448, Aug. 2022, doi: 10.3390/ijms23169448.

[189] B. A. Ahmed *et al.*, “Lower brown adipose tissue activity is associated with non-alcoholic fatty liver disease but not changes in the gut microbiota,” *Cell Rep Med*, vol. 2, no. 9, p. 100397, Sep. 2021, doi: 10.1016/j.xcrm.2021.100397.
[190] H. Shen, L. Jiang, J. D. Lin, M. B. Omary, and L. Rui, “Brown fat activation mitigates alcohol-induced liver steatosis and injury in mice,” *Journal of Clinical Investigation*, vol. 129, no. 6, pp. 2305–2317, Apr. 2019, doi: 10.1172/JCI124376.
[191] B. Bhavadharini *et al.*, “Association of dairy consumption with metabolic syndrome, hypertension and diabetes in 147 812 individuals from 21 countries,” *BMJ Open Diabetes Res Care*, vol. 8, no. 1, p. e000826, Apr. 2020, doi: 10.1136/bmjdrc-2019-000826.
[192] M. S. Da Silva, P. Julien, P. Couture, S. Lemieux, M.-C. Vohl, and I. Rudkowska, “Associations between dairy intake and metabolic risk parameters in a healthy French-Canadian population,” *Applied Physiology, Nutrition, and Metabolism*, vol. 39, no. 12, pp. 1323–1331, Dec. 2014, doi: 10.1139/apnm-2014-0154.